



Amber and the Cretaceous Resinous Interval

Xavier Delclòs ^{a,b,*¹}, Enrique Peñalver ^{c,**¹}, Eduardo Barrón ^c, David Peris ^d, David A. Grimaldi ^e, Michael Holz ^f, Conrad C. Labandeira ^{g,h,i}, Erin E. Saupe ^j, Christopher R. Scotese ^k, Mónica M. Solórzano-Kraemer ^l, Sergio Álvarez-Parra ^{a,b}, Antonio Arillo ^m, Dany Azar ^{n,o}, Edwin A. Cadena ^p, Jacopo Dal Corso ^q, Jiří Kvaček ^r, Antonio Monleón-Getino ^s, André Nel ^t, Daniel Peyrot ^u, Carlos A. Bueno-Cebollada ^c, Alejandro Gallardo ^a, Beatriz González-Fernández ^v, Marta Goula ^{b,w}, Carlos Jaramillo ^x, Iwona Kania-Kłosok ^y, Rafael López-Del Valle ^z, Rafael P. Lozano ^c, Nieves Meléndez ^{aa}, César Menor-Salván ^{ab}, Constanza Peña-Kairath ^{a,b}, Vincent Perrichot ^{ac}, Ana Rodrigo ^c, Alba Sánchez-García ^c, Maxime Santer ^{a,b}, Víctor Sarto i Monteys ^{ad}, Dieter Uhl ^l, José Luis Viejo ^{ae}, Ricardo Pérez-de la Fuente ^{af}

^a Departament de Dinàmica de la Terra i de l'Oceà, Facultat de Ciències de la Terra, Universitat de Barcelona, Spain

^b Institut de Recerca de la Biodiversitat (IRBio), Universitat de Barcelona, Spain

^c CN Instituto Geológico y Minero de España (IGME)-Consejo Superior de Investigaciones Científicas (CSIC), Madrid, Spain

^d Institut Botànic de Barcelona, CSIC-Ajuntament de Barcelona, Barcelona, Spain

^e Division of Invertebrate Zoology, American Museum of Natural History, New York, USA

^f Instituto de Geociencias, Universidade Federal da Bahia, Salvador da Bahia, Brazil

^g National Museum of Natural History, Smithsonian Institution, Washington, D.C., USA

^h Department of Entomology, University of Maryland, MD, USA

ⁱ College of Life Sciences & Academy for Multidisciplinary Studies, Capital Normal University, Beijing, China

^j Department of Earth Sciences, University of Oxford, Oxford, UK

^k Department of Earth & Planetary Sciences, Northwestern University, Evanston, IL, USA

^l Senckenberg Forschungsinstitut und Naturmuseum, Frankfurt, Frankfurt am Main, Germany

^m Departamento de Biodiversidad, Ecología y Evolución, Facultad de Biología, Universidad Complutense, Madrid, Spain

ⁿ Natural Sciences Department, Faculty of Science II, Lebanese University, Fanar-El-Matin, Lebanon

^o State Key Laboratory of Palaeobiology and Stratigraphy, Nanjing Institute of Geology and Palaeontology, Chinese Academy of Sciences, Nanjing, China

^p Facultad de Ciencias Naturales, Universidad del Rosario, Bogotá, Colombia

^q State Key Laboratory of Biogeology and Environmental Geology, China University of Geosciences, Wuhan, China

^r National Museum, Prague, Czech Republic

^s Departament de Genètica, Microbiologia i Estadística, Facultat de Biologia, Universitat de Barcelona, Spain

^t Institut de Systématique, Évolution, Biodiversité (ISYEB), Muséum national d'Histoire naturelle, CNRS, Sorbonne Université, EPHE, Université des Antilles, CP50 Paris, France

^u School of Earth Sciences, University of Western Australia, Crawley, Australia

^v Departamento de Explotación y Prospección de Minas, Universidad de Oviedo, Oviedo, Spain

^w Departament de Biología Evolutiva, Ecología i Ciències Ambientals, Facultat de Biología, Universitat de Barcelona, Spain

^x Smithsonian Tropical Research Institute, Panama

^y Department of Biology, Institute of Biology and Biotechnology, University of Rzeszów, Poland

^z Museo de Ciencias Naturales de Álava, Vitoria-Gasteiz, and Cueva El Soplao, Celis, Cantabria, Spain

^{aa} Departamento de Geodinámica, Estratigrafía y Paleontología, Facultad de Ciencias Geológicas, Universidad Complutense de Madrid, Spain

^{ab} Departamento de Biología de Sistemas, Universidad de Alcalá, Alcalá de Henares, Spain

^{ac} Géosciences Rennes - UMR 6118, University of Rennes, CNRS, Rennes, France

^{ad} Institut de Ciència i Tecnologia Ambientals (ICTA), Universitat Autònoma de Barcelona, Spain

^{ae} Departamento de Biología, Facultad de Ciencias, Centro de Investigación en Biodiversidad y Cambio Global (CIBG-UAM), Universidad Autónoma de Madrid, Cantoblanco, Madrid, Spain

^{af} Oxford University Museum of Natural History, Oxford, UK

* Corresponding author at: Departament de Dinàmica de la Terra i de l'Oceà, Facultat de Ciències de la Terra, Universitat de Barcelona, Spain.

** Corresponding author.

E-mail addresses: xdelclos@ub.edu (X. Delclòs), e.penalver@igme.es (E. Peñalver).

¹ (X. Delclòs), (E. Peñalver). These contributed equally to this work.

ARTICLE INFO

Keywords:
Cretaceous
Amber
Resin
Mass resin production
Conifers

ABSTRACT

Amber is fossilized resin that preserves biological remains in exceptional detail, study of which has revolutionized understanding of past terrestrial organisms and habitats from the Early Cretaceous to the present day. Cretaceous amber outcrops are more abundant in the Northern Hemisphere and during an interval of about 54 million years, from the Barremian to the Campanian. The extensive resin production that generated this remarkable amber record may be attributed to the biology of coniferous resin producers, the growth of resiniferous forests in proximity to transitional sedimentary environments, and the dynamics of climate during the Cretaceous. Here we discuss the set of interrelated abiotic and biotic factors potentially involved in resin production during that time. We name this period of mass resin production by conifers during the late Mesozoic, fundamental as an archive of terrestrial life, the ‘Cretaceous Resinous Interval’ (CREI).

1. Introduction

Resins are secondary metabolites synthesized by specialized cells of “gymnosperm” and angiosperm plants, whose composition consists of amorphous mixtures of carboxylic acids, essential oils and isoprene-based hydrocarbons (Langenheim, 2003). Resin production is conditioned by temperature, solar radiation, evapotranspiration, and soil water deficit (Allen et al., 2010; Rodríguez-García et al., 2015). The primary functions of resins relate to defense against herbivores and pathogens, and as a healing mechanism, sealing wounds and vulnerable parts after damage caused by physical or biological agents (Langenheim, 2003; Seyfullah et al., 2018).

Resins can remain sticky from just hours to several months after being secreted, which can ensnare organisms or parts of them—known as bioinclusions—found mostly in the same ecosystem as the resin-producing plant (Solórzano Kraemer et al., 2018). The crosslinking of resin takes place over millions of years, resulting in gradual hardening, decrease in thermal denaturation, and loss of free methyl groups, all of which lead to a relatively inert, hardened form called amber (Langenheim, 1990; Anderson et al., 1992; McCoy et al., 2017; Solórzano-Kraemer et al., 2020). Only a few types of resins can fossilize based on their chemical composition (Anderson and Crelling, 1995; Langenheim, 2003).

Most amber deposits have yielded few or no bioinclusions. The reasons for this scarcity of bioinclusions are variable, but usually relate to the paucity of resin production during some periods of time (this paper), where the resin was produced (under aerial or underground conditions; Álvarez-Parra et al., 2021), and/or how long the resin retained its stickiness (Solórzano Kraemer et al., 2018). Amber-bearing outcrops that preserve bioinclusions are a type of Konservat-Lagerstätte. Indeed, the preservation of organisms in amber is exceptional and differs from other organic or inorganic mechanisms that retain organismic detail for millions of years (Martínez-Delclòs et al., 2004; Ross, 2009; Grimaldi and Ross, 2017). Despite taphonomic biases inherent in resin entrapment (Solórzano Kraemer et al., 2018), amber can provide exceptional external and internal anatomical detail of the bioinclusions and evidence of past animal behaviors (Labandeira, 2014a; Grimaldi, 2019). Amber deposits are typically parautochthonous-allochthonous, in which resin was dislodged by gravity, transported and concentrated by water, and accumulated in a primary or secondary location (Martínez-Delclòs et al., 2004). However, a few autochthonous-paraautochthonous deposits are known, in which resin experienced minimal to virtually no transport (Schmidt et al., 2012; Seyfullah et al., 2018; Álvarez-Parra et al., 2021).

Resin crosslinking, which begins once the resin is exuded by the plant, continues after burial in sealed, anoxic sediments (e.g., within or under layers of clay) that have little interaction with meteoric water (Martínez-Delclòs et al., 2004). Resin has almost the same density as freshwater but is buoyant in sea water or in freshwater with sediments in suspension and is therefore easily transported by flotation and concentrated by currents. For these reasons, transitional settings with large

accumulations of continental organic matter, such as deltas, estuaries, swamps or oxbow lakes, are the most favorable sedimentary environments for resin fossilization (Grimaldi et al., 2000b; Martínez-Delclòs et al., 2004; Iturrealde-Vinent and MacPhee, 2019). Resiniferous trees are often located on emergent topography within these transitional environments (Álvarez-Parra et al., 2021) or close to areas where resin primarily accumulated by low-energy transport, indicated by the preservation of fragile resin structures (Grimaldi et al., 2000b; Perrichot, 2005; Rust et al., 2010; Veltz et al., 2013). The association of amber-bearing deposits with coal (lignite) or other rocks rich in organic matter suggests episodes of inland environments flooded by marine transgression (Najarro et al., 2009; Rodríguez-López et al., 2020).

Although resin is exuded by different tissues and organs of plants, amber deposits—at least those from the Cretaceous and whose taphonomy has been addressed—were formed primarily by resin produced by root tissues that generally lack bioinclusions (root resin) and, more minorly, by the trunk, branches, or above-soil plant parts (aerial resin) (Langenheim, 1995; Álvarez-Parra et al., 2021), the latter of which has the potential to contain abundant bioinclusions. Although the oldest fossil resin dates from the late Carboniferous (Bray and Anderson, 2009), oldest amber with bioinclusions dates from the Late Triassic, which preserves a few minute arthropods (Schmidt et al., 2012; Sidorchuk et al., 2015). Jurassic amber is scarce and may be associated with the tropical-equatorial zone, since it has been found primarily in Thailand, Italy, and Lebanon; no macroscopic bioinclusions have been hitherto reported from this amber (Nohra et al., 2013; Neri et al., 2016). The oldest amber deposits rich in bioinclusions are Barremian in age (Early Cretaceous) (Maksoud et al., 2017).

The Cretaceous (~145.0–66.0 Ma) represents a time of rapid evolutionary turnover and diversification of organisms. From a macroecological perspective, it was a key period in Earth history in which the Angiosperm Terrestrial Revolution (ca. 100 to 50 Ma), inclusive of the formerly defined Cretaceous Terrestrial Revolution (Lloyd et al., 2008; Benton et al., 2022), occurred. During this time, the Mesophytic paleobiome dominated by “gymnosperms” was replaced by a Cenophytic paleobiome dominated by angiosperms (Labandeira, 2014b; McElwain, 2018; Birks, 2020; Condamine et al., 2020). This turnover altered the base of trophic networks within continental ecosystems (Labandeira, 2014b), substantially modifying communities of herbivores (Labandeira, 2007; Kerfoot et al., 2014) and, therefore, affecting the composition and evolution of continental biotas (Meredith et al., 2011; McKenna et al., 2015; Peris et al., 2017; Benson et al., 2021; Peris and Condamine, 2023).

The climate of the Cretaceous was warmer and more humid than that of today, probably due to very active, sustained volcanism associated with unusually extensive seafloor spreading that elevated atmospheric CO₂ and O₂ values (Royer et al., 2004; Poulsen and Zhou, 2013). During most of the Cretaceous, polar regions were virtually devoid of ice (Scotese, 2021) and continental land masses were largely occupied by forests dominated by conifers (Hay and Floegel, 2012; Peralta-Medina and Falcon-Lang, 2012), thereby significantly reducing albedo. The

decrease in latitudinal desert belts during the Early Cretaceous and long-lasting humid conditions during the Late Cretaceous were driven by the breakup of Pangea (Chaboureau et al., 2014; Landwehrs et al., 2021).

Cretaceous amber-bearing deposits, at least those currently documented, have a limited temporal and geographical distribution (Martínez-Delclòs et al., 2004; Labandeira, 2014a). They are known from the Valanginian to the Maastrichtian, but they are particularly abundant and significant from the Barremian to the Campanian (these ages ranging from 125.77 to ~72.1 Ma at present), and, although numerous and widely distributed, occur predominately in the Northern Hemisphere, which may reflect present-day sampling biases (Fig. 1A). Several Cretaceous amber-bearing deposits yield abundant amber and bio-inclusions (Martínez-Delclòs et al., 2004; Penney, 2010; Seyfullah et al., 2018). The most studied fossiliferous amber-bearing outcrops from the Cretaceous are found in Lebanon (Barremian), Congo (Aptian), Spain (Albian), France (Cenomanian), Myanmar (Cenomanian), New Jersey in the USA (Turonian), Taimyr in Russia (Santonian) and western Canada (Campanian). In addition to these localities, amber (with or without bioinclusions) has been reported from Cretaceous deposits in many other regions worldwide (Fig. 2; Supplementary data A).

Molecularly analyzed amber, Pleistocene and Holocene copals, and Defaunation resin (produced after the beginning of the Industrial Revolution, see Solórzano-Kraemer et al., 2020) are valuable tools for interpreting the botanical origin of amber (McCoy et al., 2017, 2021).

However, the identity of Cretaceous resin-producing plants remains unknown in most cases. The taxonomic affinities of Cretaceous trees that produced abundant resin remain elusive for a variety of reasons, which include extensive chemical variation observed in the composition of Cretaceous amber samples (Menor-Salván et al., 2016; McCoy et al., 2021), molecular convergence (Bray and Anderson, 2009), and the usually scarce record of plant remains in amber as bioinclusions (Kvaček et al., 2018; Moreau et al., 2020). Nevertheless, geochemical studies have ruled out angiosperms as resin-producing plants during the Cretaceous (Anderson et al., 1992; Lambert et al., 1996; Menor-Salván et al., 2016), with a few minor exceptions (Grimaldi et al., 2000a). Most likely, angiosperms did not acquire the ability to produce resin in sufficient quantities to form amber-bearing deposits until the Early Eocene (Jossang et al., 2008). As for “gymnosperms”, the coniferous tree families of Araucariaceae, Cheirolepidiaceae†, Cupressaceae s.l., Podocarpaceae, and Pinaceae were widely distributed during the Cretaceous (Peralta-Medina and Falcon-Lang, 2012) (Fig. 2) and have been identified as likely resin sources of Cretaceous amber deposits (Azar et al., 2010; Peñalver and Delclòs, 2010; Perrichot et al., 2010; Nohra et al., 2014; Menor-Salván et al., 2016; McCoy et al., 2021) (Supplementary data B). The Erdtmanithecales†, a group of non-coniferous “gymnosperms” related to the Gnetales or the Bennettitales†, and namely known for their pollen, have been suggested as possible producers of resin that generated amber deposits in the Aptian of Brazil (Seyfullah et al., 2020).

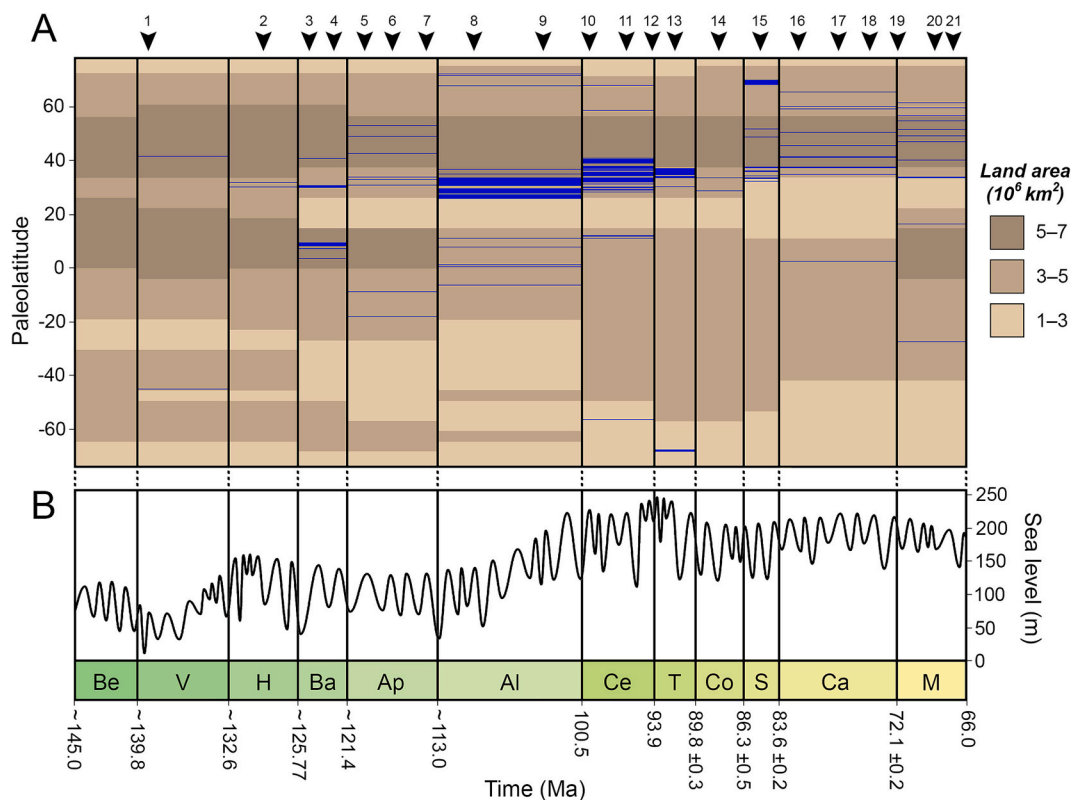


Fig. 1. Paleolatitudinal distribution of 239 Cretaceous amber-bearing deposits, grouped by geological age (A) and sea level changes (B) throughout the Cretaceous. Amber-bearing deposit data are provided in Supplementary data A. Amber deposits represented by thin blue stripes of the same thickness; deposits within the same age box and close in paleolatitude appear as stripes of greater thickness due to superposition. Proportion of area occupied by land indicated in shades of brown (modified from Landwehrs et al., 2021; Fig. 3). Representative amber deposits: 1- Hastings (UK); 2- Golling (Austria); 3- Isle of Wight (UK); 4- Twenty-nine localities in Lebanon, Zarzar Lake (Syria); 5- Chōshi (Japan); 6- Doumanga (Congo); 7- Araripe (Brazil); 8- Aríño (Spain), Hkamti (Myanmar), Estoril (Portugal), Archidona (Ecuador); 9- Eleven localities in Spain, Salignac-Eyvigues (France), Wadi Zerqa (Jordan); 10- Six localities in France, Kachin (Myanmar); 11- Nizhnyaya Agapa (Russia), Agdzakhend (Azerbaijan); 12- Chatham Island (New Zealand); 13- Sayreville in New Jersey (USA), La Garnache (France); 14- Shavarshavan (Armenia); 15- Five localities in Taymyr (Russia), Kuji (Japan), Piolenc (France); 16- Ajka (Hungary), Eutaw Fm. in Alabama (USA), Tuna-1 (Australia); 17- Cedar Lake, Grassy Lake (and other localities, Canada); 18- Tilin amber (Myanmar); 19- Arctic Coastal Plain in Alaska (USA); 20- Hanna Basin in Wyoming (USA); 21- Hell Creek Fm. in South Dakota (USA). Eustatic sea-level changes modified from Ray et al. (2019) and after Haq (2014). Geological Timetable based in the International Commission on Stratigraphy (v 2023/06), <https://stratigraphy.org/chart>. (For interpretation of the references to color in this figure legend, the reader is referred to the web version of this article.)

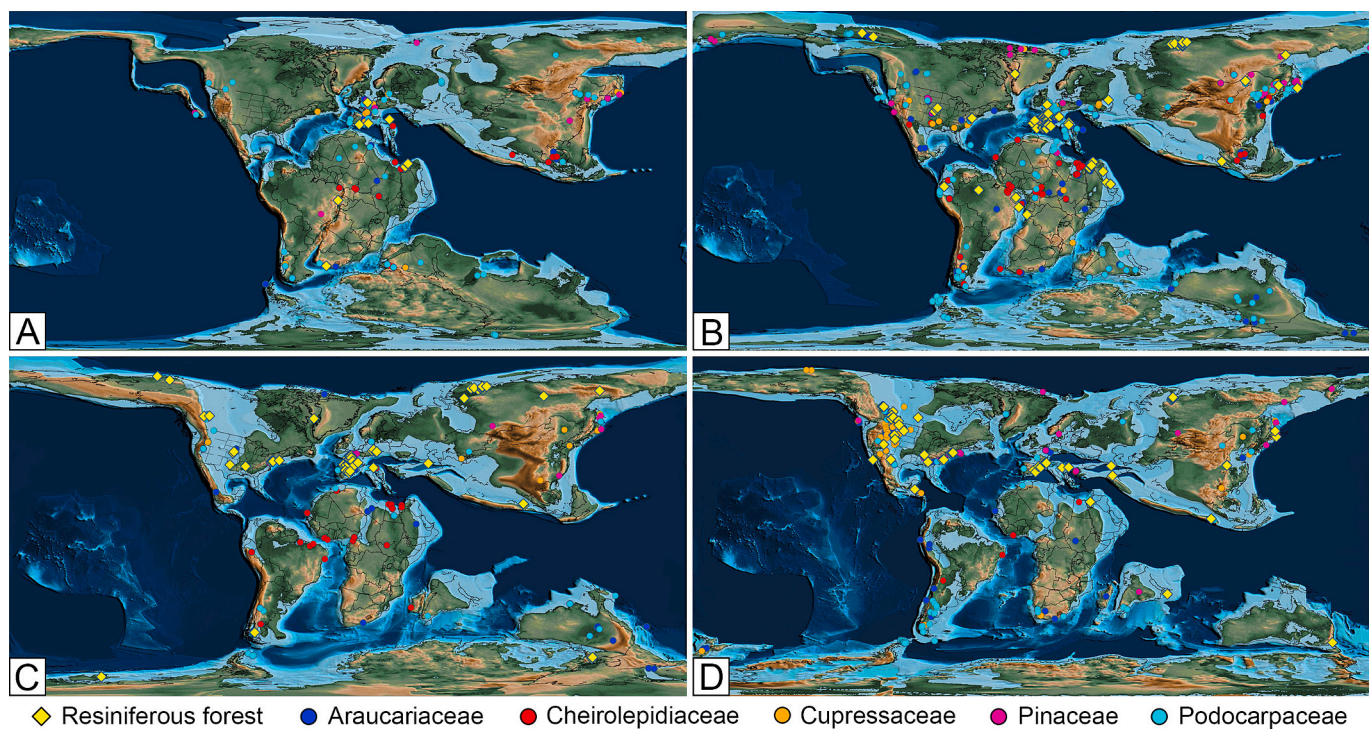


Fig. 2. Distribution of resiniferous forests based on known amber-bearing localities and known occurrences of potential coniferous resin-producing tree families throughout the Cretaceous: Araucariaceae, Cheirolepidiaceae†, Cupressaceae, Pinaceae, and Podocarpaceae. The dataset/sources related to the paleobotanical groups used to construct this figure is formed by Supplementary data B (data from Peralta-Medina and Falcon-Lang (2012) and our own bibliographic search) and data downloaded from Paleobiology Database (<https://paleobiodb.org>). A) Berriasian–Hauterivian; B) Barremian–Albian; C) Cenomanian–Turonian; D) Coniacian–Maastrichtian. Paleogeographic maps obtained from Scotese et al. (2021). The present-day spatial coordinates and ages from a total of 299 Cretaceous amber outcrops and 1252 paleobotanical records were obtained from a bibliographic survey (Supplementary data A and B, respectively). Present coordinates of amber outcrops and paleobotanic occurrences were rotated to paleocoordinates using R v.4.0.4 and GPlates v.2.2.0. Map visualization and imaging was made using QGIS v.3.22.3 software. (For interpretation of the references to color in this figure legend, the reader is referred to the web version of this article.)

Actuotaphonomic studies (Peñalver et al., 2018), plant bioinclusions (Kvaček et al., 2018; Moreau et al., 2020) (Fig. 3A–B), and examination of wood logs and cone scales with embedded amber in amber-rich levels (Perrichot, 2005; Mays et al., 2019) provide important evidence for determining specific conifer taxa involved in resin mass production during the Cretaceous. Although modern Pinaceae resin is poorly crosslinked due to its molecular composition, a few moderate-size amber deposits resulting from this resin have been found (Bray and Anderson, 2008; Menor-Salván et al., 2016). Cretaceous Cupressaceae produced resin but generally in small amounts (e.g. Otto et al., 2000). Cheirolepidiaceae† conifers lack resiniferous structures, except for some taxa presenting traumatic resin canals (Bodnar et al., 2013; Rombola et al., 2022).

In this contribution, we define and outline the Cretaceous Resinous Interval (CREI) by integrating diverse lines of evidence and analyzing the set of interrelated abiotic and biotic factors that characterized this interval. The data presented herein was compiled from the literature and our own fieldwork in Cretaceous amber localities from Lebanon, Jordan, Congo, Ecuador, Spain, France, Myanmar, USA, and New Zealand; Cenozoic amber localities from France, Mexico, Dominican Republic, New Zealand, India, China, and Ethiopia; and copal and Defaunation resin deposits from Colombia, Dominican Republic, New Caledonia, New Zealand, and Madagascar. In the latter three regions, our fieldwork focused on actuotaphonomic processes aimed at understanding the conditions of production and conservation of Defaunation resin and the formation of copal deposits.

The materials figured in this work are housed at the El Soplao Cave amber collection, Spain (Figs. 3A, E, 5C), the University of Barcelona, Spain (Figs. 3B, 5D), the Nanjing Institute of Geology and Palaeontology, China (Fig. 5A), and the Museu de Ciències Naturals de Barcelona, Spain

(Fig. 5B). Photographs and data used in the figures are our own when not specified in the captions.

2. Definition of the Cretaceous Resinous Interval

We define the Cretaceous Resinous Interval (CREI) as *global mass resin production and burial interval that occurred from the Barremian to the Campanian stages of the Cretaceous Period*. We posit that, during a relatively continuous time interval of about 54 million years, a suite of factors led to the formation of rich amber deposits with similar characteristics and of wide geographic distribution (Figs. 1, 2). This time-delimited interval is based on the known geological record, which provides evidence of numerous amber-bearing deposits (Supplementary data A) from the Barremian (Early Cretaceous), namely those from Lebanon (Maksoud et al., 2022), to the Campanian (Late Cretaceous), particularly Canadian (McKellar et al., 2008) and Tulin in Myanmar (Zheng et al., 2018) ambers. Most of these amber deposits occur in the Northern Hemisphere, between 5° and 75° N paleolatitude, and are especially abundant in low to mid latitudes from the Barremian to Coniacian and in mid to high latitudes from the Santonian to the Campanian (Fig. 1A). Some Cretaceous amber-bearing deposits are found in the Southern Hemisphere between the Aptian–Turonian, but they are scarce (Fig. 1A). Cenozoic amber deposits first appear during the Mid Paleocene of Wyoming, USA (~61 Ma) and Late Paleocene of Alaska, USA (~57 Ma) (Grimaldi et al., 2000a, 2018), and the Eocene of Oise, France (~53 Ma), Fushun, China (53–50 Ma) and Cambay, India (~52–50 Ma) (Jossang et al., 2008; Rust et al., 2010; Wang et al., 2014a).

There are five primary shared characteristics among amber deposits formed during the CREI. First, resin production was restricted to conifers

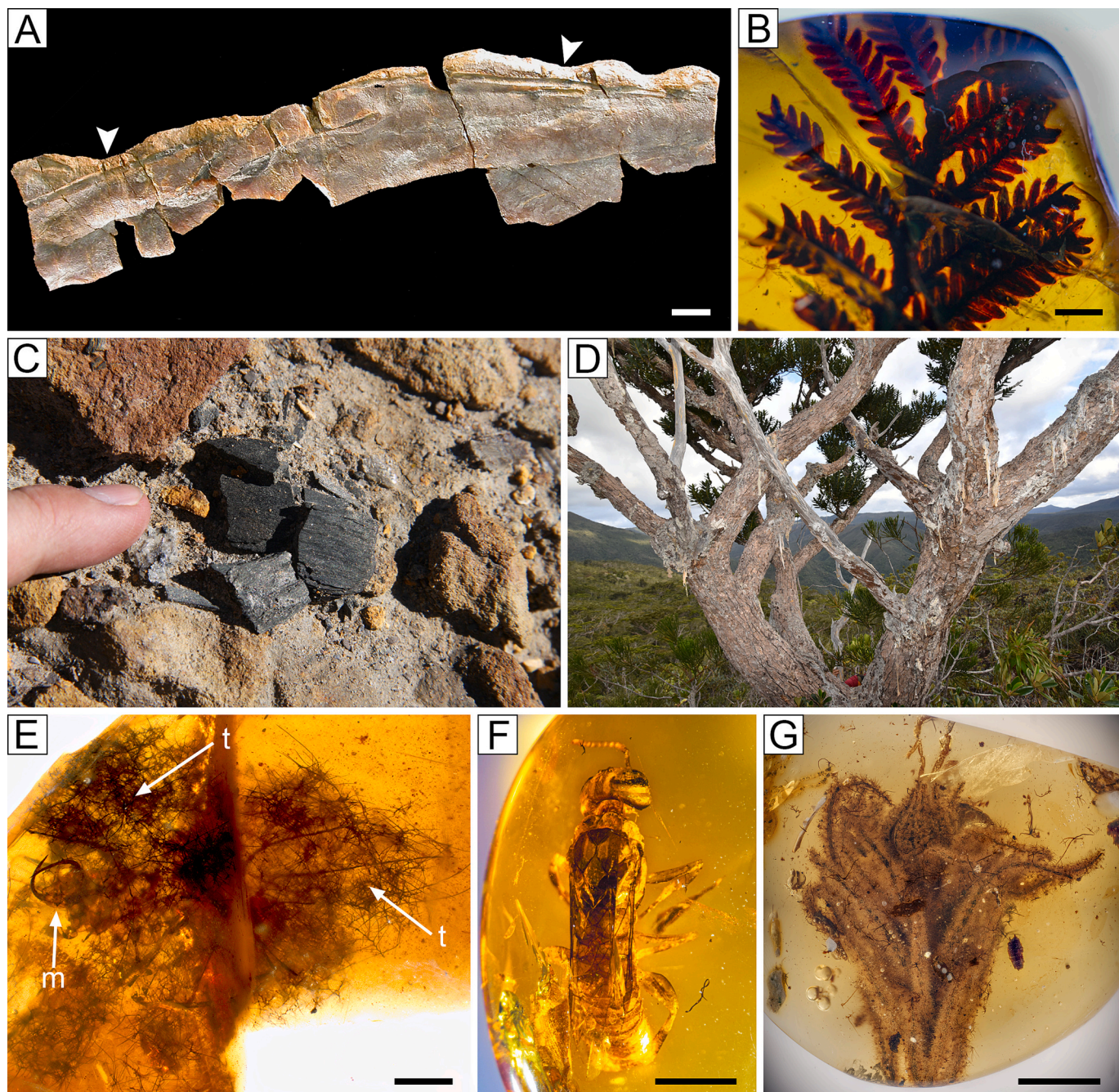


Fig. 3. Mass resin tree producers and development of fires during the Cretaceous. A) Aerial amber piece with surface imprints and bioinclusions of *Frenelopsis* (Cheirolepidiaceae†) axes, from the Albian of El Soplao (Spain); based on taphonomic studies, the largest number of plant bioinclusions corresponds to this resin-producing tree (Penalver et al., 2018); B) One of the most abundant plant remains in the Cenomanian amber of Kachin (Myanmar) are axes with leaves of araucariaceans (Poinar et al., 2007) (University of Barcelona); C) Charcoal from the Albian amber-bearing outcrop of San Just, level SJ2 (Spain), commonly found in amber-bearing levels (Peñalver and Delclòs, 2010); D) *Agathis ovata* from Col de Yaté, New Caledonia, producing copious quantities of resin in an area burned several years ago; E) The immature insect related to green lacewings, *Hallucinochrysa diogenesi* (Neuroptera: Chrysopoidea), from the Albian amber of El Soplao (Spain), preserved with a debris-carrying packet of trichomes with gleicheniaceous affinity; today, gleicheniaceous ferns opportunistically colonize burned areas (Pérez-de la Fuente et al., 2012); F) *Orthosyntexys elegans*, a wasp from the relict family Anaxyelidae (Hymenoptera: Symphyta) from the Cenomanian amber of Kachin, Myanmar; the living representatives of this family lay eggs in the sapwood of conifers, preferring recently burned wood (Gao et al., 2021), photograph courtesy of T. Gao; G) *Eophysilica priscastellata*, an angiosperm flower of the family Rhamnaceae from the Cenomanian amber of Kachin (Myanmar) showing morphological specializations identical to those of modern relatives adapted to recurrent wildfires (Shi et al., 2022); photograph courtesy of C. Shi and R. Spicer. Abbreviations: m = mandibulo-maxillary stylets (feeding structures), t = trichomes. Scale bars = 2 mm (B, F), 1 mm (E, G), 0.5 mm (A). (For interpretation of the references to color in this figure legend, the reader is referred to the web version of this article.)

(Araucariaceae, Cheirolepidiaceae†, Cupressaceae s.l., Podocarpaceae, and Pinaceae) (Langenheim, 2003; Menor-Salván et al., 2010; Seyfullah et al., 2018). Second, charcoal, resulting from plant material charred by wildfires, is commonly found in the same stratigraphic level as amber,

particularly in the Northern Hemisphere (Brown et al., 2012; Tappert et al., 2013; Supplementary data C) (Fig. 3C). Third, when bioinclusions are preserved, they correspond to similar fauna and flora under comparable biases (Penney, 2010; Solórzano Kraemer et al., 2018), although

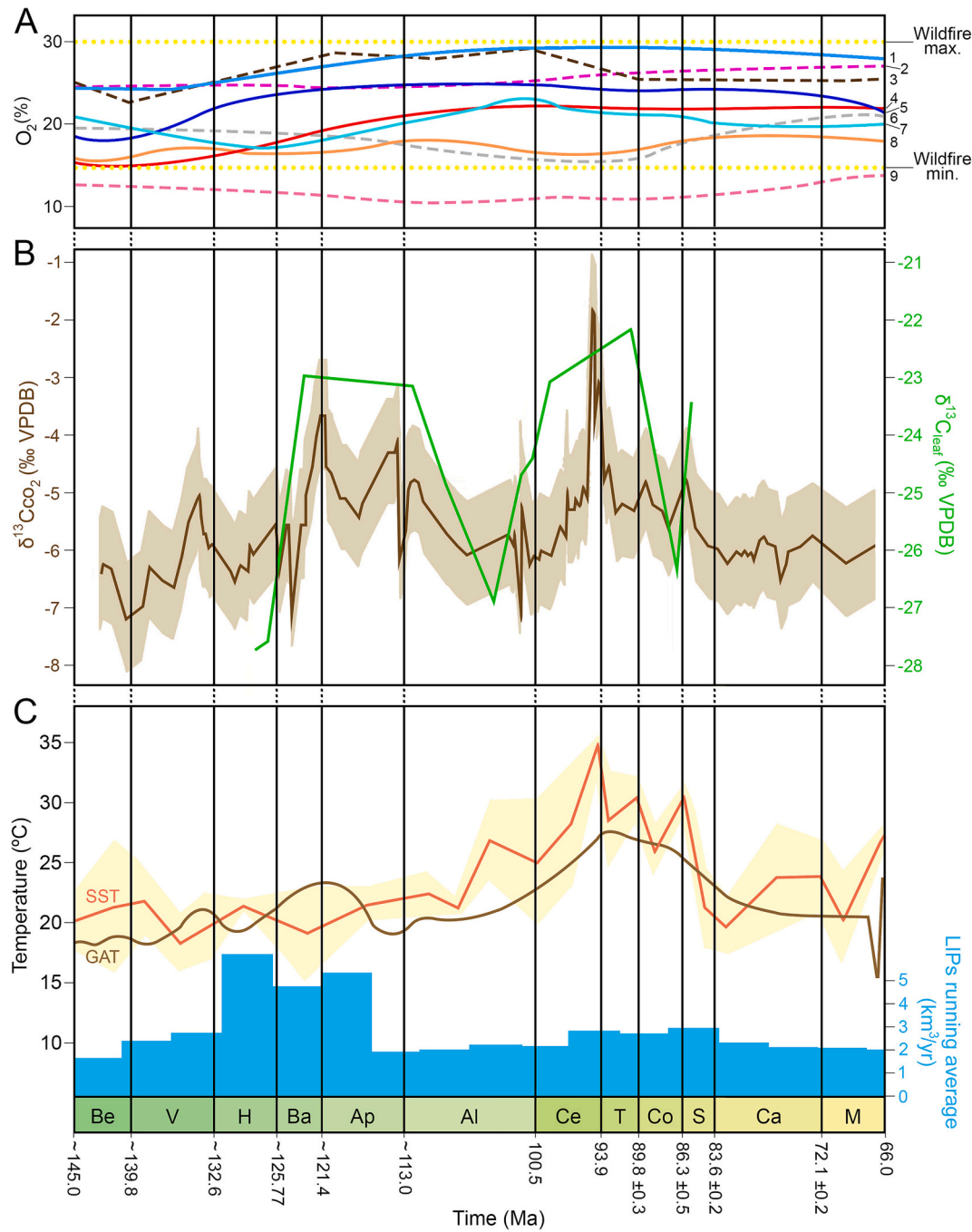


Fig. 4. Oxygen (O_2) and carbon dioxide (CO_2) atmospheric composition, temperature, and Large Igneous Province (LIP) activity throughout the Cretaceous. A) Reconstruction for Cretaceous atmospheric O_2 mixing ratio (from Mills et al., 2016). Forward models of O_2 based on nutrient/weathering (1, 5, 7), including isotope mass balance models (4, 8) and “proxy inversion” methods that estimate atmospheric oxygen by reference to geochemical data, assuming relationships between O_2 concentration and either fossil charcoal abundance (3), carbon-to-phosphorus ratios in sediments (6), carbon isotope composition of plant resins (9), or combined estimates for sedimentation rate and abundance of organic carbon and pyrite in rock samples (2). Also represented: wildfire minimum (for ignition) and maximum (in the Phanerozoic, Carboniferous–Permian). References used: 1- Bergman et al. (2004), 2- Berner and Canfield (1989), 3- Glasspool and Scott (2010), 4- Berner (2009), 5- Arvidson et al. (2013), 6- Algeo and Ingall (2007), 7- Hansen and Wallman (2003), 8- Falkowski et al. (2005), 9- Tappert et al. (2013); B) Comparison of the carbon isotope composition of leaves of the Cheirolepidiaceae† conifer *Frenelopsis* ($\delta^{13}C_{leaf}$, in green) with the evolution of the carbon isotope composition of atmospheric CO_2 ($\delta^{13}C_{CO_2}$, in brown), from Barral et al. (2017). The *Frenelopsis* samples from the upper Barremian–lower Santonian interval come from amber outcrops; C) Reconstructed Cretaceous Sea Surface Temperature (SST) (from Martin et al., 2014 in Barral et al., 2017), Global Average Temperature (GAT) (from Scotece et al., 2021) and LIP running average every 5 Ma (from Eldholm and Coffin, 2000). Geological Timetable based in the International Commission on Stratigraphy (v 2023/06), <https://stratigraphy.org/chart>. (For interpretation of the references to color in this figure legend, the reader is referred to the web version of this article.)

often bioinclusions are absent likely due to taphonomic reasons. Fourth, resin accumulation occurred in transitional sedimentary environments under subtropical and temperate paleoclimates. And fifth, resin accumulation coincides with the maximum regressive surface (or transgressive surface) (Bowen and Jux, 1987; Villagómez et al., 1996; Najarro et al., 2009) (Fig. 1B). Spatially, the CREI appears to be global in nature, since amber-bearing outcrops are distributed worldwide throughout the Cretaceous, although they are particularly concentrated in Laurasia and the northern margin of Gondwana (Figs. 1, 2). In any case, we use the term ‘global’ in its broader sense as we posit that the CREI did not necessarily take place in both hemispheres simultaneously throughout the entire interval.

3. Conditional factors on resin production and preservation

Two basic conditions need to co-occur in time and space to generate an accumulation of resin with the potential to become an amber-bearing deposit. First, there needs to exist resin-producing plants with the capacity to secrete large amounts of resin. Second, there needs to be a suitable sedimentary setting, namely a transitional environment that buries resin under anoxic conditions. Known Cretaceous amber-bearing deposits are restricted geographically despite the worldwide distribution of resin-producing conifers during various Cretaceous stages (Fig. 2). Consequently, potential lack of suitable depositional environments for the accumulation and preservation of resin may have limited the distribution of amber-bearing deposits. However, transitional sedimentary environments during major marine transgressions were equally probable anywhere on Earth’s surface, and have occurred cyclically throughout time (Haq, 2014). Thus, the two conditions noted above may not fully explain the observed distribution of Cretaceous amber-bearing deposits, such that other abiotic or biotic factors, and the confluence of several factors, likely promoted the production of resin by trees and/or its subsequent accumulation and preservation. These factors could be global or more localized in spatial scale and are not necessarily mutually exclusive.

3.1. Abiotic factors

Multiple abiotic factors were potentially related to the mass production and/or accumulation of resin during the CREI. Although these factors are interrelated and feedback on each other, we group them here to facilitate discussion: (1) atmospheric gas composition, temperature, and wildfires; (2) volcanism and changes in sea level; and (3) oceanic physicochemical properties and hurricanes. An overview of the global climate throughout the CREI is provided at the end of this section.

3.1.1. Atmospheric gas composition, temperature, and wildfires

Atmospheric gas composition (Fig. 4A–B) has a major effect on climate. Atmospheric greenhouse gases such as carbon dioxide (CO_2) and methane (CH_4), as well as oxygen (O_2) may have directly or indirectly impacted global resin production. Estimates of atmospheric CO_2 concentration during the Cretaceous vary according to the authors and proxies used (Tappert et al., 2013; Landwehrs et al., 2021) but generally is considered to have been more than twice that of preindustrial values, between 560 and 1680 ppm (Barrial et al., 2017).

High CO_2 levels are due to extensive volcanic emissions during the Cretaceous from Large Igneous Provinces (LIPs, Fig. 4C) and seafloor formation (Condé et al., 2021). Wildfires, changes in ocean chemistry, biotic respiration, and organic matter decomposition also released significant amounts of CO_2 to the atmosphere during the Cretaceous (Hu et al., 2012; Wang et al., 2014b; Scott, 2018). Methane has a greater greenhouse potential than CO_2 , and is likely to have notably increased during the Cretaceous (Jahren et al., 2001; Chang et al., 2022). Higher CH_4 levels were related to the liberation of methane hydrate from the seafloor by rising water temperatures (Wagner et al., 2007) and from seafloor spreading. Global temperatures fluctuated during the

Cretaceous (Holz, 2015; Landwehrs et al., 2021) (Fig. 4C), with generally elevated temperatures and reduced latitudinal temperature gradients between the equator and the poles of $\leq 35^\circ \text{C}$ mean annual temperature (MAT) in both hemispheres (O’Brien et al., 2017; Huber et al., 2018) compared with current values. The Northern Hemisphere thermal gradient showed a ca. 5°C decrease from the Late Jurassic into the Late Cretaceous due to increased CO_2 and associated warming, while in the Southern Hemisphere the temperature gradient increased during this time due to the migration of Antarctica towards the South Pole (Landwehrs et al., 2021). Higher temperatures also brought more extreme atmospheric precipitation regimes and the establishment of more extensive regions under arid or monsoonal climates (Hasegawa et al., 2012), although the latter would have been influenced more by palaeogeography than by atmospheric gas concentration (Farnsworth et al., 2019).

Continental precipitation during the mid-Cretaceous was roughly mirrored between the Northern and Southern Hemispheres according to coupled ocean-atmosphere general circulation simulations, with maximum precipitation at the equator that decreased steeply to a minimum around 30° paleolatitude, which then increased again to a peak at around 50° paleolatitude (Zhou et al., 2012). This pattern situates the bulk of Cretaceous amber deposits with bioinclusions (particularly during the mid-Cretaceous) (Fig. 1A) in areas of moderate to relatively low average rainfall. Remarkably, the occurrence of the first significant Triassic amber deposits with inclusions in northern Italy coincides with the Carnian Pluvial Episode, associated with an important evolutionary radiation of “gymnosperms” (Roghi et al., 2022).

The increase in atmospheric CO_2 below the RuBisCo (the enzyme ribulose-1,5-bisphosphate carboxylase/oxygenase, involved in the first major step of carbon fixation) saturation limit accelerates plant photosynthesis and growth under present conditions (Dalling et al., 2016; Olivoto et al., 2017). In principle, such acceleration would suggest that increasing atmospheric CO_2 could result in higher metabolic rates and thus increased production of secondary metabolites, such as resin (Trapp and Croteau, 2001; Novick et al., 2012). However, related plant species may show opposite responses to CO_2 changes due to differences in physiological plasticity (Berini et al., 2018; Kurepin et al., 2018), thereby limiting the ability to infer resin production by fossil plant species based on CO_2 concentration alone. Even so, CO_2 and O_2 values might be indirectly linked with resin production, as elevated levels would be expected to impact the physiological features of plants that, in turn, could increase the herbivorous, wood-boring or pathogenic activity of other organisms such as arthropods or fungi (Lake and Wade, 2009; Labandeira, 2013; Couture et al., 2015; see section 3.2 below).

Numerous proxies suggest that atmospheric O_2 increased continuously from the Barremian to the late Cenomanian (Fig. 4A) to about 29%–31% (Berner, 2006; Glasspool and Scott, 2010; Brown et al., 2012), but decreased from the Turonian to the end of the Paleocene to the current value of 21% (Wade et al., 2019). The high O_2 content in the atmosphere during the Cretaceous favored recurrent wildfires in coniferous forests (Belcher and McElwain, 2008), which were also promoted by increased electrical storms and intensive volcanism (Scott, 2018). Charcoal is indicative of paleowildfires (Brown et al., 2012; Scott, 2018) and is abundant in most Cretaceous amber-bearing deposits (Peñalver and Delclòs, 2010; Shi et al., 2012; De Lima et al., 2019) (Fig. 3C), but mainly in the Northern Hemisphere deposits (Supplementary data C), including the presence of charcoaled remains within amber (Grimaldi et al., 2000b; Najarro et al., 2010). Partially burned amber pieces have been found occasionally together with charcoaled plant material (Grimaldi et al., 2000b).

Extant trees increase resin exudation if injured by fire (Fig. 3D) as a physiological response that prevents pathogenic activity or arthropod invasion (Langenheim, 2003; Della Prasetya et al., 2017). Fire has played a key role in reshaping ecosystems, particularly after the accumulation of flammable biomass arising from increased productivity of terrestrial ecosystems linked to the predominance of angiosperms (Bond

and Scott, 2010) and from the altered ignitability and flammability of angiospermous plant matter (Belcher and Hudspith, 2017). Different groups of Cretaceous conifers exhibit pyrophilous modifications linked to recurrent wildfires (He et al., 2016), in lifestyles such as serotiny that has endured into the present (Pausas, 2018). Moreover, there are diverse instances of organisms associated with fire that are preserved in Cretaceous ambers (Ortega-Blanco et al., 2008; Pérez-de la Fuente et al., 2012; Shi et al., 2022) (Fig. 3E–G).

The above lines of evidence suggest wildfires played a role in the genesis of resin deposits during the CREI, at least in some deposits, by favoring resin exudation but also subsequent accumulation, since deforested soils experienced increased erosion. However, based on the global occurrence of wildfires (Brown et al., 2012; Scott, 2018; Supplementary data C) and the broad distribution of potential resiniferous plants during the CREI (Fig. 2; Supplementary data B), a global distribution of Cretaceous amber deposits would be expected, for which there is currently no evidence (Fig. 2). Wildfires were globally distributed but seems only involved in local and regional resin production and accumulation during the CREI (e.g., the Raritan Fm. amber in New Jersey, USA or Spanish and French ambers), but appear not to be a definitive cause of resin production on a global scale.

3.1.2. Volcanism and changes in sea level

The abundant record of volcanic rocks associated directly or laterally with Cretaceous amber-bearing deposits such as those in Lebanon (Veltz et al., 2013), Myanmar (Shi et al., 2012), Ecuador (Balseca et al., 1993), and Canada (Eberth, 2005) is evidence that resin mass production took place in environments amid local volcanic influence, with this factor intimately related to wildfires (see above). Aside from increasing atmospheric O₂ concentrations that promoted wildfires, large amounts of volcanic emissions over a long period of time in LIPs could have affected global climate in other ways (Johansson et al., 2018; Macdonald et al., 2018). The maximum development of LIPs during the last 2500 million years occurred during the Cretaceous (Eldholm and Coffin, 2000; Condie et al., 2021). This peak of LIP development (Fig. 4C) altered atmospheric composition and circulation patterns and changed the geometry of sedimentary basins and sea level. The formation of LIPs and seafloor spreading, in combination with increased global MATs, led to the melting of polar ice caps (Zhou et al., 2008; Hay, 2017) and to significant reductions in the Earth's albedo (Kent and Muttoni, 2022) during the Cretaceous. These changes produced a global marine transgression trend (Fig. 1C) from the Valanginian to the Turonian (Wagreich et al., 2020). This global transgression was only interrupted by a regression at the Aptian–Albian boundary, after global MATs (Haq, 2014) fell to 12 °C (Hay, 2017). Maximum transgression was reached in the Turonian and sea level remained at high stands into the Campanian (Olde et al., 2015). All resin-bearing deposits were developed in periods of maximum regression, onlapped by the second-order marine transgressive strata (Grimaldi et al., 2000b; Perrichot, 2005; Najarro et al., 2009) (Fig. 1C).

The globally-high sea level during the CREI increased insularization, changing the extent and distribution of land masses and epicontinental seas such as the Late Cretaceous European archipelago, and the Mid-continental Seaway of North America. Extensive regions were flooded, which produced the remobilization of abundant resin stored in the soils due to erosion resulting from the transgressions, establishing new areas of shallow deposition, reducing terrestrial biotopes, and increasing flooding stress (Erwin, 2009). Marine transgressions have been associated with higher global temperature and paleogeographic changes, both of which caused more emergent land masses at mid to high latitudes in the Northern Hemisphere (Landwehrs et al., 2021), which potentially allowed for more colonization by plants and distribution of coniferous forest (Klages et al., 2020). This pattern contrasts with what occurred in the Southern Hemisphere during the Cretaceous, wherein the proportion of emerged land masses at mid to high latitudes remained low, similar in extent to that of the present day (Figs. 1, 2).

3.1.3. Oceanic physicochemical properties and hurricanes

Amber-bearing deposits are frequently associated with transitional sea-to-land environments. Thus, the properties of ocean waters, namely salinity and sea surface temperature (SST), and paleocirculation patterns may have affected the formation of resin deposit. Salinity may have controlled the formation of resin deposits because resin has a lower density than seawater, rendering it buoyant and making its burial and preservation in environments with high salinity difficult. High salinity conditions did occur in regions where amber-bearing deposits are found in the Northern Hemisphere, such as Myanmar and New Jersey of the USA (Poulsen et al., 1998; Ladant et al., 2020; Topper et al., 2011), and Brazil and the Congo in the Southern Hemisphere (Pérez-Díaz and Eagles, 2017). However, the formation of resin deposits in high salinity zones suggest only temporary marine influence. The record of frequent, yet rarely diverse, marine protists and invertebrates, such as oysters or crinoids, and plant macroremains in amber deposits (Néraudeau et al., 2008; Barrón et al., 2015; Peyrot et al., 2019) supports a transitional depositional setting with occasional marine influence.

Global average SST during the mid-Cretaceous was >6 °C higher than that of today (Hay, 2009; Torsvik and Cocks, 2016), but disparate data exist regarding SSTs throughout the entire Cretaceous (Hay and Floegel, 2012) (Fig. 4C). Global ocean circulation changed significantly during the Cretaceous due to progressive opening of the South Atlantic Ocean and the Tethyan Circumglobal Current, providing east to west flow around the globe at low latitudes of the Northern Hemisphere. In addition, the transfer of heat from the hydrosphere to the atmosphere from water vapor played an important role in cooling the tropics and in warming at high latitudes, establishing the diminished latitudinal gradient of temperature noted earlier. These factors conditioned global temperature and climate during the CREI (Hay, 2009; Wohlwend et al., 2015), and thus may have indirectly impacted resin formation and/or accumulation.

Linked to high average SST during the Cretaceous (O'Brien et al., 2017), heavy rainfall and winds, such as those during hurricanes, have been proposed as an abiotic cause of resin production. High winds can cause severe damage to trees, which is sealed by resin to minimize opportunistic insect attacks or pathogenic infections (Langenheim, 1994; Seyfullah et al., 2018). Climate models based on marine and continental distribution and topography suggest winds were generally weaker during the Cretaceous than at present (Cousin-Rittimard et al., 2002; Hay, 2009), but the consistently high annual SST could have promoted the development of hurricanes in low to mid latitudes. The absence of high topographic relief (Hay et al., 2019) would have allowed the wind to circulate without diverting its zonal flow (Scotese et al., 2021).

3.1.4. Climatic overview throughout the CREI

Based on paleoclimate data and maps (Chumakov et al., 1995), most Cretaceous amber-bearing deposits originated in the northern mid-latitude warm humid belt. Nevertheless, during the Albian and Santonian, some amber-bearing localities were present well within the northern high-latitude temperate humid belt, and during the Albian and Cenomanian other amber-bearing localities were present within the equatorial humid belt and northern hot arid belt, respectively. Based on global circulation models, the depositional environments that gave rise to amber-bearing deposits in Lebanon (Barremian) were located within the tropical climate belt (Sewall et al., 2007; Ohba and Ueda, 2010). During the lower to middle Aptian, the climate cooled globally (Mutterlose et al., 2010), which coincides with a reduction in currently known amber deposits, although this cold interval was recently questioned (Huber and O'Brien, 2020).

At the Aptian–Albian boundary, warm greenhouse conditions were re-established due to intense volcanism, coinciding with amber deposits in Brazil, Ecuador, and the Congo at low latitudes in the Southern Hemisphere (Pereira et al., 2009; Cadena et al., 2018; Bouju and Perrichot, 2020). During the Albian, an extensive subtropical arid belt

developed in the equatorial zone, which subsequently migrated poleward (Scotese, 2021). Abundant resin accumulations were common in tropical mid latitude areas, such as Iberia, leading to the present-day Spanish amber deposits (Peñalver and Delclòs, 2010).

During the Cenomanian–Turonian, climate zones began to organize latitudinally (Sewall et al., 2007), although still under hothouse conditions (Kidder and Worsley, 2010; Mills et al., 2017), enabling the tropical biota to migrate poleward of 40°N latitude. Although currently there are important forests of conifers in very high latitudes (Fig. 2), resin deposits were formed at that time mostly between 30° and 40°N latitude, with some exceptions at higher latitudes (Fig. 1), corresponding to a MAT of around 30 °C (Hay and Floegel, 2012); these conditions may have produced the resin corresponding to amber-bearing deposits from the lower Cenomanian of France (Perrichot et al., 2010), Myanmar (Ross et al., 2010), and from the Turonian of New Jersey in the USA (Grimaldi and Nascimbene, 2010).

During the upper Turonian–Maastrichtian, climate changed considerably (Tabor et al., 2016). Simulated global mean surface air temperatures (GMST) show temperatures of 21.2 °C–19.5 °C during the Campanian. These cooling trends are associated with changes in the fraction of Earth's surface occupied by land (Fig. 1B), which has a higher average albedo than that of the ocean, caused by lower sea levels that resulted in greater exposure of continental areas (Landwehrs et al., 2021). Although average global temperatures decreased during the Turonian–Maastrichtian, most resin deposits formed at high latitudes, namely of the Northern Hemisphere, and were rare at mid to low latitudes (Fig. 1B). From this interval are known the amber deposits of the Santonian from the Taymyr region in Russia (Perkovsky and Vasilenko, 2019), from the Campanian of Cedar Lake and Grassy Lake in Canada (McKellar et al., 2008), and from the Campanian–Maastrichtian of the Arctic Coastal Plain in Alaska (Langenheim et al., 1960).

3.2. Biotic factors

The mass production of resin during the CREI may have been promoted by biotic factors acting at a regional scale (Martínez-Delclòs et al., 2004; Seyfullah et al., 2018). These factors include arthropod damage, pathogenic activity, and the emission of volatile compounds by the resins to attract pollinators and other insects (Langenheim, 1994; Pichersky and Gershenson, 2020; Peris et al., 2021).

Terrestrial arthropods (insects, mites) can cause severe damage to plants through feeding- or development-related activity. Different wood-boring insects, namely beetles (Coleoptera), but also some wasps such as wood wasps (Hymenoptera: Siricidae) and moths such as cossid millers or clearwing moths (Lepidoptera: Cossidae and Sesiidae), bore into wood for nest building and offspring development, at times cultivating fungi as a food source in galleries within woody tissues (Hulcr and Stelinski, 2017; Peris et al., 2021). The diseased tree reacts against invasive agents by developing secondary defensive compounds such as terpene-rich oleoresins in conifers, which flood the area to physically repel the invasion, while different toxins and volatiles act as a chemical defense (Raffa, 2014; Krokene, 2015). The influence of massive attacks of wood-boring beetles on resiniferous ancient forests has been widely cited in the literature based on their abundance in Cenozoic ambers, Pleistocene and Holocene copals, and Defaunation resins (Martínez-Delclòs et al., 2004; Labandeira, 2014a; Seyfullah et al., 2018; Peris, 2020). However, there is no significant direct evidence of beetle infestations in Cretaceous ambers yet found, although scarce wood boring beetles such as auger beetles (Bostrichidae), spider beetles (Ptinidae), ship timber beetles (Lymexylidae) and weevils (Curculionidae) are found occasionally (Chen and Zhang, 2020; Peris, 2020; Peris and Rust, 2020) (Fig. 5A–B). Herbivorous insect groups such as true bugs (Hemiptera), thrips (Thysanoptera) (Fig. 5D), grasshoppers and crickets (Orthoptera), and termites (Isoptera) have been found in major Cretaceous amber deposits, including taxa that currently cause significant damage to plants. However little evidence exists of intense arthropod

herbivory during the CREI in rock deposits (Labandeira, 1998, 2014b; Xiao et al., 2022a, 2022b), and there has been no assessment of the herbivory in amber due to the scarcity of damaged leaves and other photosynthetic structures (such as cheirolepidiaceous axes) as bioinclusions.

Pathogenic organisms can invade plant tissues directly or through a vector. Aside from their ability to cause direct harm, some extant species from insect groups transmit pathogens to their plant hosts, including viruses, bacteria, fungi, oomycetes, and nematodes (Labandeira and Prevec, 2014).

The development of insect-borne pathogens depends on population dynamics, dispersal ability, host selection behavior, and the feeding behavior of the insect vectors (Labandeira and Prevec, 2014; Eigenbrode et al., 2018). Bacteria and fungi are chiefly spread by adhering to the insect's body, so their vector relationship is not as specific as that which occurs in the transmission of viral diseases (Jones, 2005). Oomycetes are remarkable plant pathogens, because infection by these fungus-like microorganisms can induce copious resin exudation, as observed in the genus *Agathis* in New Zealand (Fig. 5E–G), which produces a particular variation in the color of large resin exudates (Weir et al., 2015). Unfortunately, this type of resin would be difficult to recognize once transformed into amber; future studies may be able to distinguish this resin isotopically or by the presence of oomycete spores as bioinclusions.

Plants are known to emit volatile compounds to attract or repel insects (Raffa, 2014; Pichersky and Gershenson, 2020). However, many insect species are attracted to volatile plant mixtures that indicate stress, as this signaling can allow insects to enter tissues free of defense and, potentially, competition (Hulcr and Dunn, 2011). Angiosperm resin terpenoids attract insect pollinators (Armbruster, 1984; Boncan et al., 2020). Highly specialized pollination relationships between some groups of insects and "gymnosperms" have been discovered in amber since the Albian (Fig. 5C), in some instances lacking extant representatives of such pollination interactions (Peñalver et al., 2012, 2015; Peris et al., 2017, 2020; Peña-Kairath et al., 2023). Resin exudation by conifers during the CREI could be related to the attraction of certain groups of insects to assist in pollination. This idea was proposed for Cenozoic ambers produced by angiosperms (Armbruster, 1993). The hypothesis is challenging to test at present, and the absence of Cretaceous insects with attached coniferous pollen (Peris et al., 2020) renders it unlikely. Nevertheless, cheirolepidiaceous pollen has been found on the mouth-parts of insects in compression-impression deposits from non-amber producing environments of the Middle Jurassic to the Early Cretaceous (Labandeira et al., 2016), indicating insect pollination of at least one reproductively specialized cheirolepidiaceous conifer was an exception (Labandeira et al., 2007).

4. Present limitations and future directions

We propose that the CREI represented a distinct mass resin production that occurred over a continuous time interval from the Barremian to the Campanian, despite differences in the known record of amber-bearing deposits between Cretaceous geochronologic stages (Fig. 1A). The causal mechanisms underlying such fluctuations are not well understood, although they may relate to circumstances that are best studied on a case-by-case basis by integrating multiple approaches.

Although we hypothesize that the same set of general processes that promoted resin mass production and accumulation acted for the entirety of the CREI, we posit that these were under the influence of possible local or regional controls that determined the intensity of the effect. The relative importance of the abiotic and biotic factors influencing resin production and accumulation during the CREI at regional geographical scales, among other variables, will need to be rigorously tested in future studies.

We established the CREI with a stage/age hierarchy (apud IUGS Chronochart - Gradstein et al., 2021). Finer temporal resolution would

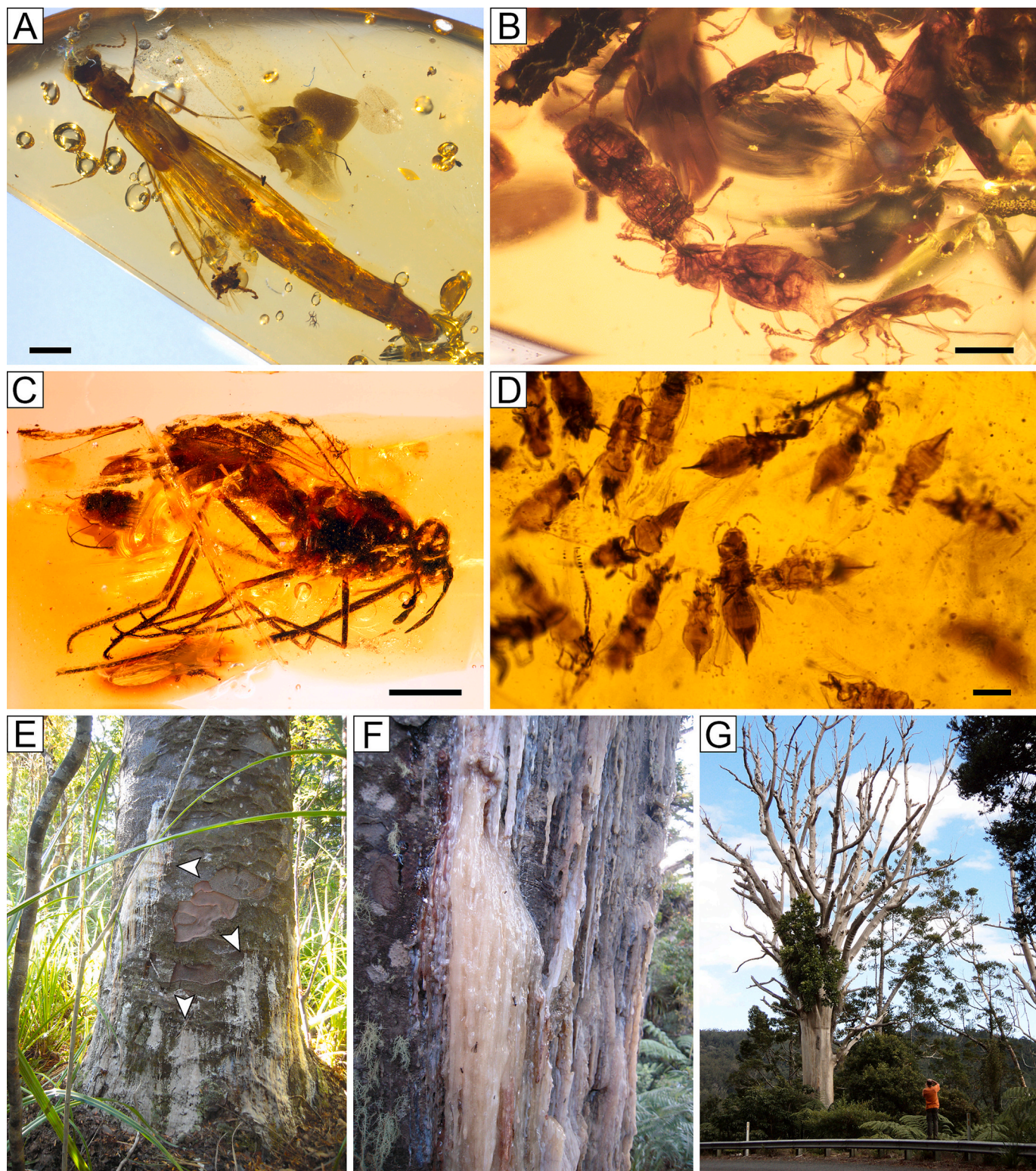


Fig. 5. Biotic factors that could have promoted resin mass production during the Cretaceous: wood-boring insects, pollination, and pathogens. A) A lymexyliid beetle; larvae of this group of beetles today penetrate living and decaying wood, consuming fungus in a symbiotic association; unpublished specimen from the Nanjing Institute of Geology and Palaeontology, China Academy of Sciences; B) Bostrichid beetles *Cretaretes minimus*, from Kachin amber (Peris and Jelínek, 2020); these beetles could have been among the first wood-boring beetles and transmitters of pathogens; C) The zhangsolvid fly *Buccinatoromyia magnifica*, from El Soplao amber (Peñalver et al., 2015); the oldest instances of “gymnosperm” pollinators in amber are found in the Albian of Spain; D) Thrips (Thysanoptera) swarm from Kachin amber with attached pollen grains (unstudied, UB); thrips were “gymnosperm” pollinators, but this group could have also been the cause of massive attacks on resinous trees; E–G) *Agathis australis* (Araucariaceae) attacked by the oomycete *Phytophthora agathidicida* (Oomycota) in Waipoua Forest, New Zealand, causing copious resin production (E, F) and the eventual death of the tree (G). Scale bars = 1 mm (A), 0.5 mm (B), 2 mm (C), 0.2 mm (D). (For interpretation of the references to color in this figure legend, the reader is referred to the web version of this article.)

reduce considerable noise to the analyses at present, as many amber deposits and conventional paleobotanical deposits are characterized by significant temporal uncertainty.

Further work to improve temporal resolution will involve more accurate dating of the deposits, more detailed identification of changes in atmospheric gas composition, more precise evaluations of meso- and macroplant remains from amber deposits, and other studies within each Cretaceous stage. These studies may provide further insight into the causal mechanisms for enhanced resin production and accumulation during the CREI. A higher-resolution temporal framework might also allow identification of distinct subintervals or even events within the Cretaceous Resinous Interval.

Although sampling bias may be an explanation for the apparently skewed presence of amber deposits towards the Northern Hemisphere during CREI (Figs. 1, 2), paleogeographical circumstances may contribute to explain the pattern. First, a greater proportion of land had emerged in the Northern Hemisphere (Landwehrs et al., 2021) during the Cretaceous, and was thus sustaining potentially greater extensions of resin-producing forests. Second, different resiniferous species distributed among both hemispheres could have had different capacities to produce resin even under comparable environmental conditions and, thus, a different potential to produce amber deposits; this has been observed at present even between closely related species (Langenheim, 1995; Seyfullah et al., 2018). It will be necessary to substantially increase reconnaissance efforts in the Southern Hemisphere to shed light on this matter.

Taphonomic knowledge on the known Cretaceous amber deposits is scarce, fundamentally limiting understanding of the CREI. It is imperative to improve efforts studying amber deposits (both the amber itself and the associated stratal context) from a detailed taphonomic standpoint. Such studies would aim to elucidate the paleoenvironmental, paleoecological, and geological circumstances surrounding the production and accumulation of resin and the formation of amber. A particular emphasis should be on improving paleobotanical analyses of meso- and macro-remains, including fossilized wood. A focus on actuataphonomic experiments, both in the field and the laboratory, will further complement our view on the subject.

5. Conclusions

The Cretaceous distribution of amber-bearing deposits is clustered around an interval of roughly 54 Ma, from the Barremian to the Campanian, and reflects global, massive resin production during the late Mesozoic. Prior to this interval, amber is remarkably scarce, appears in small quantities and, save from some Triassic amber, has not hitherto yielded macroscopic bioinclusions. We place the end of the interval in the Campanian, provided that during the Maastrichtian amber is latitudinally well distributed but appears in small quantities and is scarcely fossiliferous. Shortly before the K-Pg boundary lignite deposits exist but with the absence of amber that extends into the Paleocene, establishing a gap of several million years without amber and obviously bioinclusions.

In the Cenozoic the resin producers were no longer exclusively conifers, but rather the first deposits of angiosperm resins appeared. Shared characteristics of Cretaceous amber deposits are herein used to formally establish the Cretaceous Resinous Interval, or CREI, and are distinct from those shown by Cenozoic amber deposits. The resin that generated the amber during the CREI was produced by conifers and accumulated in transitional sedimentary environments from subtropical and temperate regions, commonly associated with charcoal and coinciding with the maximum regressive surface. Moreover, the fauna and flora preserved within the CREI share comparable group compositional characteristics, possibly due to similar original paleoenvironment, and suffered comparable taphonomic biases (Martínez-Delclòs et al., 2004; Solórzano Kraemer et al., 2018; Seyfullah et al., 2018).

The potential causal factors for the CREI are complex and

interrelated. Abiotic conditions potentially related to massive resin production and accumulation during the CREI include: (1) increased global average temperatures, including SST, with the consequent reduction in albedo due to the absence of icy poles, (2) reduced latitudinal temperature gradients, which allowed the development of forests at high latitudes, (3) higher levels of greenhouse atmospheric gases (carbon dioxide, methane) and oxygen, which promoted changes in the growth and development of the biota, (4) increased volcanic activity, which promoted an increase in temperature and changes in the composition of atmospheric gases, (5) moderate or relatively high average rainfall that could favor the development of large forests and the production of resin, (6) enhanced wildfire activity due to volcanism and high O₂ levels, (7) transgressive sea level periods and overall trend, which reduced terrestrial land area but led to the filling of large areas of lowlands and formation of resin deposits, and (8) increased storm and hurricane activity that could have promoted wildfires and/or destruction of large areas of forest, and consequently resin production. Biotic factors partially explaining the CREI at a more localized scale could include arthropod damage, pathogenic activity due to high temperatures and humidity, and the emission of insect-attracting compounds by resins. Future studies on the CREI will need to focus on elucidating the relative importance of each of these abiotic and biotic factors, enhancing the spatial and temporal resolution of the succession of paleoevents, increasing prospective efforts –particularly in the Southern Hemisphere–, and improving taphonomic understanding of Cretaceous amber deposits.

Our multidisciplinary approach will hopefully stimulate future research efforts aimed at elucidating past dynamics between the geosphere and the biosphere. Increased knowledge of when, how and why the CREI occurred will shed light on its global impact for Cretaceous terrestrial ecology and the establishment of modern terrestrial ecosystems. The exceptionally preserved record trapped in resin during the Cretaceous Resinous Interval is crucial to unravel the evolutionary history of many key terrestrial lineages, including plants, arthropods, and vertebrates, and for understanding life in a moment of critical change for terrestrial ecosystems at the transition from the Mesozoic to the Cenozoic.

Funding

This work was supported by the Spanish Ministerio de Ciencia, Innovación y Universidades [research agreement CRE CGL2017-84419 AEI/FEDER, UE] and by the Consejería de Industria, Turismo, Innovación, Transporte y Comercio of the Gobierno de Cantabria through the public enterprise EL SOPLAO S.L. [research agreement #20963 with University of Barcelona and research contract Ref. VAPC 20225428 to CN-IGME CSIC, both 2022–2025]; the Conselho Nacional de Pesquisa (Brazil) [research grant PQ 304529/19-2]; National Geographic Global Exploration Fund Northern Europa [research agreement GEFNE 127-14]; Deutsche Forschungsgemeinschaft (DFG) [research agreement SO 894/6-1]; VolkswagenStiftung [research agreement 90946]; the Secretary of Universities and Research (Government of Catalonia) and by the Horizon 2020 program of research and innovation of the European Union under the Marie-Curie [research contract no. 801370, Beatriu de Pinós]; the Secretary of Universities and Research (Government of Catalonia) and the European Social Fund [research contract 2021FI_B2 00003]; this work is a contribution to the grant RYC2021-032907-I, funded by the MCIN/AEI/10.13039/501100011033 and by the European Union «NextGenerationEU»/PRTR; and the National Agency for Research and Development (ANID) Scholarship Program [BECAS CHILE 2020-Folio 72210321].

Author contributions

Study conception and design, contributed equally: X.D. and E.P.

Data collection: X.D., E.P., D.P., D.G., M.H., C.L., Ch.S., M.M.S-K and

R.P.-d.l.F.

Conducted the fieldwork and the preparation, identification, and analysis of the field samples: X.D., E.P., E.B., D.P., D.G., C.L., M.M.S-K., S.Á.-P., D.A., E.C., R.L-D., A.N. and V.P.

Analysis and interpretation of results: X.D., E.P., D.P., D.G., M.H., C.L., Ch.S., M.M.S-K., S.Á.-P. and R.P.-d.l.F.

Database creation: X.D., S.Á.-P. and A.M.-G.

Manuscript preparation. Wrote the manuscript: X.D., E.P., D.P. and R.P.-d.l.F. All authors contributed to the discussion, reviewed the results, and approved the final version of the manuscript.

Imaging and figure preparation: X.D., D.P., S.Á.-P., C.P.-K.

Funding acquisition and project administration: X.D., E.B., M.M.S.-K.

Declaration of Competing Interest

The authors declare that they have no known competing financial interests or personal relationships that could have appeared to influence the work reported in this paper.

Data availability

All data is available as supplementary files. Part of the dataset of plants plotted in the paleomaps in Fig. 2 was downloaded from Paleobiology Database (<https://paleobiodb.org>) on 17 September 2022.

Acknowledgements

This study is a contribution to the activity of the laboratory "Advanced Micropalaeontology, Biodiversity and Evolution Researches" (AMBER) led by DA at the Lebanese University.

Appendix A. Supplementary data

Supplementary data to this article can be found online at <https://doi.org/10.1016/j.earscirev.2023.104486>.

References

- Algeo, T.J., Ingall, E., 2007. Sedimentary Corg: P ratios, paleocean ventilation, and Phanerozoic atmospheric pO₂. *Palaeogeogr. Palaeoclimatol. Palaeoecol.* 256, 130–155. <https://doi.org/10.1016/j.palaeo.2007.02.029>.
- Allen, C.D., Macalady, A.K., Chenchouni, H., Bachelet, D., McDowell, N., et al., 2010. A global overview of drought and heat-induced tree mortality reveals emerging climate change risks for forests. *For. Ecol. Manag.* 259, 660–684. <https://doi.org/10.1016/j.foreco.2009.09.001>.
- Álvarez-Parra, S., Pérez-de la Fuente, R., Peñalver, E., Barrón, E., Alcalá, L., et al., 2021. Dinosaur bonebed amber from an original swamp forest soil. *eLife* 10, e72477. <https://doi.org/10.7554/eLife.72477>.
- Anderson, K.B., Crelling, J.C., 1995. In: *Amber, Resinite, and Fossil Resins. ACS Symposium Series No. 617*, p. 297. Washington.
- Anderson, K.B., Winans, R.E., Botto, R.E., 1992. The nature and fate of natural resins in the geosphere—II. Identification, classification and nomenclature of resinites. *Org. Geochem.* 18, 829–841. [https://doi.org/10.1016/0146-6380\(92\)90051-X](https://doi.org/10.1016/0146-6380(92)90051-X).
- Armbuster, W.S., 1984. The Role of Resin in Angiosperm Pollination: Ecological and Chemical Considerations. *Am. J. Bot.* 71, 1149–1160. <https://doi.org/10.1002/j.1537-2197.1984.tb11968.x>.
- Armbuster, W.S., 1993. Evolution of Plant Pollination Systems: Hypotheses and Tests with the Neotropical Vine Dalechampia. *Evolution* 47, 1480–1505. <https://doi.org/10.1111/j.1558-5646.1993.tb02170.x>.
- Arvidson, R.S., Mackenzie, F.T., Guidry, M.W., 2013. Geologic history of seawater: a MAGIC approach to carbon chemistry and ocean ventilation. *Chem. Geol.* 362, 287–304. <https://doi.org/10.1016/j.chemgeo.2013.10.012>.
- Azar, D., Géze, R., Acrà, F., 2010. Lebanese amber. In: Penney, D. (Ed.), *Biodiversity of Fossils in Amber from the Major World Deposits*. Siri Scientific Press, pp. 271–298.
- Balseca, W., Ferrari, L., Pasquare, G., Tibaldi, A., 1993. Structural evolution of the Northern sub-Andes of Ecuador: the Napo uplift. *Second ISAG. Oxford (UK)* 9, 163–166.
- Barral, A., Gomez, B., Fourel, F., Daviero-Gomez, V., Lécuyer, Ch., 2017. CO₂ and temperature decoupling at the million-year scale during the cretaceous Greenhouse. *Sci. Rep.* 7, 8310. <https://doi.org/10.1038/s41598-017-08234-0>.
- Barrón, E., Peyrot, D., Rodríguez-López, J.P., Meléndez, N., López Del Valle, R., et al., 2015. Palynology of Aptian and upper Albian (Lower Cretaceous) amber-bearing outcrops of the southern margin of the Basque-Cantabrian basin (northern Spain). *Cretac. Res.* 52, 292–312. <https://doi.org/10.1016/j.cretres.2014.10.003>.
- Belcher, C.A., Hudspith, V.A., 2017. Changes to cretaceous surface fire behaviour influenced the spread of the early angiosperms. *New Phytol.* 213, 1521–1532. <https://doi.org/10.1111/nph.14264>.
- Belcher, C.M., McElwain, J.C., 2008. Limits for combustion in low O₂ redefine paleoatmospheric predictions for the Mesozoic. *Science* 321, 1197–1200. <https://doi.org/10.1126/science.1160978>.
- Benson, R.B.J., Butler, R., Close, R.A., Saupe, E., Rabosky, D.L., 2021. Biodiversity across space and time in the fossil record. *Curr. Biol.* 31, R1225–R1236. <https://doi.org/10.1016/j.cub.2021.07.071>.
- Benton, M.J., Wilf, P., Sauquet, H., 2022. The Angiosperm Terrestrial Revolution and the origins of modern biodiversity. *New Phytol.* 233, 2017–2035. <https://doi.org/10.1111/nph.17822>.
- Berini, J.L., Brockman, S.A., Hegeman, A.D., Reich, P.B., Muthukrishnan, R., et al., 2018. Combinations of Abiotic Factors Differentially Alter production of Plant secondary Metabolites in five Woody Plant Species in the Boreal-Temperate transition Zone. *Front. Plant Sci.* 9, 1257. <https://doi.org/10.3389/fpls.2018.01257>.
- Bergman, N.M., Lenton, T.M., Watson, A.J., 2004. COPSE: a new model of biogeochemical cycling over Phanerozoic time. *Am. J. Sci.* 304, 397–437. <https://doi.org/10.2475/ajs.304.5.397>.
- Berner, R.A., 2006. GEOCARBSULF: a combined model for Phanerozoic atmospheric O₂ and CO₂. *Geochim. Cosmochim. Acta* 70, 5653–5664. <https://doi.org/10.1016/j.gca.2005.11.032>.
- Berner, R.A., 2009. Phanerozoic atmospheric oxygen: New results using the GEOCARBSULF model. *Am. J. Sci.* 309, 603–606. <https://doi.org/10.2475/07.2009.03>.
- Berner, R.A., Canfield, D.E., 1989. A new model for atmospheric oxygen over Phanerozoic time. *Am. J. Sci.* 289, 333–361. <https://doi.org/10.2475/ajs.289.4.333>.
- Birks, H.J.B., 2020. Angiosperms versus gymnosperms in the Cretaceous. *Proc. Natl. Acad. Sci.* 117, 30879–30881. <https://doi.org/10.1073/pnas.2021186117>.
- Bodnar, J., Escapa, I., Cúneo, N.R., Gnaedinger, S., 2013. First Record of Conifer Wood from the Cañadón Asfalto Formation (Early–Middle Jurassic), Chubut Province, Argentina. *Ameghiniana* 50, 227–239. <https://doi.org/10.5710/AMGH.26.04.2013.620>.
- Boncan, D.A.T., Tsang, S.S., Li, C., Lee, I.H., Lam, H.M., Chan, T.F., Hui, J.H., 2020. Terpenes and terpenoids in plants: interactions with environment and insects. *Int. J. Mol. Sci.* 21, 7382. <https://doi.org/10.3390/ijms21197382>.
- Bond, W.J., Scott, A.C., 2010. Fire and the spread of flowering plants in the cretaceous. *New Phytol.* 188, 1137–1150. <https://doi.org/10.1111/j.1469-8137.2010.03418.x>.
- Bouju, V., Perrichot, V., 2020. A review of amber and copal occurrences in Africa and their paleontological significance. *BSGF - Earth Sci. Bull.* 191, 1–11. <https://doi.org/10.1051/bsgf/20200018>.
- Bowen, R., Jux, U., 1987. *Afro-Arabian Geology*. In: Chapman & Hall, London, New York, A kinematic view, p. 296.
- Bray, P.S., Anderson, K.B., 2008. The nature and fate of natural resins in the geosphere XIII: a probable pinaceous resin from the early cretaceous (Barremian), Isle of Wight. *Geochim. Trans.* 9, 1–5. <https://doi.org/10.1186/1467-4866-9-3>.
- Bray, P.S., Anderson, K.B., 2009. Identification of Carboniferous (320 million years old) class 1c amber. *Science* 326 (5949), 132–134. <https://doi.org/10.1126/science.1177539>.
- Brown, S.A.E., Scott, A.C., Glasspool, I.J., Collinson, M.E., 2012. Cretaceous wildfires and their impact on the Earth system. *Cretac. Res.* 36, 162–190. <https://doi.org/10.1016/j.cretres.2012.02.008>.
- Cadena, E.A., Mejía-Molina, A., Brito, C.M., Peñaflor, S., Sanmartín, K.J., et al., 2018. New Mesozoic and Cenozoic fossils from Ecuador: Invertebrates, vertebrates, plants, and microfossils. *J. S. Am. Earth Sci.* 83, 27–36. <https://doi.org/10.1016/j.jsames.2018.02.004>.
- Chang, B., Huang, J., Algeo, T.J., Pancost, R.D., Wan, X., et al., 2022. Episodic massive release of methane during the mid-Cretaceous greenhouse. *Geol. Soc. Am. Bull.* 134, 2958–2970. <https://doi.org/10.1130/B36169.1>.
- Chen, X.Y., Zhang, H.C., 2020. A new fossil record of Lymexylidae (Insecta: Coleoptera) from mid-cretaceous amber of northern Myanmar. *Zootaxa* 4878. <https://doi.org/10.1164/zootaxa.4878.1.11>.
- Chumakov, N.M., Zharkov, M.A., Herman, A.B., Doludenko, M.P., Kalandadze, N.N., et al., 1995. Climatic Belts of the Mid-cretaceous Time. *Stratigr. Geol. Correl.* 3, 241–260.
- Condamine, F.L., Silvestro, D., Koppelman, E.B., Antonelli, A., 2020. The rise of angiosperms pushed conifers to decline during global cooling. *Proc. Natl. Acad. Sci.* 117, 28867–28875. <https://doi.org/10.1073/pnas.2005571117>.
- Condie, K.C., Pisarevsky, S.A., Puetz, S.J., 2021. LIPs, orogens and supercontinents: the ongoing saga. *Gondwana Res.* 96, 105–121. <https://doi.org/10.1016/j.gr.2021.05.002>.
- Cousin-Rittmard, N.M.M., Dijkstra, H.A., Zwagers, T., 2002. Was there a wind-driven Tethys Circum-global current in the late Cretaceous? *Earth Planet. Sci. Lett.* 203, 741–753. [https://doi.org/10.1016/S0012-821X\(02\)00899-3](https://doi.org/10.1016/S0012-821X(02)00899-3).
- Couture, J., Meehan, T., Kruger, E., Lindroth, R.L., 2015. Insect herbivory alters impact of atmospheric change on northern temperate forests. *Nat. Plants* 1, 15016. <https://doi.org/10.1038/nplants.2015.16>.
- Chaboureau, A.C., Sepulchre, P., Donnadieu, Y., Franc, A., 2014. Tectonic-driven climate change and the diversification of angiosperms. *Proc. Natl. Acad. Sci.* 111, 14066–14070. <https://doi.org/10.1073/pnas.1324002111>.
- Dalling, J.W., Cernusak, L.A., Winter, K., Aranda, J., Garcia, M., et al., 2016. Two tropical conifers show strong growth and water-use efficiency responses to altered CO₂ concentration. *Ann. Bot.* 118, 1113–1125. <https://doi.org/10.1093/aob/mcw162>.
- De Lima, F.J., Pires, E.F., Jasper, A., Uhl, D., Feitosa Saraiva, A.A., et al., 2019. Fire in the paradise: evidence of repeated palaeo-wildfires from the Araripe Fossil Lagerstätte

- (Araripe Basin, Aptian-Albian), Northeast Brazil. *Palaeobiodiv. Palaeoenviron.* 99, 367–378. <https://doi.org/10.1007/s12549-018-0359-7>.
- De la Prasetya, Ch., Syaufina, L., Santosa, G., 2017. The effect of various types of forest fires on pine resin productivity in Gunung Walat University Forest, Sukabumi, Indonesia. *Biodiversitas* 18, 476–482. <https://doi.org/10.13057/biodiv/d180105>.
- Eberth, D.A., 2005. The Geology. In: Currie, P.J., Koppelhus, E.B. (Eds.), *Dinosaur Provincial Park: A Spectacular Ancient Ecosystem Revealed*. Indiana University Press, pp. 54–82.
- Eigenbrode, S.D., Bosque-Pérez, N.A., Davis, Th.S., 2018. Insect-Borne Plant Pathogens and their Vectors: Ecology, Evolution, and complex Interactions. *Annu. Rev. Entomol.* 63, 169–191. <https://doi.org/10.1146/annurev-ento-020117-043119>.
- Elldholm, O., Coffin, L.F., 2000. Large Igneous Provinces and Plate Tectonics. In: Richards, M.A., Gordon, R.G., Van Der Hilst, R.D. (Eds.), *The History and Dynamics of Global Plate Motions*, 121. American Geophysical Union, pp. 309–326. <https://doi.org/10.1029/GM121p0309>. Geophysical Monograph Series.
- Erwin, D.H., 2009. Climate as a driver of Evolutionary Change. *Curr. Biol.* 19, 575–583. <https://doi.org/10.1016/j.cub.2009.05.047>.
- Falkowski, P.G., Katz, M.E., Milligan, A.J., Fennel, K., Cramer, B.S., et al., 2005. The rise of oxygen over the past 205 million years and the evolution of large placental mammals. *Science* 309, 2202–2204. <https://doi.org/10.1126/science.1116047>.
- Farnsworth, A., Lunt, D.J., Robinson, S.A., Valdes, P.J., Roberts, W.H.G., 2019. Past East Asian monsoon evolution controlled by paleogeography, not CO₂. *Sci. Adv.* 5, eaax169. <https://doi.org/10.1126/sciadv.aax1697>.
- Gao, J., Engel, M.S., Shih, Ch., Ren, D., Gao, T., 2021. A new genus of anaxyelid wood wasps from the mid-cretaceous and the phylogeny of Anaxyelidae (Hymenoptera). *J. Hymenopt. Res.* 86, 151–169. <https://doi.org/10.3897/jhr.86.73161>.
- Glasspool, I.J., Scott, A.C., 2010. Phanerozoic concentrations of atmospheric oxygen reconstructed from sedimentary charcoal. *Nat. Geosci.* 3, 627–630. <https://doi.org/10.1038/ngeo923>.
- Gradstein, F.M., Ogg, J.G., Schmitz, M.D., Ogg, G.M., 2021. In: *Geologic Time Scale 2020*. Elsevier, Amsterdam, p. 1176, 2 vols.
- Grimaldi, D.A., 2019. *Amber. Curr. Biol.* 29, 861–862. <https://doi.org/10.1016/j.cub.2019.08.047>.
- Grimaldi, D.A., Nascimbene, P., 2010. Raritan (New Jersey) amber. In: Penney, D. (Ed.), *Biodiversity of Fossils in Amber from the Major World Deposits*. Siri Scientific Press, pp. 167–191.
- Grimaldi, D.A., Ross, A.J., 2017. Extraordinary Lagerstätten in Amber, with particular reference to the cretaceous of Burma. In: Fraser, N.C., Stues, H.-D. (Eds.), *Terrestrial Conservation Lagerstätten: Windows into the Evolution of Life on Land*. Dunedin Academic Press Ltd, pp. 287–342.
- Grimaldi, D.A., Lillegraven, J.A., Wampler, T., Bookwalter, D., Shadrinsky, A.M., 2000a. Amber from Upper cretaceous through Paleocene strata of the Hanna Basin, Wyoming, with evidence for source and taphonomy of fossil resins. *Rocky Mountain Geol.* 35, 163–204.
- Grimaldi, D.A., Shadrinsky, A., Wampler, Th.P., 2000b. A remarkable deposit of fossiliferous amber from the Upper cretaceous (Turonian) of New Jersey. In: Grimaldi, D. (Ed.), *Studies on fossils in amber, with particular reference to the Cretaceous of New Jersey*. Backhuys Publishers, pp. 1–76.
- Grimaldi, D.A., Sunderlin, D., Aaroe, G.A., Dempsey, M.R., Parker, N.E., et al., 2018. Biological Inclusions in Amber from the Paleogene Chickaloon Formation of Alaska. *Am. Mus. Novit.* 3908, 1–37. <https://doi.org/10.1206/3908.1>.
- Haq, B.U., 2014. Cretaceous eustasy revisited. *Glob. Planet. Chang.* 113, 44–58. <https://doi.org/10.1016/j.gloplacha.2013.12.007>.
- Hansen, K.W., Wallman, K., 2003. Cretaceous and Cenozoic evolution of seawater composition, atmospheric O₂ and CO₂: A model perspective. *Am. J. Sci.* 303, 94–148. <https://doi.org/10.2475/ajs.303.2.94>.
- Hasegawa, H., Tada, R., Jiang, X., Suganuma, Y., Imsamut, S., et al., 2012. Drastic shrinking of the Hadley circulation during the mid-cretaceous Supergreenhouse. *Clim. Past* 8, 1323–1337. <https://doi.org/10.5194/cp-8-1323-2012>.
- Hay, W.W., 2009. Cretaceous Oceans and Ocean Modelling. In: Scott, R.W., Wagreich, M., Jansa, L., Hu, X., Wang, C. (Eds.), *Cretaceous Oceanic Red Beds: Stratigraphy, Composition, Origins, and Paleoceanographic and Paleoclimatic Significance*. SEPM Special Publication 91, pp. 243–271. <https://doi.org/10.2110/sepm.091.233>.
- Hay, W.W., 2017. Toward understanding cretaceous climate—An updated review. *Sci. China Earth Sci.* 60, 5–19. <https://doi.org/10.1007/s11430-016-0095-9>.
- Hay, W.W., Floegl, S., 2012. New thoughts about the cretaceous climate and oceans. *Earth Sci. Rev.* 115, 262–272. <https://doi.org/10.1016/j.earscirev.2012.09.008>.
- Hay, W.W., DeConto, R.M., de Boer, P., Flögel, S., Song, Y., et al., 2019. Possible solutions to several enigmas of cretaceous climate. *Int. J. Earth Sci.* 108, 587–620. <https://doi.org/10.1007/s00531-018-1670-2>.
- He, T., Lamont, B., Manning, J.A., 2016. Cretaceous origin for fire adaptations in the Cape flora. *Sci. Rep.* 6, 34880. <https://doi.org/10.1038/srep34880>.
- Holz, M., 2015. Mesozoic paleogeography and paleoclimates – a discussion of the diverse greenhouse and hothouse conditions of an alien world. *J. S. Am. Earth Sci.* 61, 91–107. <https://doi.org/10.1016/j.jjsames.2015.01.001>.
- Hu, X., Scott, R.W., Cai, Y., Wang, Ch., Melinte-Dobrinescu, M.C., 2012. Cretaceous oceanic red beds (CORBs): different time scales and models of origin. *Earth Sci. Rev.* 115, 217–248. <https://doi.org/10.1016/j.earscirev.2012.09.007>.
- Huber, B.T., O'Brien, Ch.L., 2020. Cretaceous climate. In: Scott, E., Alderton, D. (Eds.), *Encyclopedia of Geology*, 2nd edition. Elsevier, pp. 497–503.
- Huber, B.T., MacLeod, K.G., Watkins, D.K., Coffin, M.F., 2018. The rise and fall of the cretaceous Hot Greenhouse climate. *Glob. Planet. Chang.* 167, 1–23. <https://doi.org/10.1016/j.gloplacha.2018.04.004>.
- Hulcr, J., Dunn, R.R., 2011. The sudden emergence of pathogenicity in insect-fungus symbioses threatens naive forest ecosystems. *Proc. R. Soc. B Biol. Sci.* 278 (1720), 2866–2873. <https://doi.org/10.1098/rspb.2011.1130>.
- Hulcr, J., Stelinski, L.L., 2017. The Ambrosia Symbiosis: from Evolutionary Ecology to Practical Management. *Annu. Rev. Entomol.* 62, 285–303. <https://doi.org/10.1146/annurev-ento-031616-035105>.
- Iturralde-Vinent, M.A., MacPhee, R.D.E., 2019. Remarks on the age of Dominican amber. *Palaeoentomology* 2, 236–240. <https://doi.org/10.11646/palaeoentomology.2.3.7>.
- Jahren, H., Arens, N.C., Sarmiento-Pérez, G.A., Guerrero, J., Amundson, R., 2001. Terrestrial record of methane hydrate dissociation in the early cretaceous. *Geology* 29, 159–162. [https://doi.org/10.1130/0091-7613\(2001\)029<0159:TROMHD>2.0.CO;2](https://doi.org/10.1130/0091-7613(2001)029<0159:TROMHD>2.0.CO;2).
- Johansson, L., Zahirovic, S., Dietmar Müller, R., 2018. The Interplay between the Eruption and Weathering of large Igneous Provinces and the Deep-Time Carbon Cycle. *Geophys. Res. Lett.* 45, 5380–5389. <https://doi.org/10.1029/2017GL076691>.
- Jones, D.R., 2005. Plant Viruses Transmitted by Thrips. *Eur. J. Plant Pathol.* 113, 119–157. <https://doi.org/10.1007/s10658-005-2334-1>.
- Jossang, J., Bel-Kassouui, H., Jossang, A., Seuleiman, M., Nel, A., 2008. Quesnoi, a Novel Pentacyclic ent-Diterpene from 55 Million Years Old Oise Amber. *J. Organ. Chem.* 73, 412–417. <https://doi.org/10.1021/jo701544k>.
- Kent, D.V., Muttoni, G., 2022. Latitudinal land-sea distributions and global surface albedo since the cretaceous. *Palaeogeogr. Palaeoclimatol. Palaeoecol.* 585, 110718. <https://doi.org/10.1016/j.palaeo.2021.110718>.
- Kergoat, G.J., Bouchard, P., Clamens, A.-L., Abbate, J.L., Jourdan, H., et al., 2014. Cretaceous environmental changes led to high extinction rates in a hyperdiverse beetle family. *BMC Evol. Biol.* 14, 1–13. <https://doi.org/10.1186/s12862-014-0220-1>.
- Kidder, D.L., Worsley, T.R., 2010. Phanerozoic large Igneous Provinces (LIPs), HEATT (Haline Euxinic Acidic thermal Transgression) episodes, and mass extinctions. *Palaeogeogr. Palaeoclimatol. Palaeoecol.* 295, 162–191. <https://doi.org/10.1016/j.palaeo.2010.05.036>.
- Klages, J.P., Salzmann, U., Bickert, T., Hillenbrand, C.-D., Gohl, K., et al., 2020. Temperate rainforests near the South Pole during peak cretaceous warmth. *Nature* 580, 81–86. <https://doi.org/10.1038/s41586-020-2148-5>.
- Krokene, P., 2015. Conifer Defence and Resistance to Bark Beetles. In: Vega, F.E., Hofstetter, R.W. (Eds.), *Bark Beetles: Biology and Ecology of Native and Invasive Species*. Academic Press, Elsevier, London, pp. 177–207.
- Kurepin, L.V., Stangl, Z.R., Ivanov, A.G., Bui, V., Memet, M., et al., 2018. Contrasting acclimation abilities of two dominant boreal conifers to elevated CO₂ and temperature. *Plant Cell Environ.* 41, 1331–1345. <https://doi.org/10.1111/pce.13158>.
- Kvaček, J., Barrón, E., Hermanová, Z., Mendes, M.M., Karch, J., et al., 2018. Araucarian conifer from late Albian amber of northern Spain. *Pap. Palaeontol.* 4, 643–656. <https://doi.org/10.1002/spp.21223>.
- Labandeira, C.C., 1998. The role of insects in late Jurassic to Middle Cretaceous ecosystems. In: Lucas, S.G., Kirkland, J.I., Estep, J.W. (Eds.), *Lower and Middle Cretaceous Terrestrial Ecosystems*, 14. New Mexico Museum of Natural History and Science Bulletin, pp. 105–124. <http://hdl.handle.net/10088/5968>.
- Labandeira, C.C., 2007. The origin of herbivory on land: initial patterns of plant tissue consumption by arthropods. *Insect Sci.* 14, 259–275. <https://doi.org/10.1111/j.1744-7917.2007.00141.x>.
- Labandeira, C.C., 2013. A paleobiologic perspective on plant-insect interactions. *Curr. Opin. Plant Biol.* 16, 414–421. <https://doi.org/10.1016/j.pbi.2013.06.003>.
- Labandeira, C.C., 2014. Amber. In: LaFlamme, M., Schiffbauer, J.D., Darroch, S.A.F. (Eds.), *Reading and Writing of the Fossil Record: Preservational Pathways to Exceptional Fossilization*. Paleontological Society Papers 20, pp. 163–215. <https://repository.si.edu/handle/10088/24696>.
- Labandeira, C.C., 2014b. Why did Terrestrial Insect Diversity not increase during the Angiosperm Radiation? Mid-Mesozoic, Plant-Associated Insect Lineages Harbor Clues. In: Pontarotti, P. (Ed.), *Evolutionary Biology: Genome Evolution, Speciation, Coevolution and Origin of Life*. Springer International Publishing, pp. 261–299. https://doi.org/10.1007/978-3-319-07623-2_13.
- Labandeira, C.C., Kvaček, J., Mostovski, M.B., 2007. Pollination drops, pollen, and insect pollination of Mesozoic gymnosperms. *Taxon* 56, 663–695. <https://doi.org/10.2307/25065852>.
- Labandeira, C.C., Prevec, R., 2014. Plant paleopathology and the roles of pathogens and insects. *Int. J. Paleopathol.* 4, 1–16. <https://doi.org/10.1016/j.ijpp.2013.10.002>.
- Labandeira, C.C., Yang, Q., Santiago-Blay, J.A., Hotton, C.L., Monteiro, A., et al., 2016. The evolutionary convergence of mid-Mesozoic lacewings and Cenozoic butterflies. *Proc. R. Soc. B* 283, 20152893. <https://doi.org/10.1098/rspb.2015.2893>.
- Ladant, J.B., Poulsen, C.J., Fluteau, P., Tabor, C.R., MacLeod, K.G., et al., 2020. Paleogeographic controls on the evolution of late cretaceous ocean circulation. *Clim. Past* 16 (3), 973–1006. <https://doi.org/10.5194/cp-16-973-2020>.
- Lake, J.A., Wade, R.N., 2009. Plant-pathogen interactions and elevated CO₂: morphological changes in favour of pathogens. *J. Exp. Bot.* 60, 3123–3131. <https://doi.org/10.1093/jxb/erp147>.
- Lambert, J.B., Johnson, S.C., Poinar Jr., G.O., 1996. Nuclear magnetic resonance characterization of cretaceous amber. *Archaeometry* 38, 325–335. <https://doi.org/10.1111/j.1475-4754.1996.tb00780.x>.
- Landwehr, J., Feulner, G., Petri, S., Sames, B., Wagreich, M., 2021. Investigating Mesozoic climate Trends and Sensitivities with a large Ensemble of Climate Model Simulations. *Paleoceanogr. Paleoclimatol.* 36, e2020PA004134. <https://doi.org/10.1029/2020PA004134>.

- Langenheim, R.L., Smiley, C.J., Gray, J., 1960. Cretaceous amber from the Arctic Coastal Plain of Alaska. *GSA Bull.* 71, 1345–1356. [https://doi.org/10.1130/0016-606\(1960\)71\[1345:CAFTAC\]2.0.CO;2](https://doi.org/10.1130/0016-606(1960)71[1345:CAFTAC]2.0.CO;2).
- Langenheim, J.H., 1990. Plant resins. *Am. Sci.* 78, 16–24.
- Langenheim, J.H., 1994. Higher plant terpenoids: a phytocentric overview of their ecological roles. *J. Chem. Ecol.* 20, 1223–1280. <https://doi.org/10.1007/BF02598090>.
- Langenheim, J.H., 1995. Biology of Amber-Producing Trees: Focus on Case Studies of Hymenaea and Agathis. In: Anderson, K.B., Crelling, J.C. (Eds.), *Amber, Resinite, and Fossil Resins*, ACS Symposium Series, 617, pp. 1–31.
- Langenheim, J.H., 2003. Plant Resins: Chemistry. In: Timber Press, Portland, Cambridge, Evolution, Ecology, Ethnobotany, p. 586.
- Lloyd, G.T., Davis, K.E., Pisani, D., Tarver, J.E., Ruta, M., et al., 2008. Dinosaurs and the cretaceous Terrestrial Revolution. *Proc. R. Soc. B* 275, 2483–2490. <https://doi.org/10.1098/rspb.2008.0715>.
- Macdonald, F., Wordsworth, R., Swanson-Hysell, N., 2018. LIPs and climate change. Abstract. In: Goldschmidt2018. <https://goldschmidt.info/2018/abstracts/abstractVi ew?id=2018003432>.
- McKellar, R., Wolfe, A., Tappert, R., Muehlenbachs, K., 2008. Correlation of Grassy Lake and Cedar Lake ambers using infrared spectroscopy, stable isotopes, and palaeoentomology. *Can. J. Earth Sci.* 45, 1061–1082. <https://doi.org/10.1139/E08-049>.
- Maksoud, S., Granier, B.R.C., Azar, D., 2022. Palaeoentomological (fossil insects) outcrops in Lebanon. *Carnets Geol.* 22, 699–743. <https://doi.org/10.2110/carnets.2022.2216>.
- Maksoud, S., Azar, D., Granier, B., Gèze, R., 2017. New data on the age of the lower cretaceous amber outcrops of Lebanon. *Palaeoworld* 26, 331–338. <https://doi.org/10.1016/j.palwor.2016.03.003>.
- Martínez-Delclos, X., Briggs, D.E.G., Peñalver, E., 2004. Taphonomy of insects in carbonates and amber. *Palaeogeogr. Palaeoclimatol. Palaeoecol.* 203, 19–64. [https://doi.org/10.1016/S0031-0182\(03\)00643-6](https://doi.org/10.1016/S0031-0182(03)00643-6).
- Mays, Ch., Coward, A.J., O'Dell, L.A., Tappert, R., 2019. The botanical provenance and taphonomy of late cretaceous Chatham amber, Chatham Islands, New Zealand. *Rev. Palaeobot. Palynol.* 260, 16–26. <https://doi.org/10.1016/j.revpalbo.2018.08.004>.
- McCoy, V.E., Barthel, J.H., Boom, A., Peñalver, E., Delclos, X., et al., 2021. Volatile and semi-volatile composition of cretaceous amber. *Cretac. Res.* 127, 104958 <https://doi.org/10.1016/j.cretres.2021.104958>.
- McCoy, V.E., Boom, A., Kraemer, M.M.S., Gabbott, S.E., 2017. The chemistry of American and african amber, copal, and resin from the genus Hymenaea. *Org. Geochem.* 113, 43–54. <https://doi.org/10.1016/j.orggeochem.2017.08.005>.
- McElwain, J.C., 2018. Paleobotany and Global Change: Important Lessons for Species to Biomes from Vegetation responses to Past Global Change. *Annu. Rev. Plant Biol.* 69, 761–787. <https://doi.org/10.1146/annurev-arplant-042817-040405>.
- McKenna, D.D., Wild, A., Kanda, K., Bellamy, C., Beutel, R.G., et al., 2015. The beetle tree of life reveals that Coleoptera survived end-Permian mass extinction to diversify during the cretaceous terrestrial revolution. *Syst. Entomol.* 40, 835–880. <https://doi.org/10.1111/syen.12132>.
- Menor-Salván, C., Najarro, M., Velasco, F., Rosales, I., Tornos, F., et al., 2010. Terpenoids in extracts of lower cretaceous ambers from the Basque-Cantabrian Basin (El Soplao, Cantabria, Spain): Palaeohemotaxonomic aspects. *Org. Geochem.* 41, 1089–1103. <https://doi.org/10.1016/j.orggeochem.2010.06.013>.
- Menor-Salván, C., Simoneit, B.R.T., Ruiz-Bermejo, M., Alonso, J., 2016. The molecular composition of cretaceous ambers: Identification and chemosystematic relevance of 1,6-dimethyl-5-alkyltetralins and related bisnorlabdane biomarkers. *Org. Geochem.* 93, 7–21. <https://doi.org/10.1016/j.orggeochem.2015.12.010>.
- Meredith, R.W., Janečka, J.E., Gatesy, J., Ryder, O.A., Fisher, C.A., et al., 2011. Impacts of the cretaceous Terrestrial Revolution and KPg Extinction on Mammal diversification. *Science* 334, 521–524. <https://doi.org/10.1126/science.1211028>.
- Mills, B.J.W., Belcher, C.M., Lenton, T.M., Newton, R.J., 2016. A modeling case for high atmospheric oxygen concentrations during the Mesozoic and Cenozoic. *Geology* 44, 1023–1026. <https://doi.org/10.1130/G38231.1>.
- Mills, J.V., Gomes, M.L., Kristall, B., Sageman, B.B., Jacobson, A.D., et al., 2017. Massive volcanism, evaporite deposition, and the chemical evolution of the early cretaceous ocean. *Geology* 45, 475–478. <https://doi.org/10.1130/G38667.1>.
- Moreau, J.-D., Néraudeau, D., Perrichot, V., 2020. Conifers from the Cenomanian amber of Fouras (Charente-Maritime, western France). *BSGF – Earth Sci. Bull.* 191, 1–5. <https://doi.org/10.1051/bsgf/2020017>.
- Mutterlose, J., Malkoc, M., Schouten, S., Sinninghe Damsté, J.S., Forster, A., 2010. TEX86 and stable δ¹⁸O paleothermometry of early cretaceous sediments: Implications for belemnite ecology and paleotemperature proxy application. *Earth Planet. Sci. Lett.* 298, 286–298. <https://doi.org/10.1016/j.epsl.2010.07.043>.
- Najarro, M., Peñalver, E., Rosales, I., Pérez-de-la-Fuente, R., Daviero-Gómez, V., et al., 2009. Unusual concentration of early Albian arthropod-bearing amber in the Basque-Cantabrian Basin (El Soplao, Cantabria, Northern Spain): Palaeoenvironmental and palaeobiological implications. *Geol. Acta* 7, 363–387. <https://doi.org/10.1344/105.000001443>.
- Najarro, M., Peñalver, E., Pérez-de-la-Fuente, R., Ortega-Blanco, J., Menor-Salván, C., et al., 2010. A review of the El Soplao amber outcrop, early cretaceous of Cantabria, Spain. *Acta Paleontol. Sin.* 84, 959–976. <https://doi.org/10.1111/j.1755-6724.2010.00258.x>.
- Néraudeau, D., Perrichot, V., Colin, J.-P., Girard, V., Gomez, B., et al., 2008. A new amber deposit from the cretaceous (uppermost Albian–lowermost Cenomanian) of southwestern France. *Cretac. Res.* 29, 925–929. <https://doi.org/10.1016/j.cretres.2008.05.009>.
- Neri, M., Roghi, G., Ragazzi, E., Papazzonia, C.A., 2016. First record of Pliensbachian (Lower Jurassic) amber and associated palynoflora from the Monti Lessini (northern Italy). *Geobios* 50, 49–63. <https://doi.org/10.1016/j.geobios.2016.10.001>.
- Nohra, Y.A., Azar, D., Gèze, R., Maksoud, S., El-Samrani, A., et al., 2013. New Jurassic amber outcrops from Lebanon. *Terrest. Arthropod. Rev.* 6, 27–51. <https://doi.org/10.1163/18749836-06021056>.
- Nohra, Y.A., Perrichot, V., Boura, A., Jeanneau, L., Néraudeau, D., et al., 2014. Cupressacean origin of the Cretaceous Vendean amber (northwestern France): evidence from fossil wood and chemical signatures. In: 9th European Palaeobotany-Palynology Conference, 189. Padova.
- Novick, K., Katul, G.G., McCarthy, H.R., Oren, R., 2012. Increased resin flow in mature pine trees growing under elevated CO₂ and moderate soil fertility. *Tree Physiol.* 32, 752–763. <https://doi.org/10.1093/treephys/tpr133>.
- O'Brien, C.L., Robinson, S.A., Pancost, R.D., Sinninghe Damsté, J.S., Schouten, S., et al., 2017. Cretaceous sea-surface temperature evolution: Constraints from TEX86 and planktonic foraminiferal oxygen isotopes. *Earth Sci. Rev.* 172, 224–247. <https://doi.org/10.1016/j.earscirev.2017.07.01>.
- Ohba, M., Ueda, H., 2010. A GCM Study on Effects of Continental Drift on Tropical climate at the early and late cretaceous. *J. Meteorol. Soc. Jpn.* 88, 869–881. <https://doi.org/10.2131/jmsj.2010-601>.
- Olde, K., Jarvis, I., Uličník, D., Pearce, M.A., Trabucho-Alexandre, J., et al., 2015. Geochemical and palynological sea-level proxies in hemipelagic sediments: a critical assessment from the Upper cretaceous of the Czech Republic. *Palaeogeogr. Palaeoclimatol. Palaeoecol.* 435, 222–243. <https://doi.org/10.1016/j.palaeo.2015.06.018>.
- Olivoto, T., Nardino, M., Carvalho, I.R., Follmann, D.N., Szareski, V.J., et al., 2017. Plant secondary metabolites and its dynamical systems of induction in response to environmental factors: a review. *Afr. J. Agric. Res.* 12, 71–84. <https://doi.org/10.5897/AJAR2016.11677>.
- Ortega-Blanco, J., Rasnitsyn, A., Delclos, X., 2008. First record of anaxyelid woodwasps (Hymenoptera: Anaxyelidae) in lower cretaceous spanish amber. *Zootaxa* 1937, 39–50. <https://doi.org/10.11646/zootaxa.1937.1.3>.
- Otto, A., Kváček, J., Goth, K., 2020. Biomarkers from the taxodiaceous conifer *Sphenoletipus pecinovincens* Kváček and resin from Bohemian Cenomanian. *Acta Palaeobot. Suppl.* 2, 153–157.
- Pausas, J.G., 2018. Generalized fire response strategies in plants and animals. *Oikos* 128, 147–153. <https://doi.org/10.1111/oik.05907>.
- Penney, D. (Ed.), 2010. *Biodiversity of Fossils in Amber from the Major World Deposits*. Siri Scientific Press, Manchester, p. 304.
- Peña-Kairath, C., Delclos, X., Álvarez-Parras, S., Peñalver, E., Engel, M.S., et al., 2023. Insect pollination in deep time. *Trends Ecol. Evol.* <https://doi.org/10.1016/j.tree.2023.03.008>.
- Peñalver, E., Delclos, X., 2010. Spanish Amber. In: Penney, D. (Ed.), *Biodiversity of Fossils in Amber from the Major World Deposits*. Siri Scientific Press, pp. 236–270.
- Peñalver, E., Arillo, A., Pérez-de la Fuente, R., Riccio, M.L., Delclos, X., et al., 2015. Long-Proboscid Flies as Pollinators of cretaceous Gymnosperms. *Curr. Biol.* 14, 1917–1923. <https://doi.org/10.1016/j.cub.2015.05.062>.
- Peñalver, E., Delclos, X., Solórzano Kraemer, M.M., 2018. A new approach to determine the resiniferous trees involved in the origin of the Cretaceous amber deposits. In: 1st Paleontological Virtual Congress, 140, Valencia. <https://www.uv.es/everlab/PUBLICACIONES/1stSVP%20BOOK%20OF%20ABSTRACTS.pdf>.
- Peñalver, E., Labandeira, C.C., Barrón, E., Delclos, X., Nel, P., 2012. Thrips pollination of Mesozoic gymnosperms. *Abstract Proc. Natl. Acad. Sci.* 109, 8623–8628. <https://doi.org/10.1073/pnas.1120499109>.
- Peralta-Medina, E., Falcon-Lang, H.J., 2012. Cretaceous forest composition and productivity inferred from a global fossil wood database. *Geology* 40, 219–222. <https://doi.org/10.1130/G32733.1>.
- Pereira, R., de Souza Carvalho, I., Simoneit, B.R.T., de Almeida Azevedo, D., 2009. Molecular composition and chemosystematic aspects of cretaceous amber from the Amazonas, Araripe and Recôncavo basins, Brazil. *Org. Geochem.* 40, 863–875. <https://doi.org/10.1016/j.orggeochem.2009.05.002>.
- Pérez-de la Fuente, R., Delclos, X., Peñalver, E., Speranza, M., Wierzos, J., 2012. Early evolution and ecology of camouflage in insects. *Proc. Natl. Acad. Sci.* 109, 21414–21419. <https://doi.org/10.1073/pnas.121377511>.
- Pérez-Díaz, L., Eagles, G., 2017. South Atlantic paleobathymetry since early cretaceous. *Sci. Rep.* 7, 11819. <https://doi.org/10.1038/s41598-017-11959-7>.
- Peris, D., 2020. Coleoptera in amber from cretaceous resiniferous forests. *Cretac. Res.* 113, 104484. <https://doi.org/10.1016/j.cretres.2020.104484>.
- Peris, D., Condamine, F.L., 2023. The dual role of the angiosperm radiation on insect diversification. *BioRxiv*. <https://doi.org/10.1101/2023.02.07.527317>.
- Peris, D., Jelfnek, J., 2020. Syninclusions of two new species of short-winged flower beetle (Coleoptera: Kateretidae) in mid-cretaceous Kachin amber (Myanmar). *Cretac. Res.* 116, 104264. <https://doi.org/10.1016/j.cretres.2019.104264>.
- Peris, D., Rust, J., 2020. Cretaceous beetles (Insecta: Coleoptera) in amber: the palaeoecology of this most diverse group of insects. *Zool. J. Linnean Soc.* 189, 1085–1104. <https://doi.org/10.1093/zoolinnean/zlz118>.
- Peris, D., Delclos, X., Jordal, B.H., 2021. Origin and evolution of fungus farming in wood-boring Coleoptera – a palaeontological perspective. *Biol. Rev.* 96, 2476–2488. <https://doi.org/10.1111/brv.12763>.
- Peris, D., Labandeira, C.C., Barrón, E., Delclos, X., Rust, J., et al., 2020. Generalist Pollen-Feeding Beetles during the Mid-cretaceous. *iScience* 23, 100913. <https://doi.org/10.1016/j.isci.2020.100913>.
- Peris, D., la Fuente, Pérez-de, Peñalver, E., Delclos, X., Barrón, E., et al., 2017. False Blister Beetles and the expansion of Gymnosperm-Insect Pollination Modes before Angiosperm Dominance. *Curr. Biol.* 27, 897–904. <https://doi.org/10.1016/j.cub.2017.02.009>.

- Perkovsky, E.E., Vasilenko, D.V., 2019. A summary of recent results in the study of Taimyr amber. *Paleontol. J.* 53, 984–993. <https://doi.org/10.1134/S0031030119100149>.
- Perrichot, V., 2005. Environnements paralliques à ambre et à végétaux du Crétacé Nord-Aquitain (Charentes, Sud-Ouest de la France), 213 pp. + annexes, 118. Mémoires Géosciences Rennes, Thèse de l'Université de Rennes 2003. <https://tel.archives-ouvertes.fr/tel-00011639>.
- Perrichot, V., Néraudeau, D., Tafforeau, P., 2010. Charentese Amber. In: Penney, D. (Ed.), *Biodiversity of Fossils in Amber from the Major World Deposits*. Siri Scientific Press, pp. 193–208.
- Peyrot, D., Barrón, E., Polette, F., Batten, D.J., Néraudeau, D., 2019. Early Cenomanian palynofloras and inferred resiniferous forests and vegetation types in Charente (southwestern France). *Cretac. Res.* 94, 168–189. <https://doi.org/10.1016/j.cretres.2018.10.011>.
- Pichersky, E., Gershenson, J., 2020. The formation and function of plant volatiles: Perfumes for pollinator attraction and defense. *Curr. Opin. Plant Biol.* 5, 237–243. [https://doi.org/10.1016/S1369-5266\(02\)00251-0](https://doi.org/10.1016/S1369-5266(02)00251-0).
- Poinar Jr., G., Lambert, J.B., Wu, Y., 2007. Araucarian source of fossiliferous Burmese amber: Spectroscopic and anatomical evidence. *J. Bot. Res. Inst. Texas* 1, 449–455.
- Poulsen, C.J., Zhou, J., 2013. Sensitivity of Arctic climate variability to mean State: Insights from the cretaceous. *J. Clim.* 26, 7003–7022. <https://doi.org/10.1175/JCLI-D-12-00825.1>.
- Poulsen, C.J., Seidov, D., Barron, E.J., Peterson, W.H., 1998. The impact of paleogeographic evolution on the surface oceanic circulation and the marine environment within the mid-cretaceous Tethys. *Paleoceanogr. Paleoclimatol.* 13, 546–559. <https://doi.org/10.1029/98PA01789>.
- Raffa, K.F., 2014. Terpenes tell different tales at different scales: glimpses into the Chemical Ecology of conifer – bark beetle – microbial interactions. *J. Chem. Ecol.* 40, 1–20. <https://doi.org/10.1007/s10886-013-0368-y>.
- Ray, D.C., van Buchem, F.S.P., Baines, G., Davies, A., Gréselle, B., et al., 2019. The magnitude and cause of short-term eustatic cretaceous sea-level change: a synthesis. *Earth Sci. Rev.* 197, 102901 <https://doi.org/10.1016/j.earscirev.2019.102901>.
- Rodríguez-García, A., Martín, J.A., López, R., Mutke, S., Pinillos, F., Gil, L., 2015. Influence of climate variables on resin yield and secretory structures in tapped *Pinus pinaster* Ait. In: Central Spain. *Agric. For. Meteorol.* 202, 83–93. <https://doi.org/10.1016/j.agrformet.2014.11.023>.
- Rodríguez-López, J.P., Peyrot, D., Barrón, E., 2020. Complex sedimentology and palaeohabitats of Holocene coastal deserts, their topographic controls, and analogues for the mid-cretaceous of northern Iberia. *Earth Sci. Rev.* 201, 103075 <https://doi.org/10.1016/j.earscirev.2019.103075>.
- Roghi, G., Gianolla, P., Kustatscher, E., Schmidt, A.R., Seyfullah, L.J., 2022. An Exceptionally Preserved Terrestrial Record of LIP Effects on Plants in the Carnian (Upper Triassic) Amber-Bearing Section of the Dolomites, Italy. *Front. Earth Sci.* 10 (900586), 1–18. <https://doi.org/10.3389/feart.2022.900586>.
- Rombola, C.F., Greppi, C.D., Pujana, R.R., García Massini, J.L., Bellosi, E.S., et al., 2022. Brachyoxylon fossil woods with traumatic resin canals from the Upper cretaceous Cerro Fortaleza Formation, southern Patagonia (Santa Cruz Province, Argentina). *Cretac. Res.* 130, 105065 <https://doi.org/10.1016/j.cretres.2021.105065>.
- Ross, A., 2009. In: *Amber, the Natural Time Capsule*, 2nd ed. Natural History Museum, London, p. 112.
- Ross, A., Mellish, C., York, P., Crighton, B., 2010. Burmese Amber. In: Penney, D. (Ed.), *Biodiversity of Fossils in Amber from the Major World Deposits*. Siri Scientific Press, pp. 208–225.
- Royer, D.L., Berner, A., Montañez, I.P., Tabor, N.J., Beerling, D.J., 2004. CO₂ as a primary driver of Phanerozoic climate. *GSA Today* 14, 4–10. [https://doi.org/10.1130/1052-5173\(2004\)014<4:CAAPDO>2.0.CO;2](https://doi.org/10.1130/1052-5173(2004)014<4:CAAPDO>2.0.CO;2).
- Rust, J., Singh, H., Rana, R.S., McCann, T., Singh, L., 2010. Biogeographic and evolutionary implications of a diverse paleobiota in amber from the Early Eocene of India. *Proc. Natl. Acad. Sci.* 107, 18360–18365. <https://doi.org/10.1073/pnas.1007407107>.
- Scotes, C.R., Song, H., Mills, B.J.W., van der Meer, D., 2021. Phanerozoic paleotemperatures: the earth's changing climate during the last 540 million years. *Earth Sci. Rev.* 215, 103503 <https://doi.org/10.1016/j.earscirev.2021.103503>.
- Scotes, C.R., 2021. An Atlas of Phanerozoic Paleogeographic Maps: the Seas come in and the Seas Go out. *Annu. Rev. Earth Planet. Sci.* 49, 669–718. <https://doi.org/10.1146/annurev-earth-081320-064052>.
- Scott, A.C., 2018. In: *Burning Planet: The Story of Fire through Time*. Oxford University Press, Oxford, p. 256.
- Schmidt, A.R., Jancke, S., Lindquist, E.E., Ragazzi, E., Roghi, G., 2012. Arthropods in amber from the Triassic Period. *Proc. Natl. Acad. Sci.* 109, 14796–14801. <https://doi.org/10.1073/pnas.1208464109>.
- Sewall, J.O., van de Wal, R.S.W., van der Zwan, K., van Oosterhout, C., Dijkstra, H.A., et al., 2007. Climate model boundary conditions for four cretaceous time slices. Climate of the past. *Eur. Geosci. Union (EGU)* 3, 647–657. <https://doi.org/10.5194/cp-3-647-2007>.
- Seyfullah, L.J., Beimforde, Ch., Dal Corso, J., Perrichot, V., Rikkinen, J., et al., 2018. Production and preservation of resins – past and present. *Biol. Rev.* 93, 1684–1714. <https://doi.org/10.1111/brv.12414>.
- Seyfullah, L.J., Roberts, E.A., Schmidt, A.R., Ragazzi, E., Anderson, K.B., et al., 2020. Revealing the diversity of amber source plants from the Early Cretaceous Crato Formation Brazil. *BMC Evol. Biol.* 20, 107. <https://doi.org/10.1186/s12862-020-01651-2>.
- Shi, C., Wang, S., Cai, H., Zhang, H., Long, X., et al., 2022. Fire-prone Rhamnaceae with South African affinities in cretaceous Myanmar amber. *Nat. Plants* 8, 125–135. <https://doi.org/10.1038/s41477-021-01091-w>.
- Shi, G., Grimaldi, D.A., Harlow, G.E., Wang, J., Wang, M., et al., 2012. Age constraint on Burmese amber based on U-Pb dating of zircons. *Cretac. Res.* 37, 155–163. <https://doi.org/10.1016/j.cretres.2012.03.014>.
- Sidorchuk, E.A., Schmidt, A.R., Ragazzi, E., Roghi, G., Lindquist, E.E., 2015. Plant-feeding mite diversity in Triassic amber (Acar: Tetrapodili). *J. Syst. Palaeontol.* 13, 129–151. <https://doi.org/10.1080/14772019.2013.867373>.
- Solórzano Kraemer, M.M., Delclòs, X., Clapham, M.E., Arillo, A., Peris, D., 2018. Arthropods in modern resins reveal if amber accurately recorded forest arthropod communities. *Proc. Natl. Acad. Sci.* 115, 6739–6744. <https://doi.org/10.1073/pnas.18021138115>.
- Solórzano-Kraemer, M.M., Delclòs, X., Engel, M., Peñalver, E., 2020. A revised definition for copal and its significance for palaeontological and Anthropocene biodiversity-loss studies. *Sci. Rep.* 10, 19904. <https://doi.org/10.1038/s41598-020-76808-6>.
- Tabor, C.R., Poulsen, C.J., Lunt, D.J., Rosenbloom, N.A., Otto-Btiesner, B.L., et al., 2016. The cause of late cretaceous cooling: a multimodel-proxy comparison. *Geology* 44, 963–966. <https://doi.org/10.1130/G38363.1>.
- Tappert, R., McKellar, R.C., Wolfe, A.P., Tappert, M.C., Ortega-Blanco, J., et al., 2013. Stable carbon isotopes of C3 plant resins and ambers record changes in atmospheric oxygen since the Triassic. *Geochim. Cosmochim. Acta* 121, 240–262. <https://doi.org/10.1016/j.gca.2013.07.011>.
- Topper, M., Trabucho Alexandre, J., Tuenter, E., Meijer, P.Th., 2011. A regional ocean circulation model for the mid-cretaceous North Atlantic Basin: implications for black shale formation. *Clim. Past* 7, 277–297. <https://doi.org/10.5194/cp-7-277-2011>.
- Torsvik, T., Cocks, L., 2016. Cretaceous. In: Torsvik, T.H., Cocks, L.R.M. (Eds.), *Earth History and Palaeogeography*. Cambridge University Press, pp. 219–239. <https://doi.org/10.1017/9781316225523.014>.
- Trapp, S., Croteau, R., 2001. Defensive Resin Biosynthesis in Conifers. *Annu. Rev. Plant Physiol. Plant Mol. Biol.* 52, 689–724. <https://doi.org/10.1146/annurev.arplant.52.1.689>.
- Veltz, I., Paicheler, J.-C., Maksoud, S., Gèze, R., Azar, D., 2013. Context and genesis of the lebanese amberiferous palaeoenvironments at the Jurassic-cretaceous transition. *Terrest. Arthropod. Rev.* 6, 11–26. <https://doi.org/10.1163/18749836-06021055>.
- Villagómez, R., Jaillard, E., Bulot, L., Rivadeneira, M., Vera, R., 1996. The Aptian-late Albian marine transgression in the Oriente Basin of Ecuador. In: *Third ISAG, St Malo (France)*, pp. 521–524.
- Wade, D.C., Abraham, N.L., Farnsworth, A., Valdes, P.J., Bragg, F., et al., 2019. Simulating the climate response to atmospheric oxygen variability in the Phanerozoic: a focus on the Holocene, cretaceous and Permian. *Clim. Past* 15, 1463–1483. <https://doi.org/10.5194/cp-15-1463-2019>.
- Wagner, Th., Wallmann, K., Herrle, J.O., Hofmann, P., Stuesser, I., 2007. Consequences of moderate ~25,000 yr lasting emission of light CO₂ into the mid-cretaceous ocean. *Earth Planet. Sci. Lett.* 259, 200–211. <https://doi.org/10.1016/j.epsl.2007.04.045>.
- Cretaceous climate events and Short-Term Sea-Level changes. In: Wagreich, M., Hart, M. B., Sames, B., Yilmaz, I.O. (Eds.), *Geol. Soc. Lond., Spec. Publ.* 498, 1–8. <https://doi.org/10.1146/SP498-2019-156>.
- Wang, B., Rust, J., Engel, M.S., Szwedo, J., Dutta, S., et al., 2014a. A Diverse Paleobiota in early Eocene Fushun Amber from China. *Curr. Biol.* 24, 1606–1610. <https://doi.org/10.1016/j.cub.2014.05.048>.
- Wang, Y., Huang, Ch., Sun, B., Quan, Ch., Wu, J., Lin, Z., 2014b. Paleo-CO₂ variation trends and the cretaceous greenhouse climate. *Earth Sci. Rev.* 129, 136–147. <https://doi.org/10.1016/j.earscirev.2013.11.001>.
- Weir, B.S., Paderes, E.P., Anand, N., Uchida, J.Y., Pennycook, S.R., 2015. A taxonomic revision of Phytophthora Clade 5 including two new species, *Phytophthora agathidicida* and *P. cocois*. *Phytotaxa* 205, 21–38. <https://doi.org/10.11646/phytotaxa.205.1.2>.
- Wohlwend, S., Hart, M., Weissert, H., 2015. Ocean current intensification during the cretaceous oceanic anoxic event 2 – evidence from the northern Tethys. *Terra Nova* 27, 147–155. <https://doi.org/10.1111/ter.12142>.
- Xiao, L.F., Labandeira, C.C., Dilcher, D.L., Ren, D., 2022a. Arthropod and fungal herbivory at the dawn of angiosperm diversification: the Rose Creek plant assemblage of Nebraska, U.S.A. *Cretac. Res.* 131, 105088 <https://doi.org/10.1016/j.cretres.2021.105088>.
- Xiao, L.F., Labandeira, C.C., Dilcher, D.L., Ren, D., 2022b. Data, metrics, and methods for arthropod and fungal herbivory at the dawn of angiosperm diversification: the Rose Creek plant assemblage of Nebraska, U.S.A. *Data Brief* 42, 108170. <https://doi.org/10.1016/j.dib.2022.108170>.
- Zheng, D., Chang, S.-Ch., Perrichot, V., Dutta, S., Rudra, A., et al., 2018. A late cretaceous amber biota from Central Myanmar. *Nat. Commun.* 9, 3170. <https://doi.org/10.1038/s41467-018-05650-2>.
- Zhou, J., Poulsen, C.J., Pollard, D., White, T.S., 2008. Simulation of modern and middle cretaceous marine δ₁₈O with an ocean-atmosphere general circulation model. *Paleoceanogr. Paleoclimatol.* 23, PA3223. <https://doi.org/10.1029/2008PA001596>.
- Zhou, J., Poulsen, C.J., Rosenbloom, N., Shields, C., Briegleb, B., 2012. Vegetation-climate interactions in the warm mid-cretaceous. *Clim. Past* 8, 565–576. <https://doi.org/10.5194/cp-8-565-2012>.

Supplementary data A. Database of the Cretaceous amber-bearing outcrops worldwide

Outcrop name	Longitude	Latitude	Stage/s	Stage/s	Maps	Quantity amber (0=Scarce/mention; 1=Abundant)	Bioinclusions (0=No; 1= Yes)	References	Other references
Bath (Saint Thomas, Jamaica)	-76,354919	17,953601	Maastrichtian–Paleocene	12	4	0	0	Iturralde-Vinent (2001)	
Danek Bonebed Quarry 1 (Alberta, Canada)	-113,545832	53,436108	Maastrichtian	12	4	0	0	https://doi.org/10.1139/cjes-2014-0057	
Danek Bonebed Quarry 2 (Alberta, Canada)	-113,544974	53,436293	Maastrichtian	12	4	0	0	https://doi.org/10.1139/cjes-2014-0057	
Edmonton River Valley (Alberta, Canada)	-113,490833	53,527222	Maastrichtian	12	4	0	0	https://doi.org/10.1139/E08-049	
Morrin Bridge in Drumheller (Alberta, Canada)	-112,908556	51,647306	Maastrichtian	12	4	0	0	https://doi.org/10.1139/E08-049	
Horseshoe Canyon (Alberta, Canada)	-112,868556	51,539417	Maastrichtian	12	4	0	0	https://doi.org/10.1139/E08-049	
Royal Tyrrell Museum in Drumheller (Alberta, Canada)	-112,788889	51,478056	Maastrichtian	12	4	0	0	https://doi.org/10.1139/E08-049	
Tyrannosaurus Bonebed (Saskatchewan, Canada)	-108,499106	49,402238	Maastrichtian	12	4	0	0	https://doi.org/10.1016/j.cretres.2006.12.005	
Vansandt Site (Saskatchewan, Canada)	-108,257445	49,486959	Maastrichtian	12	4	0	0	Boulding (2019)	
Garfield County (Montana, USA)	-106,901625	47,615675	Maastrichtian	12	4	0	0	Wilson (2006)	
Ferris Fm. 1 (Wyoming, USA)	-106,880933	41,931502	Maastrichtian	12	4	0	0	https://doi.org/10.2113/35.2.163	
Medicine Bow Fm. (Wyoming, USA)	-106,669145	42,058093	Maastrichtian	12	4	0	0	https://doi.org/10.2113/35.2.163	
Ferris Fm. 2 (Wyoming, USA)	-106,592069	42,065867	Maastrichtian	12	4	0	0	https://doi.org/10.2113/35.2.163	
Boulder (Colorado, USA)	-105,243843	39,910218	Maastrichtian	12	4	0	0	Cockerell (1909)	
Hell Creek Fm. (South Dakota, USA)	-103,196625	45,236546	Maastrichtian	12	4	1	1	DePalma et al. (2010)	
Sewell (New Jersey, USA)	-75,143417	39,772944	Maastrichtian	12	4	0	0	Grimaldi et al. (1989)	
Serraduy (Huesca, Spain)	0,516363	42,350048	Maastrichtian	12	4	0	0	https://doi.org/10.1016/j.cretres.2018.02.016	
Figols (Barcelona, Spain)	1,839807	42,178607	Maastrichtian	12	4	0	0	Own data	
La Nou de Berguedà (Barcelona, Spain)	1,882722	42,168175	Maastrichtian	12	4	1	0	Own data	
Mina Esperanza (Barcelona, Spain)	1,945893	42,154305	Maastrichtian	12	4	0	0	Own data	
Mishor Rotem (Southern District, Israel)	35,128863	31,040633	Maastrichtian	12	4	0	0	https://doi.org/10.2113/176.1.37	
Therria (Meghalaya, India)	91,764444	25,18775	Maastrichtian	12	4	0	0	https://doi.org/10.1016/j.coal.2010.09.006	
Marlboro (New Jersey, USA)	-74,280025	40,358029	Campanian–Maastrichtian	11–12	4	0	0	Grimaldi et al. (1989)	
Lo Hueco (Cuenca, Spain)	-2,053211	39,96494	Campanian–Maastrichtian	11–12	4	0	0	https://doi.org/10.1111/i.1502-3931.2012.00331.x	
La Solana (Valencia, Spain)	-0,586799	39,202529	Campanian–Maastrichtian	11–12	4	0	0	Own data	
Red Willow River <i>Hadrosaurus</i> Skeleton (Alberta, Canada)	-119,520786	55,080688	Campanian	11	4	0	0	Tanke (2004)	
Wapiti River/Pipestone Creek Bonebed (Alberta, Canada)	-119,107382	55,051616	Campanian	11	4	0	0	Tanke (2004)	
Pipestone Creek <i>Pachyrhinosaurus</i> Bonebed (Alberta, Canada)	-119,102391	55,062508	Campanian	11	4	1	1	https://doi.org/10.1016/j.gr.2019.12.005	
Spring Creek Bonebed (Alberta, Canada)	-118,924046	55,075784	Campanian	11	4	0	0	https://doi.org/10.7717/peerj.11290	
Punta Baja (Baja California, Mexico)	-115,807023	29,957801	Campanian	11	4	0	0	https://doi.org/10.5962/p.168367	
Grassy Lake (Alberta, Canada)	-111,949575	49,896776	Campanian	11	4	1	1	McKellar and Wolfe (2010)	
Dinosaur Provincial Park (Alberta, Canada)	-111,484237	50,758061	Campanian	11	4	1	1	https://doi.org/10.1038/s41598-019-54400-x	
San Juan Basin (New Mexico, USA)	-108,1932	36,284962	Campanian	11	4	0	0	https://doi.org/10.1017/s2475262200009655	
Allen Ridge Fm. (Wyoming, USA)	-106,385368	41,989152	Campanian	11	4	0	0	https://doi.org/10.2113/35.2.163	
Brewster County (Texas, USA)	-103,568819	29,203749	Campanian	11	4	0	0	https://doi.org/10.1306/8626CE33-173B-11D7-8645000102C1865D	
Cedar Lake (Manitoba, Canada)	-100,970456	53,438313	Campanian	11	4	1	1	McKellar and Wolfe (2010)	
Neuse River (North Carolina, USA)	-78,04321	35,363653	Campanian	11	4	0	0	https://doi.org/10.1016/j.cretres.2017.10.011	
Tar River (North Carolina, USA)	-77,480933	35,679194	Campanian	11	4	0	0	Berry (1907)	
Ellisdale (New Jersey, USA)	-74,585604	40,130104	Campanian	11	4	0	0	Grimaldi et al. (1989)	
Cheesequake (New Jersey, USA)	-74,287069	40,422098	Campanian	11	4	0	0	Grimaldi et al. (1989)	
Martigues north (Provence-Alpes-Côte d'Azur, France)	5,038903	43,424552	Campanian	11	4	0	0	https://doi.org/10.1051/bsgf/2020048	
Tilin (Mangway, Myanmar)	94,083333	21,683333	Campanian	11	4	1	1	https://doi.org/10.1038/s41467-018-05650-2	
Tuna-1 (Victoria, Australia)	148,419348	-38,173452	Santonian–Campanian	10–11	4	1	0	https://doi.org/10.1038/s41598-020-62252-z	
Ajka (Bakony Mts, Hungary)	17,586446	47,088728	Santonian	10	4	1	1	Borkent (1997)	https://doi.org/10.1016/j.cretres.2022.105314
Coffee Bluff (Tennessee, USA)	-88,249204	35,282826	Santonian	10	4	0	0	Wade (1920)	
Parsons (Tennessee, USA)	-88,172014	35,641774	Santonian	10	4	0	0	Wade (1920)	
Ingersoll shale (Alabama, USA)	-84,996031	32,44106	Santonian	10	4	0	0	https://doi.org/10.1016/j.cretres.2009.09.008	
Kinkora (New Jersey, USA)	-74,750999	40,118816	Santonian	10	4	0	0	Grimaldi et al. (1989)	
Cliffwood (New Jersey, USA)	-74,221207	40,442886	Santonian	10	4	0	0	Grimaldi et al. (1989)	
Piolenc 2 (Provence-Alpes-Côte d'Azur, France)	4,762482	44,182905	Santonian	10	4	1	1	https://doi.org/10.1051/bsgf/2020048	
Piolenc 1 (Provence-Alpes-Côte d'Azur, France)	4,765538	44,184572	Santonian	10	4	1	1	https://doi.org/10.1016/S1631-0683(03)00041-1	https://doi.org/10.1051/bsgf/2020048
Martigues-La Mède (Provence-Alpes-Côte d'Azur, France)	5,073071	43,398163	Santonian	10	4	0	0	https://doi.org/10.1016/j.crpv.2006.05.005	https://doi.org/10.1051/bsgf/2020048
Ensùes-la-Redonne 1 (Provence-Alpes-Côte d'Azur, France)	5,202521	43,330107	Santonian	10	4	0	0	https://doi.org/10.1051/bsgf/2020048	
Ensùes-la-Redonne 2 (Provence-Alpes-Côte d'Azur, France)	5,20641	43,329551	Santonian	10	4	0	0	https://doi.org/10.1051/bsgf/2020048	
Belcodène (Provence-Alpes-Côte d'Azur, France)	5,578364	43,408449	Santonian	10	4	0	1	https://doi.org/10.1016/j.janpal.2013.03.001	https://doi.org/10.1051/bsgf/2020048
Plan d'Aups/La Brasque (Provence-Alpes-Côte d'Azur, France)	5,705315	43,322615	Santonian	10	4	0	0	https://doi.org/10.1051/bs	

Saint-Marcel-de-Careiret (Provence-Alpes-Côte d'Azur, France)	4,483409	44,150055	Turonian	8	3	0	0	Perrichot et al. (2007)	
THAO1 (Victoria, Australia)	142,90215	-39,237336	Turonian	8	3	0	0	https://doi.org/10.1371/journal.pone.0121307	
Thylacine-1 (Victoria, Australia)	142,913649	-39,239509	Turonian	8	3	0	0	https://doi.org/10.1371/journal.pone.0121307	
Minerva-1 (Victoria, Australia)	142,954795	-38,701905	Turonian	8	3	0	0	https://doi.org/10.1371/journal.pone.0121307	
Minerva-2a (Victoria, Australia)	142,957147	-38,716434	Turonian	8	3	0	0	https://doi.org/10.1371/journal.pone.0121307	
Iona-4 (Victoria, Australia)	142,974889	-38,605287	Turonian	8	3	0	0	https://doi.org/10.1371/journal.pone.0121307	
Chatham Islands (New Zealand)	-176,223832	-44,245421	Cenomanian-Turonian	7-8	3	1	0	https://doi.org/10.1038/s41598-020-6225z-2	
Quality Creek (British Columbia, Canada)	-120,954293	55,167777	Cenomanian-Turonian	7-8	3	0	0	Quinney (2015)	
Timmerdyakh-Khaya (Sakha Republic (Yakutia), Russian Federation)	123,569722	64,054444	Cenomanian-Turonian	7-8	3	1	1	http://dx.doi.org/10.1016/i.cretres.2015.12.025	
Tal-Yuryakh (Magadan Oblast, Russian Federation)	146,664805	63,294907	Cenomanian-Turonian	7-8	3	0	0	Zherickin and Escov (1999)	
Dunvegan (Alberta, Canada)	-118,571736	55,931305	Cenomanian	7	3	0	0	Quinney (2015)	
Grayson County (Texas, USA)	-96,710549	33,65432	Cenomanian	7	3	0	0	https://doi.org/10.9784/LEB5(3)Friedman.01	
Woodbridge (New Jersey, USA)	-74,271099	40,555977	Cenomanian	7	3	0	0	Grimaldi et al. (1989)	
Mata Amarilla Fm. (Santa Cruz, Argentina)	-71,484137	-49,526933	Cenomanian	7	3	0	0	Petrulevičius and Iglesias (2018)	
Alto de El Caleyu (Asturias, Spain)	-5,874667	43,323627	Cenomanian	7	3	0	0	Own data	
Pruvia (Asturias, Spain)	-5,767591	43,452634	Cenomanian	7	3	0	0	Own data	
Torrelaguna (Madrid, Spain)	-3,542636	40,842191	Cenomanian	7	3	0	0	Own data	
Hoz Seca (Guadalajara, Spain)	-1,871413	40,5328	Cenomanian	7	3	0	0	https://doi.org/10.3989/tp.2012.12098	
Aix Island (Nouvelle-Aquitaine, France)	-1,15607	46,019394	Cenomanian	7	3	1	1	Néraudeau et al. (2009)	
Enet Island (Nouvelle-Aquitaine, France)	-1,143324	46,003307	Cenomanian	7	3	0	0	Perrichot et al. (2007)	
Fouras/Bois-Vert (Nouvelle-Aquitaine, France)	-1,100376	45,992477	Cenomanian	7	3	0	0	Perrichot et al. (2007)	
Saint-Lon (Nouvelle-Aquitaine, France)	-1,099688	43,611196	Cenomanian	7	3	0	0	Perrichot et al. (2007)	
Fouras (Nouvelle-Aquitaine, France)	-1,079191	45,974085	Cenomanian	7	3	0	1	https://doi.org/10.1016/S1631-0683(03)00032-0	
Cadeuil (Nouvelle-Aquitaine, France)	-0,939347	45,767241	Cenomanian	7	3	1	1	https://doi.org/10.1016/i.cretres.2008.05.009	
Losa del Obispo (Valencia, Spain)	-0,879237	39,71653	Cenomanian	7	3	0	0	Own data	
Les Renardières (Nouvelle-Aquitaine, France)	-0,829285	45,965954	Cenomanian	7	3	1	1	https://doi.org/10.1016/i.cretres.2018.10.011	
Briollay (Pays de la Loire, France)	-0,513936	47,555998	Cenomanian	7	3	0	0	Perrichot et al. (2007)	
Hucheloup (Pays de la Loire, France)	-0,502208	47,533926	Cenomanian	7	3	0	0	https://doi.org/10.1016/i.annpal.2013.10.001	
Le Brouillard (Pays de la Loire, France)	-0,492037	47,53565	Cenomanian	7	3	0	0	https://doi.org/10.1016/i.annpal.2013.10.001	
Neau (Pays de la Loire, France)	-0,459807	48,159989	Cenomanian	7	3	1	1	https://doi.org/10.1051/bsgf/2020039	
Précigné (Pays de la Loire, France)	-0,325368	47,772811	Cenomanian	7	3	0	0	https://doi.org/10.1344/105.000001873	
Durtal (Pays de la Loire, France)	-0,281249	47,683508	Cenomanian	7	3	1	1	https://doi.org/10.1021/acs.inatprod.5b00093	
La Brousse (Pays de la Loire, France)	-0,054578	47,776108	Cenomanian	7	3	0	0	https://doi.org/10.1344/105.000001873	
Saint-Jean-du-Bois (Pays de la Loire, France)	-0,03422	47,868666	Cenomanian	7	3	0	0	https://doi.org/10.1344/105.000001873	
Mézéray (Pays de la Loire, France)	-0,025052	47,825517	Cenomanian	7	3	0	0	https://doi.org/10.1344/105.000001873	
La-Suze-sur-Sarthe (Pays de la Loire, France)	0,014017	47,898511	Cenomanian	7	3	0	0	https://doi.org/10.1344/105.000001873	
Röezé-sur-Sarthe (Pays de la Loire, France)	0,071942	47,902842	Cenomanian	7	3	0	0	https://doi.org/10.1344/105.000001873	
La Bazoge (Pays de la Loire, France)	0,127984	48,099435	Cenomanian	7	3	0	0	https://doi.org/10.1344/105.000001873	
Fessard (Pays de la Loire, France)	0,136578	47,82726	Cenomanian	7	3	0	0	https://doi.org/10.1344/105.000001873	
Mansigné (Pays de la Loire, France)	0,144061	47,751894	Cenomanian	7	3	0	0	https://doi.org/10.1344/105.000001873	
Moncé-en-Belin (Pays de la Loire, France)	0,185164	47,889764	Cenomanian	7	3	0	0	https://doi.org/10.1344/105.000001873	
La Buzinie (Nouvelle-Aquitaine, France)	0,19365	45,705148	Cenomanian	7	3	1	1	https://doi.org/10.1016/i.cretres.2018.10.011	
Écommoy (Pays de la Loire, France)	0,259718	47,810306	Cenomanian	7	3	1	1	https://doi.org/10.1344/105.000001873	
Scorbé-Clairvaux-La Bergeonneau (Nouvelle-Aquitaine, France)	0,387262	46,800977	Cenomanian	7	3	0	0	https://doi.org/10.1051/bsgf/2020034	
Châtelerault-La Désirée (Nouvelle-Aquitaine, France)	0,540599	46,831536	Cenomanian	7	3	0	0	https://doi.org/10.1051/bsgf/2020034	
Saint-Cyprien (Nouvelle-Aquitaine, France)	1,07674	44,874946	Cenomanian	7	3	0	0	Perrichot et al. (2007)	
Veyrines (Nouvelle-Aquitaine, France)	1,079551	44,802915	Cenomanian	7	3	0	0	https://doi.org/10.1016/i.annpal.2013.07.001	
Simeyrols (Nouvelle-Aquitaine, France)	1,338992	44,923328	Cenomanian	7	3	0	0	https://doi.org/10.1016/i.annpal.2013.07.001	
Fourtou (Occitanie, France)	2,429223	42,902994	Cenomanian	7	3	1	1	https://doi.org/10.1016/i.annpal.2013.06.002	
Schliersee (Bavaria, Germany)	11,877551	47,717066	Cenomanian	7	3	0	0	https://doi.org/10.1006/cres.2001.0267	
Nové Strašeci (Central Bohemian Region, Czech Republic)	13,910101	50,132583	Cenomanian	7	3	0	0	https://doi.org/10.1016/i.jenvrad.2016.04.004	
Křižany (Liberec, Czech Republic)	14,855637	50,708399	Cenomanian	7	3	0	0	https://doi.org/10.1016/i.jenvrad.2016.04.004	
Nová Ves (South Moravian, Czech Republic)	16,310337	49,113592	Cenomanian	7	3	0	0	https://doi.org/10.1135/cccc19763138	
Valchov (South Moravian, Czech Republic)	16,712453	49,482615	Cenomanian	7	3	0	0	https://doi.org/10.1135/cccc19763138	
Agdzakend (Goranboy District, Azerbaijan)	46,493611	40,404167	Cenomanian	7	3	1	1	https://doi.org/10.1016/i.cretres.2015.12.025	
Nizhnyaya Agapa (Krasnoyarsk Krai, Russia Federation)	86,817831	70,165067	Cenomanian	7	3	1	1	https://doi.org/10.1016/i.cretres.2	

Qeqertarsuatsiaq/Hare Island (Greenland)	-54,879139	70,421907	Albian–Cenomanian	6–7	2	0	0	https://doi.org/10.1111/i.1475-4754.1996.tb00780.x	https://www.science.org/doi/10.1126/science.163.3872.1157
San Claudio (Asturias, Spain)	-5,914707	43,352554	Albian–Cenomanian	6–7	2	0	0	Own data	
La Manjoya (Asturias, Spain)	-5,860553	43,341174	Albian–Cenomanian	6–7	2	0	0	Own data	
Fonfría (Cantabria, Spain)	-4,265705	43,391447	Albian–Cenomanian	6–7	2	0	0	https://doi.org/10.1016/j.orggeochem.2015.12.010	
Oreña (Cantabria, Spain)	-4,138525	43,392009	Albian–Cenomanian	6–7	2	0	0	https://doi.org/10.1016/j.orggeochem.2015.12.010	
Cuchiá (Cantabria, Spain)	-4,016127	43,445557	Albian–Cenomanian	6–7	2	0	0	Own data	
Somocueva (Cantabria, Spain)	-3,945295	43,469855	Albian–Cenomanian	6–7	2	1	1	Own data	
Archingeay-Les Nouillers (Nouvelle-Aquitaine, France)	-0,696843	45,93744	Albian–Cenomanian	6–7	2	1	1	https://doi.org/10.1016/S0016-6995(02)00024-4	
Estercuel (Teruel, Spain)	-0,640288	40,855012	Albian–Cenomanian	6–7	2	1	0	Own data	
Logata (Krasnoyarsk Krai, Russia)	99,098412	73,781097	Albian–Cenomanian	6–7	2	0	0	https://doi.org/10.1134/S0031030119100149	
Novaya (Krasnoyarsk Krai, Russian Federation)	101,045395	72,576578	Albian–Cenomanian	6–7	2	0	0	https://doi.org/10.1134/S0031030119100149	
Baikura (Krasnoyarsk Krai, Russian Federation)	101,426389	73,833056	Albian–Cenomanian	6–7	2	1	1	https://doi.org/10.1016/j.cretres.2015.12.025	https://doi.org/10.1134/S0031030119100149
Gubina Gora (Krasnoyarsk Krai, Russian Federation)	102,59996	71,976294	Albian–Cenomanian	6–7	2	0	0	https://doi.org/10.1134/S0031030119100149	
Moroskop (Krasnoyarsk Krai, Russia)	103,489853	72,492496	Albian–Cenomanian	6–7	2	0	0	https://doi.org/10.1134/S0031030119100149	
Nikon-Yuryakh (Krasnoyarsk Krai, Russia)	105,132309	73,168606	Albian–Cenomanian	6–7	2	0	0	https://doi.org/10.1134/S0031030119100149	
Bediye (Krasnoyarsk Krai, Russia)	106,324326	73,597126	Albian–Cenomanian	6–7	2	0	0	https://doi.org/10.1134/S0031030119100149	
Syndasko in Khatangskaya Guba (Krasnoyarsk Krai, Russian Federation)	108,235947	73,280064	Albian–Cenomanian	6–7	2	0	0	https://doi.org/10.1134/S0031030119100149	
Ellsworth County (Kansas, USA)	-98,03351	38,658596	Albian	6	2	0	0	Ward Aber and Kosmowska-Ceramowicz (2001)	
Pungarayacu (Napo, Ecuador)	-77,741328	-0,706706	Albian	6	2	0	0	https://doi.org/10.1016/j.jsames.2018.02.004	Own data
Washington D.C. (District of Columbia, USA)	-76,96074	38,872161	Albian	6	2	0	0	Lanhengim and Beck (1968)	
Cape Sable (Maryland, USA)	-76,501509	39,083242	Albian	6	2	0	0	https://doi.org/10.1126/science.3.68.582	https://doi.org/10.26879/847
Maguito (Lisboa, Portugal)	-9,449777	38,865081	Albian	6	2	0	0	Barrón et al. (2001)	Peñalver et al. (2018a)
Corte Caleyu (Asturias, Spain)	-5,873173	43,323392	Albian	6	2	0	0	Peñalver et al. (2018b)	
El Caleyu (Asturias, Spain)	-5,870998	43,322488	Albian	6	2	1	1	Peñalver and Delclòs (2010)	
La Rodada (Asturias, Spain)	-5,862788	43,331092	Albian	6	2	0	1	Peñalver and Delclòs (2010)	
Pola de Siero (Asturias, Spain)	-5,653265	43,383003	Albian	6	2	0	1	Peñalver and Delclòs (2010)	
Puerto del Boyar (Cádiz, Spain)	-5,418143	36,749342	Albian	6	2	0	0	Own data	
Trambarria (Asturias, Spain)	-5,39535	43,365272	Albian	6	2	0	0	Own data	
El Soplao (Cantabria, Spain)	-4,447222	43,305556	Albian	6	2	1	1	https://doi.org/10.1344/105.000001443	
San Vicente de la Barquera (Cantabria, Spain)	-4,398027	43,37878	Albian	6	2	0	0	Own data	
Basconcillos del Tozo-Aguilar de Campoo (Burgos, Spain)	-4,075919	42,753345	Albian	6	2	0	0	Own data	
Olleros (Palencia, Spain)	-4,023417	42,784019	Albian	6	2	0	0	Own data	
Ensenada del Camello (Cantabria, Spain)	-3,776067	43,470615	Albian	6	2	0	1	Own data	
Pancorbo (Burgos, Spain)	-3,109928	42,645703	Albian	6	2	0	0	Own data	
Salinillas de Buradón (Álava, Spain)	-2,856625	42,638969	Albian	6	2	1	1	https://doi.org/10.11158/saa.13.3.13	
San Felices (La Rioja, Spain)	-2,84788	42,625397	Albian	6	2	0	0	Own data	
Peñacerrada II (Álava, Spain)	-2,724882	42,620316	Albian	6	2	1	1	https://doi.org/10.1007/s12371-010-0030-9	
Peñacerrada I (Burgos, Spain)	-2,714722	42,678611	Albian	6	2	1	1	https://doi.org/10.1666/0022-3360/2000/0742.0.CO;2	
Zubielki (Navarra, Spain)	-2,065931	42,680208	Albian	6	2	0	0	Own data	
Moratalla (Murcia, Spain)	-1,995206	38,232161	Albian	6	2	0	0	Peñalver et al. (2013)	
Vilel (Teruel, Spain)	-1,178101	40,239746	Albian	6	2	0	0	Own data	
Puy-Puy (Nouvelle-Aquitaine, France)	-0,880909	45,963866	Albian	6	2	1	1	https://doi.org/10.1016/j.cretres.2019.03.022	
San Just (Teruel, Spain)	-0,834283	40,777977	Albian	6	2	1	1	https://doi.org/10.1016/j.cretres.2006.12.004	
Palomas de Arroyos (Teruel, Spain)	-0,744598	40,766372	Albian	6	2	0	0	Own data	
Alcaine-Oliete (Teruel, Spain)	-0,67808	40,96797	Albian	6	2	0	0	Own data	
Quesa (Valencia, Spain)	-0,672706	39,082456	Albian	6	2	0	0	Own data	
Arroyo de la Pascueta Teruel, Spain)	-0,604085	40,214037	Albian	6	2	1	1	Peñalver and Delclòs (2010)	
San Vicente del Raspeig (Alicante, Spain)	-0,574628	38,363295	Albian	6	2	0	0	Own data	
Ariño (Teruel, Spain)	-0,558794	41,031691	Albian	6	2	1	1	https://doi.org/10.7554/elife.72477	
Molino de Arriba (Castellón, Spain)	-0,549492	40,149465	Albian	6	2	0	0	Own data	
La Hoya (Castellón, Spain)	-0,52761	40,198551	Albian	6	2	1	1	Peñalver and Delclòs (2010)	
Valle de Andorra (Teruel, Spain)	-0,47221	40,992126	Albian	6	2	0	0	Own data	
Mina Tremedal (Teruel, Spain)	-0,429879	40,9302	Albian	6	2	0	0	Own data	
Serra Gelada (Alicante, Spain)	-0,061944	38,554207	Albian	6	2	0	0	Own data	
Son Vida (Mallorca, Spain)	2,591447	39,599691	Albian	6	2	0	0	Own data	
Bédoïn (Provence-Alpes-Côte d'Azur, France)	5,191942	44,125688	Albian	6	2	0	0	https://doi.org/10.1051/bsgf/2020048	
Aubignosc (Provence-Alpes-Côte d'Azur, France)	5,963911	44,115422	Albian	6	2	0	0	https://doi.org/10.1051/bsgf/2020048	
Salignac 2 (Provence-Alpes-Côte d'Azur, France)	5,990576	44,175147	Albian	6	2	1	1	https://doi.org/10.1051/bsgf/2020048	
Ra Stua (Veneto, Italy)	12,095667</								

Maknouniyeh (South, Lebanon)	35,539527	33,528022	Barremian	4	2	1	1	https://doi.org/10.11646/palaeoentomology.3.2.2	
Roum-Aazour Hornsiyeh (South, Lebanon)	35,560668	33,552665	Barremian	4	2	1	1	https://doi.org/10.11646/palaeoentomology.3.2.2	
Rihane (South, Lebanon)	35,561993	33,448601	Barremian	4	2	1	1	https://doi.org/10.11646/palaeoentomology.3.2.2	
Jezzine (South, Lebanon)	35,572052	33,547825	Barremian	4	2	1	1	https://doi.org/10.11646/palaeoentomology.3.2.2	
Wadi Jezzine (South, Lebanon)	35,57909	33,552797	Barremian	4	2	1	1	https://doi.org/10.11646/palaeoentomology.3.2.2	
Daychouniyeh (Mount Lebanon, Lebanon)	35,582019	33,85171	Barremian	4	2	1	1	https://doi.org/10.11646/palaeoentomology.3.2.2	
Ain Zalta (Mount Lebanon, Lebanon)	35,687719	33,731856	Barremian	4	2	1	1	https://doi.org/10.11646/palaeoentomology.3.2.2	
Hammana-Mdeyrif (Mount Lebanon, Lebanon)	35,731235	33,806256	Barremian	4	2	1	1	https://doi.org/10.11646/palaeoentomology.3.2.2	
Ain Dara 2 (Mount Lebanon, Lebanon)	35,731536	33,794078	Barremian	4	2	1	1	https://doi.org/10.11646/palaeoentomology.3.2.2	https://doi.org/10.11646/palaeoentomology.4.1.4
Ain Dara 1 (Mount Lebanon, Lebanon)	35,735827	33,794399	Barremian	4	2	1	1	https://doi.org/10.11646/palaeoentomology.3.2.2	https://doi.org/10.11646/palaeoentomology.4.1.4
Falougha (Mount Lebanon, Lebanon)	35,75707	33,838379	Barremian	4	2	1	1	https://doi.org/10.11646/palaeoentomology.3.2.2	
Ouata El-Jacou (Mount Lebanon, Lebanon)	35,759023	34,021883	Barremian	4	2	1	1	https://doi.org/10.11646/palaeoentomology.3.2.2	
Kfar Selouan (Mount Lebanon, Lebanon)	35,779858	33,848538	Barremian	4	2	1	1	https://doi.org/10.11646/palaeoentomology.3.2.2	
Dahr Qloum Hachem (Mount Lebanon, Lebanon)	35,789799	33,997378	Barremian	4	2	0	0	https://doi.org/10.11646/palaeoentomology.3.4.14	
Baskinta (Mount Lebanon, Lebanon)	35,791466	33,942932	Barremian	4	2	0	0	https://doi.org/10.11646/palaeoentomology.3.6.7	
Red Rock/Mazraat Kfarlibiane (Mount Lebanon, Lebanon)	35,797855	33,978488	Barremian	4	2	1	1	https://doi.org/10.11646/palaeoentomology.3.4.14	https://doi.org/10.11646/palaeoentomology.4.1.4
Jabal Er Roueis (Mount Lebanon, Lebanon)	35,815911	34,008211	Barremian	4	2	0	0	https://doi.org/10.11646/palaeoentomology.3.4.14	
Bouarji (Beqaa, Lebanon)	35,82478	33,821506	Barremian	4	2	1	1	https://doi.org/10.11646/palaeoentomology.3.2.2	
Tannourine (North, Lebanon)	35,897961	34,169385	Barremian	4	2	1	1	https://doi.org/10.11646/palaeoentomology.3.2.2	
Aita El-Foukhar (Beqaa, Lebanon)	35,925207	33,629598	Barremian	4	2	1	1	https://doi.org/10.11646/palaeoentomology.3.2.2	
Hadath El-Joubbeh (North, Lebanon)	35,938645	34,247394	Barremian	4	2	1	1	https://doi.org/10.11646/palaeoentomology.3.2.2	
Beqaa Kafra (North, Lebanon)	36,020013	34,234764	Barremian	4	2	1	1	https://doi.org/10.11646/palaeoentomology.3.2.2	
Bcharreh (North, Lebanon)	36,035634	34,250374	Barremian	4	2	1	1	https://doi.org/10.11646/palaeoentomology.3.2.2	
Zarzar Lake (Rif Dimashq, Syria)	36,043994	33,618295	Barremian	4	2	1	1	https://doi.org/10.1016/j.cretres.2014.12.006	
Nimrin/El-Dabsheh (North, Lebanon)	36,061641	34,380956	Barremian	4	2	1	1	https://doi.org/10.11646/palaeoentomology.3.2.2	
Hrar (Akkar, Lebanon)	36,145641	34,462113	Barremian	4	2	0	0	https://doi.org/10.11646/palaeoentomology.2.4.6	
Brissa (North, Lebanon)	36,169015	34,401566	Barremian	4	2	1	1	https://doi.org/10.11646/palaeoentomology.3.2.2	
Mechmech/El-Rassif (Akkar, Lebanon)	36,182864	34,46378	Barremian	4	2	0	0	https://doi.org/10.11646/palaeoentomology.2.4.6	
Mechmech/Aqabet Raqiya (Akkar, Lebanon)	36,195365	34,451836	Barremian	4	2	0	0	https://doi.org/10.11646/palaeoentomology.2.4.6	
Jord Hrar (North, Lebanon)	36,200643	34,386834	Barremian	4	2	0	0	https://doi.org/10.11646/palaeoentomology.3.6.7	
Mechmech/Ain El-Khyar (Akkar, Lebanon)	36,215643	34,438224	Barremian	4	2	1	1	https://doi.org/10.11646/palaeoentomology.2.4.6	https://doi.org/10.11646/palaeoentomology.4.1.4
Esh-Sheaybeh (Baalbek-Hermel, Lebanon)	36,244363	33,927009	Barremian	4	2	1	1	https://doi.org/10.11646/palaeoentomology.3.2.2	
East Baghdad Oilfield (Iraq)	44,527626	33,304931	Barremian	4	2	0	0	https://doi.org/10.2113/geoarabia020329	https://doi.org/10.1111/j.1747-5457.1993.tb00344.x
Orcera (Jaén, Spain)	-2,640384	38,320313	Hauterivian–Barremian	3–4	2	0	0	Own data	
Maracangalha Fm. (Bahia, Brazil)	-38,455995	-12,359701	Berriasian–Barremian	1–4	2	0	0	https://doi.org/10.1016/j.orggeochem.2009.05.002	
Orcera (Jaén, Spain)	-2,640384	38,320313	Hauterivian–Barremian	3–4	1	0	0	Own data	
Alaró (Mallorca, Spain)	2,842847	39,716434	Hauterivian	3	1	0	0	Own data	
Golling (Salzburg, Austria)	13,176145	47,574799	Hauterivian	3	1	1	1	Borkent et al. (1997)	
Baboor (Southern District, Israel)	35,114071	31,134232	Valanginian–Hauterivian	2–3	1	0	0	https://doi.org/10.1016/0899-5362(92)90106-M	
Kokhov (Southern District, Israel)	34,657849	31,64491	Valanginian–Hauterivian	2–3	1	0	0	https://doi.org/10.1016/0899-5362(92)90106-M	
Qiryat Shermona (Northern District, Israel)	35,558083	33,218157	Valanginian–Hauterivian	2–3	1	0	0	https://doi.org/10.1016/0899-5362(92)90106-M	
Mount Hermon (Northern District, Israel)	35,751543	33,267612	Valanginian–Hauterivian	2–3	1	0	0	https://doi.org/10.1016/0899-5362(92)90106-M	
Bexhill (East Sussex, England)	0,440242	50,860536	Valanginian	2	1	0	0	https://doi.org/10.1144/0016-76492008-158	
Kirkwood (Eastern Cape, South Africa)	25,47847	-33,413099	Valanginian	2	1	0	0	https://doi.org/10.1016/S1631-0683(02)00014-3	https://doi.org/10.1111/j.1502-3931.2002.tb00090.x
Hastings (East Sussex, England)	0,51837	50,843742	Berriasian–Valanginian	1–2	1	0	1	https://doi.org/10.1144/0016-76492008-158	
Maracangalha Fm. (Bahia, Brazil)	-38,455995	-12,359701	Berriasian–Barremian	1–4	1	0	0	https://doi.org/10.1016/j.orggeochem.2009.05.002	

Country	Longitude	Latitude	Wood Taxon	Family	Stage/s	Stages	Maps	Geological and geographical info	DOI or authors
Antarctica	-60	-62	<i>Agathoxylon chapmannae</i>	Araucariaceae	Cenomanian–Campanian	7–11	4	Williams Point Beds, Dragon Cove, Williams Point	https://doi.org/10.1130/G32733.1 Peralta-Medina & Falcon-Lang (2012)
Antarctica	-60	-62	<i>Agathoxylon floresii</i>	Araucariaceae	Cenomanian–Campanian	7–11	4	Williams Point, Livingston Island	https://doi.org/10.1130/G32733.1
Antarctica	-60	-62	<i>Araucarioptis antarcticus</i>	Araucariaceae	Cenomanian–Campanian	7–11	4	Williams Point Beds, Dragon Cove, Williams Point	https://doi.org/10.1130/G32733.1
Antarctica	-56	-64	<i>Agathoxylon pseudoporechymatosum</i>	Araucariaceae	Maastrichtian	12	4	Lopez de Bertodano Fm., Seymour Island	https://doi.org/10.1130/G32733.1
Antarctica	-56	-64	<i>Agathoxylon</i>	Araucariaceae	Maastrichtian	12	4	Lopez de Bertodano Fm., Seymour Island	https://doi.org/10.1130/G32733.1
Antarctica	-56	-64	<i>Araucarioptis</i>	Araucariaceae	Maastrichtian	12	4	Lopez de Bertodano Fm., Seymour Island	https://doi.org/10.1130/G32733.1
Antarctica	-58	-62	<i>Dadoxylon</i>	Araucariaceae	Maastrichtian	12	4	Barton Peninsula, King George Island	https://doi.org/10.1130/G32733.1
Antarctica	-57,918325	-63,862606	<i>Agathoxylon antarcticus</i>	Araucariaceae	Santonian–Lower Campanian	10–11	4	Santa Marta Fm., Brandy Bay, James Ross Island	https://doi.org/10.1016/j.cretres.2017.04.016
Antarctica	-57,918325	-63,862606	<i>Agathoxylon pseudoporechymatosum</i>	Araucariaceae	Santonian–Lower Campanian	10–11	4	Santa Marta Fm., Brandy Bay, James Ross Island	https://doi.org/10.1016/j.cretres.2017.04.016
Antarctica	-57,918325	-63,862606	<i>Agathoxylon kellerense</i>	Araucariaceae	Santonian–Lower Campanian	10–11	4	Santa Marta Fm., Brandy Bay, James Ross Island	https://doi.org/10.1016/j.cretres.2017.04.016
Argentina	-69	-45	<i>Agathoxylon</i> sp.	Araucariaceae	Cenomanian–Coniacian	7–9	4	Bajo Barreal Fm., Puesto Confluencia, Chubut	https://doi.org/10.1130/G32733.1
Argentina	-67,80152801	-43,3483566	<i>Agathoxylon antarcticum</i>	Araucariaceae	Campanian–Maastrichtian	11–12	4	Puntudo Chico Fm., El Mirasol, Chubut	https://doi.org/10.1016/j.cretres.2019.01.022
Belgium	5	50	<i>Dammoxylon aachense</i>	Araucariaceae	Santonian	10	4	Aachen Fm., Kaskorb quarry, La Calamine	https://doi.org/10.1130/G32733.1
Belgium	6	50	<i>Dadoxylon</i>	Araucariaceae	Santonian	10	4	Kelmis, literature, Kunzmann	https://doi.org/10.1130/G32733.1
Chile	-70	-30	<i>Agathoxylon pichasquensis</i>	Araucariaceae	Campanian–Maastrichtian	11–12	4	Pichasca, Ovalle, literature, Torres	https://doi.org/10.1130/G32733.1
Chile	-70	-30	<i>Agathoxylon pichasensis</i>	Araucariaceae	Campanian–Maastrichtian	11–12	4	Pichasca	https://doi.org/10.1130/G32733.1
Chile	-73,05133955	-36,6170815	<i>Agathoxylon pluriserratum</i>	Araucariaceae	Maastrichtian	12	4	Quiriquina Fm., bahía de las Tablas, Isla Quiriquina	Torres & Biro-Bagozky (1986)
Chile	-73,05133955	-36,6170815	<i>Agathoxylon resinosum</i>	Araucariaceae	Maastrichtian	12	4	Quiriquina Fm., bahía de las Tablas, Isla Quiriquina	Torres & Biro-Bagozky (1986)
Germany	8	49	<i>Agathoxylon subhercynicum</i>	Araucariaceae	Coniacian	9	4	Heidelberg Fm.	https://doi.org/10.1130/G32733.1
Hungary	17	47	<i>Agathoxylon angustifolium</i>	Araucariaceae	Santonian	10	4	Ajka, literature, Greguss	https://doi.org/10.1130/G32733.1
Japan	142	42	<i>Agathoxylon tankoensis</i>	Araucariaceae	Cenomanian–Santonian	7–10	4	Hokkaido, Yubari, literature	https://doi.org/10.1130/G32733.1
Japan	141,6385382	40,3833263	<i>Agathoxylon</i>	Araucariaceae	Santonian–Campanian	10–11	4	Honshu, Iwate Prefecture, Taneichi (Outer Zone), Taneichi Fm.	https://doi.org/10.1016/j.iseaes.2010.11.010
Korea	122	34	<i>Agathoxylon byeongpungense</i>	Araucariaceae	Campanian?	11	4	Byeongpong Island, southern extremity of Jindo County, South Jeolla Province	https://doi.org/10.1130/G32733.1
Madagascar	47	-19	<i>Agathoxylon madagascariense</i>	Araucariaceae	Turonian–Maastrichtian	8–12	4	literature, Fliche	https://doi.org/10.1130/G32733.1
Mexico	-101	27	<i>Agathoxylon</i> sp.	Araucariaceae	Maastrichtian	12	4	Olmos Fm., Barreroan, Coahuila	https://doi.org/10.1130/G32733.1
Mexico	-101	27	<i>Dadoxylon</i>	Araucariaceae	Maastrichtian	12	4	Olmos Fm., Coahuila	https://doi.org/10.1130/G32733.1
New Caledonia	165	-21	<i>Agathoxylon pancheri</i>	Araucariaceae	Turonian–Maastrichtian	8–12	4	Main island, literature	https://doi.org/10.1130/G32733.1
New Zealand	172	-42	<i>Araucarioptis hectorii</i>	Araucariaceae	Campanian–Maastrichtian	11–12	4	Amuri Bluffs, literature, NHStopes	https://doi.org/10.1130/G32733.1
New Zealand	172	-42	<i>Agathoxylon novaezealandii</i>	Araucariaceae	Campanian–Maastrichtian	11–12	4	Amuri Bluffs, literature, NHStopes	https://doi.org/10.1130/G32733.1
New Zealand	172	-42	<i>Agathoxylon ettigense</i>	Araucariaceae	Campanian–Maastrichtian	11–12	4	Amuri Bluffs, literature, NHStopes	https://doi.org/10.1130/G32733.1
New Zealand	172	-42	<i>Agathoxylon</i>	Araucariaceae	Campanian?	11	4	Bull's Point and Batley, Kaipara Harbour	https://doi.org/10.1130/G32733.1
New Zealand	173	-42	<i>Agathoxylon kaiparaense</i>	Araucariaceae	Campanian?	11	4	Bull's Point and Batley, Kaipara Harbour	https://doi.org/10.1130/G32733.1
Peru	-75	-9	<i>Agathoxylon</i>	Araucariaceae	Campanian–Maastrichtian	11–12	4	O.L.T.4	https://doi.org/10.1130/G32733.1
Peru	-80	-5	<i>Agathoxylon</i>	Araucariaceae	Campanian	11	4	La Mesa	https://doi.org/10.1130/G32733.1
Romania	23	46	<i>Agathoxylon formosum</i>	Araucariaceae	Campanian–Maastrichtian	11–12	4	South Apuseni Mts.	https://doi.org/10.1130/G32733.1
Romania	23	46	<i>Agathoxylon ultimus</i>	Araucariaceae	Campanian–Maastrichtian	11–12	4	South Apuseni Mts.	https://doi.org/10.1130/G32733.1
Romania	23	46	<i>Agathoxylon</i> sp.	Araucariaceae	Campanian–Maastrichtian	11–12	4	South Apuseni Mts.	https://doi.org/10.1130/G32733.1
Russia/Japan	142	47	<i>Agathoxylon pseudohochense</i>	Araucariaceae	Turonian–Santonian	8–10	4	Saghalien, Miho River	https://doi.org/10.1130/G32733.1
Russia/Japan	142	47	<i>Planoxylon inaiii</i>	Araucariaceae	Turonian–Maastrichtian	8–12	4	Urakawa Series, South Saghalien, right valley of	https://doi.org/10.1130/G32733.1
Russia/Japan	142	47	<i>Dadoxylon</i> cf. <i>tankense</i>	Araucariaceae	Turonian–Maastrichtian	8–12	4	Urakawa Series, South Saghalien, The Minami Rokusenzawa, Namikawa	https://doi.org/10.1130/G32733.1
Russia/Japan	142	47	<i>Agathoxylon kiense</i>	Araucariaceae	Turonian–Santonian	8–10	4	Miho Group, South Saghalien, Miho River	https://doi.org/10.1130/G32733.1
South Africa	27	-33	<i>Agathoxylon umzambense</i>	Araucariaceae	Turonian–Maastrichtian	8–12	4	East Pondoland	https://doi.org/10.1130/G32733.1
South Africa	27	-33	<i>Agathoxylon africanum</i>	Araucariaceae	Turonian–Maastrichtian	8–12	4	East Pondoland	https://doi.org/10.1130/G32733.1
South Africa	30,18222486	-31,1019584	<i>Agathoxylon</i>	Araucariaceae	Santonian	10	4	Mzambe Fm., Mzambe (=Umzamba) River Estuary, south of Port Edward, Pondoland region	https://doi.org/10.1016/j.cretres.2022.04.008
USA	-103	29	Undetermined wood	Araucariaceae	Maastrichtian	11	4	Javelina Fm., Texas, literature	https://doi.org/10.1130/G32733.1
USA	-103	29	<i>Agathoxylon</i>	Araucariaceae	Maastrichtian	12	4	Javelina Fm., Big Bend National Park, Texas	https://doi.org/10.1016/j.palaeo.2005.05.014
USA	-103	29	<i>Araucarioptid wood type 2</i>	Araucariaceae	Maastrichtian	12	4	Javelina Fm., Big Bend National Park, Texas	https://doi.org/10.1016/j.palaeo.2005.05.014
USA	-103	29	Undetermined wood	Araucariaceae	Campanian	11	4	Aguja Fm., Texas, literature	https://doi.org/10.1130/G32733.1
USA	-103	29	<i>Araucarioptid wood type 2</i>	Araucariaceae	Campanian	11	4	Aguja Fm., Big Bend National Park, Texas	https://doi.org/10.1016/j.palaeo.2005.05.014
USA	-103	29	<i>Araucarioptid wood type 3</i>	Araucariaceae	Campanian	11	4	Aguja Fm., Big Bend National Park, Texas	https://doi.org/10.1016/j.palaeo.2005.05.014
USA	-75	39	<i>Agathoxylon nobrevarcense</i>	Araucariaceae	Turonian				

Russia/Japan	142	47	<i>Protocedroxylon shimakurae</i>	Pinaceae	Turonian–Santonian	8–10	4	Miho Group, South Sakhalin Island, Juhachirinpan-zawa affluent of Nayba	https://doi.org/10.1130/G32733.1
Russia/Japan	142	47	<i>Pinuxylon transiens</i>	Pinaceae	Turonian–Santonian	8–10	4	South Saghalien, Kawakami Coal mine, Englanduryu	https://doi.org/10.1130/G32733.1
Russia/Japan	142	47	<i>Pinuxylon dakotense</i>	Pinaceae	Turonian–Santonian	8–10	4	South Saghalien, Kawakami Coal mine, Englanduryu	https://doi.org/10.1130/G32733.1
Sweden	13	59	<i>Pityoxylon</i>	Pinaceae	Campanian	11	4	Asen, literature, Conwentz	https://doi.org/10.1130/G32733.1
USA	-76	39	<i>Pityoxylon</i>	Pinaceae	Turonian–Santonian	8–10	4	Maryland, literature, Berry	https://doi.org/10.1130/G32733.1
USA	-75	39	<i>Pinoxylon sp.</i>	Pinaceae	Turonian–Santonian	8–10	4	Magothy Fm., Summit Bridge, Magothy, Delaware	https://doi.org/10.1130/G32733.1
USA	-75	39	<i>Piceoxylon cretacea</i>	Pinaceae	Turonian–Santonian	8–10	4	Magothy Fm., Summit Bridge, Magothy, Delaware	https://doi.org/10.1130/G32733.1
USA	-75	39	<i>Protocedroxylon traumaticum</i>	Pinaceae	Turonian–Santonian	8–10	4	Magothy Fm., Summit Bridge, Magothy, Delaware	https://doi.org/10.1130/G32733.1
USA	-88	34	<i>Pinuxylon</i>	Pinaceae	Coniacian–Santonian	9–10	4	Eutaw Fm., Prentiss County, Mississippi	https://doi.org/10.1130/G32733.1
USA	-74	40	<i>Pityoxylon</i>	Pinaceae	Campanian	11	4	Marshalltown Fm., Morgans, New Jersey	https://doi.org/10.1130/G32733.1
USA	-70	41	<i>Pityoxylon</i>	Pinaceae	Campanian	11	4	Gay's Head, Martha's Vineyard	https://doi.org/10.1130/G32733.1
USA	-76	39	<i>Pityoxylon</i>	Pinaceae	Turonian–Santonian	8–10	4	Maryland, literature, Berry	https://doi.org/10.1130/G32733.1
Antarctica	-60	-62	<i>Podocarpoxylon chapmanae</i>	Podocarpaceae	Cenomanian–Campanian	7–11	4	Williams Point Beds, Dragon Cove, Williams Point	https://doi.org/10.1130/G32733.1
Antarctica	-60	-62	<i>Podocarpoxylon verticalis</i>	Podocarpaceae	Cenomanian–Campanian	7–11	4	Williams Point Beds, Williams Point	https://doi.org/10.1130/G32733.1
Antarctica	-60	-62	<i>Podocarpoxylon sp.</i>	Podocarpaceae	Cenomanian–Campanian	7–11	4	Williams Point Beds, Williams Point	https://doi.org/10.1130/G32733.1
Antarctica	-56	-64	<i>Podocarpoxylon sp. 2</i>	Podocarpaceae	Maastrichtian	12	4	Lopez de Bertodano Fm., Seymour Island	https://doi.org/10.1130/G32733.1
Antarctica	-56	-64	<i>Podocarpoxylon sp. 1</i>	Podocarpaceae	Maastrichtian	12	4	Lopez de Bertodano Fm., Seymour Island	https://doi.org/10.1130/G32733.1
Antarctica	-56	-64	<i>Protopodocarpoxylon antarcticum</i>	Podocarpaceae	Maastrichtian?	12	4	Lopez de Bertodano Fm., Seymour Island	https://doi.org/10.1130/G32733.1
Antarctica	-56	-64	<i>Podocarpoxylon aparchymatum</i>	Podocarpaceae	Maastrichtian	12	4	Lopez de Bertodano Fm., Seymour Island	https://doi.org/10.1130/G32733.1
Antarctica	-57	-63	<i>Podocarpoxylon sp.</i>	Podocarpaceae	Maastrichtian	12	4	Lopez de Bertodano Fm., Cape Lamb, Vega Island	https://doi.org/10.1130/G32733.1
Antarctica	-57,918325	-63,862606	<i>Phyllocladoxylon antarcticum</i>	Podocarpaceae	Santonian–Lower Campanian	10–11	4	Santa Marta Fm., Brandy Bay, James Ross Island	https://doi.org/10.1016/j.cretres.2017.04.016
Argentina	-67	-40	<i>Podocarpoxylon garciae</i>	Podocarpaceae	Campanian–Maastrichtian	11–12	4	Allen Fm., Rio Negro Province	https://doi.org/10.1130/G32733.2
Argentina	-67	-40	<i>Circoproxylon gregussii</i>	Podocarpaceae	Campanian–Maastrichtian	11–12	4	Allen Fm., Rio Negro Province	https://doi.org/10.1130/G32733.2
Argentina	-69	-49	<i>Podocarpoxylon sp.</i>	Podocarpaceae	Campanian–Maastrichtian	11–12	4	Mata Amarilla Fm., Tres Lagos	https://doi.org/10.1130/G32733.3
Argentina	-67,80152801	-43,3483566	<i>Podocarpoxylon mazzoni</i>	Podocarpaceae	Campanian–Maastrichtian	11–12	4	Puntudo Chico Fm., El Mirasol, Chubut	https://doi.org/10.1016/j.cretres.2019.01.022
Canada	-113	53	<i>Podocarpoxylon ajkense</i>	Podocarpaceae	Campanian	11	4	Oldman Fm., Denhart area, in the Red	https://doi.org/10.1130/G32733.1
Canada	-111,4748967	50,7458503	<i>Podocarpoxylon</i>	Podocarpaceae	Campanian	11	4	Oldman Fm., Alberta	https://doi.org/10.1016/j.palaeo.2005.05.014
France	4	44	<i>Podocarpoxylon ajkense</i>	Podocarpaceae	Santonian	10	4	Piolenc	https://doi.org/10.1130/G32733.1
France	0	46	<i>Protopodocarpoxylon</i>	Podocarpaceae	Santonian	10	4	La Garnache, Vendee	https://doi.org/10.1130/G32733.1
Hungary	17	47	<i>Podocarpoxylon ajkense</i>	Podocarpaceae	Santonian	10	4	Ajka, literature, Greguss	https://doi.org/10.1130/G32733.1
India	78	11	<i>Podocarpoxylon</i>	Podocarpaceae	Maastrichtian	12	4	Kallamedu Fm., Tamil Nadu, Cauvery Basin	https://doi.org/10.1130/G32733.1
Korea	128	35	<i>Circoproxylon</i>	Podocarpaceae	Campanian	11	4	Dadaepo Fm., Dadaepo, southern part of Saha-gu, Busan	https://doi.org/10.1130/G32733.1
Mexico	-101	27	<i>Podocarpoxylon</i>	Podocarpaceae	Maastrichtian	12	4	Olmos Fm., Barroteran, Coahuila	https://doi.org/10.1130/G32733.1
Morocco	-7	32	<i>Protopodocarpoxylon</i>	Podocarpaceae	Cenomanian–Campanian	7–11	4	literature, Dupuron & Laoudoueneix	https://doi.org/10.1130/G32733.1
Portugal	-8	40	<i>Protopodocarpoxylon aveiroense</i>	Podocarpaceae	Turonian–Maastrichtian	8–12	4	Esgueira near Aveiro	https://doi.org/10.1130/G32733.1
Russia	147	44	<i>Podocarpoxylon jurii</i>	Podocarpaceae	Campanian–Maastrichtian	11–12	4	Lesser, Kuril Islands	https://doi.org/10.1130/G32733.1
Russia/Japan	142	47	<i>Podocarpoxylon sp. dokotense ?</i>	Podocarpaceae	Turonian–Maastrichtian	8–12	4	Urakawa Series, South Saghalien, The Kisegawa	https://doi.org/10.1130/G32733.1
Russia/Japan	142	47	<i>Podocarpoxylon sp.</i>	Podocarpaceae	Turonian–Maastrichtian	8–12	4	Urakawa Series, South Saghalien, Kawakami Coal mine, Kawakami	https://doi.org/10.1130/G32733.1
Russia/Japan	142	47	<i>Phyllocladoxylon gothani</i>	Podocarpaceae	Turonian–Maastrichtian	8–12	4	Urakawa Series, South Saghalien, Kawakami Coal mine, Kawakami	https://doi.org/10.1130/G32733.1
South Africa	19	-31	<i>Podocarpoxylon woburnense</i>	Podocarpaceae	Coniacian	9	4	Namaqualand, South Africa–Namibia	https://doi.org/10.1130/G32733.1
South Africa	19	-31	<i>Podocarpoxylon umzambense ?</i>	Podocarpaceae	Coniacian	9	4	Namaqualand, South Africa–Namibia	https://doi.org/10.1130/G32733.1
South Africa	19	-31	<i>Podocarpoxylon stokesii</i>	Podocarpaceae	Coniacian	9	4	Namaqualand, South Africa–Namibia	https://doi.org/10.1130/G32733.1
South Africa	19	-31	<i>Podocarpoxylon sp.</i>	Podocarpaceae	Coniacian	9	4	Namaqualand, South Africa–Namibia	https://doi.org/10.1130/G32733.1
South Africa	19	-31	<i>Podocarpoxylon sahii</i>	Podocarpaceae	Coniacian	9	4	Namaqualand, South Africa–Namibia	https://doi.org/10.1130/G32733.1
South Africa	14	-27	<i>Podocarpoxylon jago</i>	Podocarpaceae	Coniacian	9	4	Namaqualand, South Africa–Namibia	https://doi.org/10.1130/G32733.1
South Africa	19	-31	<i>Podocarpoxylon umzambense</i>	Podocarpaceae	Coniacian	9	4	Namaqualand, literature, Bamford	https://doi.org/10.1130/G32733.1
South Africa	30,18224846	-31,1019584	<i>Podocarpoxylon umzambense</i>	Podocarpaceae	Coniacian	9	4	Mzamba Fm., Mzamba (=Umzamba) River Estuary, south of Port Edward, Pondoland region	https://doi.org/10.1016/j.gr.2022.04.008
South Africa	18,46217255	-29,6139414	<i>Podocarpoxylon umzambense</i>	Podocarpaceae	Coniacian	9	4	Umzamba beds, Namaqualand continental shelf	https://doi.org/10.1130/G32733.1
USA	-103	29	Undetermined wood type	Podocarpaceae	Campanian	11	4	Aguja Fm., Texas, literature	https://doi.org/10.1016/j.palaeo.2005.05.014
USA	-103	29	<i>Podocarpoid wood type</i>	Podocarpaceae	Campanian	11	4	Aguja Fm., Big Bend National Park, Texas	https://doi.org/10.1016/j.palaeo.2005.05.014
Antarctica	-60	-62	<i>Agathoxylon chapmannae</i>	Araucariaceae	Cenomanian–Campanian	7–11	3	Williams Point Beds, Dragon Cove, Williams Point	https://doi.org/10.1130/G32733.1
Antarctica	-60	-62	<i>Agathoxylon floresii</i> </						

Japan	141	43	<i>Piceoxylon macroporosum</i>	Pinaceae	Turonian	8	3	Hokkaido, Omakizawa, tributary of Yubari River	https://doi.org/10.1130/G32733.1
Japan	141	43	<i>Pinuxylon microporum</i>	Pinaceae	Turonian	8	3	Hokkaido, Dam site of Yubari	https://doi.org/10.1130/G32733.1
Japan	141	43	<i>Piceoxylon scleromedullosum</i>	Pinaceae	Cenomanian	7	3	Hokkaido, Dam site of Yubari	https://doi.org/10.1130/G32733.1
Japan	141	43	<i>Protocedroxylon</i> sp.	Pinaceae	Turonian–Maastrichtian	8–12	3	Hokkaido, Kikumenzawa, Mikasayamamura, Soratigun	https://doi.org/10.1130/G32733.1
Japan	142	42	<i>Piceoxylon transiens</i>	Pinaceae	Turonian–Maastrichtian	8–12	3	Urakawa Series, Hokkaido, The left valley of	https://doi.org/10.1130/G32733.1
Japan	141	43	<i>Pinoxylon dakotense</i>	Pinaceae	Hauterivian–Albian?	3–6	3	Honkei Beds, Hokkaido, Pen-hsi-hu, Fengtien Province	https://doi.org/10.1130/G32733.1
Russia	165	62	<i>Piceoxylon talovskiene</i>	Pinaceae	Coniacian	9	3	Penzhina, Fm., northwestern Kamchatka, eastern coast of	https://doi.org/10.1134/S0031030106060104
Russia	88,94527778	53,8177778	<i>Keteleeriioxylon kamtschatkicense</i>	Pinaceae	Turonian–Coniacian	8–9	3	Penzhina Fm., leftbank of the lower course of the Talovka River	https://doi.org/10.1134/S0031030106060104
Russia/Japan	142	47	<i>Piceoxylon scleromedullosum</i>	Pinaceae	Turonian–Maastrichtian	8–12	3	Urakawa Series, South Saghalien, The Santangawa	https://doi.org/10.1130/G32733.1
Russia/Japan	142	47	<i>Piceoxylon</i> sp. <i>antiquus</i> ?	Pinaceae	Turonian–Maastrichtian	8–12	3	Urakawa Series, South Saghalien, Mirami Hassenzawa, Namikawa, Toyohara	https://doi.org/10.1130/G32733.1
Russia/Japan	142	47	<i>Protocedroxylon</i> cf. <i>yendoii</i>	Pinaceae	Turonian–Maastrichtian	8–12	3	Urakawa Series, South Saghalien, Kawakami Coal mine, Kawakami	https://doi.org/10.1130/G32733.1
Russia/Japan	142	47	<i>Protocedroxylon</i> <i>shimokurae</i>	Pinaceae	Turonian–Santonian	8–10	3	Miho Group, South Sakkha Island, Juahachiripan-zawa affluent of Nayba	https://doi.org/10.1130/G32733.1
Russia/Japan	142	47	<i>Pinuxylon transiens</i>	Pinaceae	Turonian–Santonian	8–10	3	South Saghalien, Kawakami Coal mine, Englandury	https://doi.org/10.1130/G32733.1
Russia/Japan	142	47	<i>Pinuxylon dakotense</i>	Pinaceae	Turonian–Santonian	8–10	3	South Saghalien, Kawakami Coal mine, Englandury	https://doi.org/10.1130/G32733.1
Russia/Japan	142	49	<i>Pinuxylon microporum</i>	Pinaceae	Turonian	8	3	Saghalien, Aika River and tributary streams	https://doi.org/10.1130/G32733.1
Russia/Japan	142	49	<i>Piceoxylon scleromedullosum</i>	Pinaceae	Cenomanian	7	3	Saghalien, Aika River and tributary streams	https://doi.org/10.1130/G32733.1
Russia/Japan	143	50	<i>Pinuxylon</i>	Pinaceae	Turonian–Santonian	8–10	3	Saghalien, literature	https://doi.org/10.1130/G32733.1
USA	-74	40	<i>Pityoxylon protostrophopitys</i>	Pinaceae	Turonian	8	3	Raritan Fm., Cliffwood, New Jersey	https://doi.org/10.1130/G32733.1
USA	-74	40	<i>Pityoxylon foliosum</i>	Pinaceae	Turonian	8	3	Raritan Fm., Cliffwood, New Jersey	https://doi.org/10.1130/G32733.1
USA	-74	40	<i>Pityoxylon anomalous</i>	Pinaceae	Turonian	8	3	Raritan Fm., Cliffwood, New Jersey	https://doi.org/10.1130/G32733.1
USA	-75	39	<i>Pinuxylon</i> sp.	Pinaceae	Turonian–Santonian	8–10	3	Magothy Fm., Summit Bridge, Magothy, Delaware	https://doi.org/10.1130/G32733.1
USA	-75	39	<i>Piceoxylon cretacea</i>	Pinaceae	Turonian–Santonian	8–10	3	Magothy Fm., Summit Bridge, Magothy, Delaware	https://doi.org/10.1130/G32733.1
USA	-75	39	<i>Protocedroxylon traumaticum</i>	Pinaceae	Turonian–Santonian	8–10	3	Magothy Fm., Summit Bridge, Magothy, Delaware	https://doi.org/10.1130/G32733.1
Japan	142	42	<i>Abiocaulis yesoensis</i>	Pinaceae	Cenomanian–Santonian	7–10	3	Hokkaido, Yubari, literature	https://doi.org/10.1130/G32733.1
Antarctica	-60	-62	<i>Podocarpoxylon chapmanae</i>	Podocarpaceae	Cenomanian–Campanian	7–11	3	Williams Point Beds, Dragon Cove, Williams Point	https://doi.org/10.1130/G32733.1
Antarctica	-60	-62	<i>Podocarpoxylon communis</i>	Podocarpaceae	Cenomanian–Campanian	7–11	3	Williams Point Beds, Dragon Cove, Williams Point	https://doi.org/10.1130/G32733.1
Antarctica	-60	-62	<i>Podocarpoxylon verticalis</i>	Podocarpaceae	Cenomanian–Campanian	7–11	3	Williams Point Beds, Dragon Cove, Williams Point	https://doi.org/10.1130/G32733.1
Argentina	-68	-38	<i>Circoporoxylon krausei</i>	Podocarpaceae	Cenomanian	7	3	Huinul Fm., Cerros Colorados, Neuquen	Martínez & Lutz (2007)
Australia	142,620865	-21,924336	<i>Protophyllocadopxylon owensii</i>	Podocarpaceae	Cenomanian–Turonian boundary	7–8	3	Winton Fm., Eromanga Basin, N Winton, central-western Queensland	https://doi.org/10.1016/j.revpalbo.2014.05.004
Czech Republic	14	50	<i>Podocarpoxylon</i> sp.	Podocarpaceae	Cenomanian	7	3	Peruc-Koryčany Fm., Bohemian Cretaceous Basin	https://doi.org/10.1016/j.revpalbo.2020.104311
Denmark	14	55	<i>Circoporoxylon</i>	Podocarpaceae	Cenomanian	7	3	Arnager	https://doi.org/10.1130/G32733.1
Egypt	30,5991477	25,4446691	<i>Metapodocarpoxylon leuchsii</i>	Podocarpaceae	Turonian	8	3	Taref Fm., Al-Umm, El-Dabadi, El-Kharga	https://doi.org/10.1016/j.cretres.2021.104901
France	-1	46	<i>Podocarpoxylon</i>	Podocarpaceae	Cenomanian	7	3	Île d'Aix, Charente-Maritime	https://doi.org/10.1130/G32733.1
France	4	44	<i>Podocarpoxylon</i>	Podocarpaceae	Cenomanian	7	3	Saint Andre d'Olerargues	https://doi.org/10.1130/G32733.1
France	-1	45	<i>Protopodocarpoxylon</i>	Podocarpaceae	Cenomanian	7	3	Fouras, Vendée	https://doi.org/10.1130/G32733.1
France	0	49	<i>Protopodocarpoxylon</i>	Podocarpaceae	Cenomanian	7	3	Fouras, Vendée	https://doi.org/10.1130/G32733.1
France	0	49	<i>Podocarpoxylon</i>	Podocarpaceae	Cenomanian	7	3	Mont Saint Laurent	https://doi.org/10.1130/G32733.1
France	0	49	<i>Podocarpoxylon</i>	Podocarpaceae	Cenomanian	7	3	Mont Saint Laurent	https://doi.org/10.1130/G32733.1
France	4	44	<i>Protopodocarpoxylon</i>	Podocarpaceae	Cenomanian	7	3	Puy Puy, Charente, Rochefort	https://doi.org/10.1130/G32733.1
France	4	44	<i>Podocarpoxylon</i>	Podocarpaceae	Cenomanian	7	3	Puy Puy, Charente, Rochefort	https://doi.org/10.1130/G32733.1
France	4	44	<i>Podocarpoxylon</i>	Podocarpaceae	Cenomanian	7	3	Saint Laurent, La Venede, literature, unpublished	https://doi.org/10.1130/G32733.1
France	0	45	<i>Protopodocarpoxylon</i>	Podocarpaceae	Cenomanian	7	3	Vacheres, literature, unpublished	https://doi.org/10.1130/G32733.1
India	79,01325023	10,8737947	<i>Podocarpoxylon kulkulankaitamensis</i>	Podocarpaceae	Turonian	8	3	Garudamangalam Fm., Cauvery Basin, Kulakkannattam Sandstone, Sattanur Village	https://doi.org/10.5499/jio.2004.201
Kazakhstan	71	43	<i>Podocarpoxylon</i>	Podocarpaceae	Cenomanian	7	3	Central Kyzylkum, literature	https://doi.org/10.1130/G32733.1
Kazakhstan	71	43	<i>Phyllocladoxylon</i>	Podocarpaceae	Cenomanian	7	3	Central Kyzylkum, literature	https://doi.org/10.1130/G32733.1
Morocco	-7	32	<i>Protopodocarpoxylon</i>	Podocarpaceae	Cenomanian–Campanian	7–11	3	literature, Dupéron & Laudoueix	https://doi.org/10.1130/G32733.1
Portugal	-8	40	<i>Protopodocarpoxylon aveiroense</i>	Podocarpaceae	Turonian–Maastrichtian	8–12	3	Esgueira near Aveiro	https://doi.org/10.1130/G32733.1
Russia/Japan	142	47	<i>Podocarpoxylon</i> sp. <i>dakotense</i> ?	Podocarpaceae	Turonian–Maastrichtian	8–12	3	Urakawa Series, South Saghalien, The Kisegawa	https://doi.org/10.1130/G32733.1
Russia/Japan	142	47	<i>Podocarpoxylon</i> sp.	Podocarpaceae	Turonian–Maastrichtian	8–12	3	Urakawa Series, South Saghalien, Kawakami Coal mine, Kawakami	https://doi.org/10.1130/G32733.1
Russia/Japan	142	47	<i>Phyllocladoxylon gothani</i>	Podocarpaceae	Turonian–Maastrichtian	8–12	3	Urakawa Series, South Saghalien, Kawakami Coal mine, Kawakami	https://doi.org/10.1130/G32733.1
Alaska	-155	69	<i>Agathoxylon</i> ?	Araucariaceae	Albian	6	2	Naushuk Group, North slope, Colville River	https://doi.org/10.1130/G32733.1
Algeria	2	28	<i>Agathoxylon</i> sp.	Araucariaceae	A				

India	85	23	<i>Agathoxylon amraparens</i>	Araucariaceae	Aptian	5	2 Rajmahal hills, Jharkhand, Amrapara	https://doi.org/10.1130/G32733.1
India	85	23	<i>Agathoxylon rajmahalense</i>	Araucariaceae	Aptian	5	2 Rajmahal hills, Jharkhand, Banchapa	https://doi.org/10.1130/G32733.1
India	85	23	<i>Agathoxylon agathoides</i>	Araucariaceae	Aptian	5	2 Rajmahal hills, Jharkhand, Mandro	https://doi.org/10.1130/G32733.1
India	85	23	<i>Agathoxylon jurasicum</i>	Araucariaceae	Aptian	5	2 Rajmahal hills, Jharkhand, Amarjoli	https://doi.org/10.1130/G32733.1
India	85	23	<i>Agathoxylon benderi</i>	Araucariaceae	Aptian	5	2 Rajmahal hills, Jharkhand	https://doi.org/10.1130/G32733.1
India	85	23	<i>Agathoxylon sp.</i>	Araucariaceae	Aptian	5	2 Rajmahal hills, Jharkhand	https://doi.org/10.1130/G32733.1
India	87,74656757	25,0832251	<i>Agathoxylon cf. rajmahalense</i>	Araucariaceae	Aptian	5	2 Rajmahal Fm., Bartala and Banchapa, Rajmahal Hills, Jharkhand	https://doi.org/10.1016/j.palwor.2017.12.004
India	81	16	<i>Agathoxylon amraparens</i>	Araucariaceae	Barremian-Aptian	4-5	2 Gangapur Fm., Pranhita-Godavari valley, Adilabad District, Andhra Pradesh	https://doi.org/10.1130/G32733.1
India	79,43467758	19,2654655	<i>Agathoxylon parenchymatosum</i>	Araucariaceae	Barremian-Aptian	4-5	2 Gangapur Fm., Near village Gangapur, Adilabad, Telangana	https://doi.org/10.1016/j.palwor.2017.12.004
Italy	12	43	<i>Agathoxylon sp.</i>	Araucariaceae	Aptian-Albian	5-6	2 « marne a fucidi » dell'Appennino Umbro-Marchigiano	https://doi.org/10.1080/00837792.1980.10670204
Italy	12	43	<i>Agathoxylon sp.</i>	Araucariaceae	Aptian-Albian	5-6	2 Apennini, Biondi	https://doi.org/10.1130/G32733.1
Italy	12	43	<i>Agathoxylon sp.</i>	Araucariaceae	Aptian-Albian	5-6	2 « marne a fucidi » dell'Appennino Umbro-Marchigiano	https://doi.org/10.1080/00837792.1980.10670204
Italy	11,81569801	46,5825384	<i>Agathoxylon</i>	Araucariaceae	Albian	6	2 Puez-Marl Member, Puez Fm., Puez-Geisler Nature Park in the Dolomites	https://doi.org/10.1080/00837792.1980.10670204
Italy	12	43	<i>Agathoxylon sp.</i>	Araucariaceae	Aptian-Albian	5-6	2 Apennini, Biondi	https://doi.org/10.1130/G32733.1
Japan	140	35	<i>Agathoxylon inubense</i>	Araucariaceae	Barremian-Aptian	4-5	2 Choshi Group, Honshu, Chiba Prefecture, Choshi	https://doi.org/10.1130/G32733.1
Japan	140	35	<i>Agathoxylon choshiense</i>	Araucariaceae	Barremian-Aptian	4-5	2 Choshi Group, Honshu, Chiba Prefecture, Choshi	https://doi.org/10.1130/G32733.1
Japan	139	35	<i>Agathoxylon japonicum</i>	Araucariaceae	Barremian-Aptian	4-5	2 Sebayashi Fm., Kwanto, Mountains of central Honshu	https://doi.org/10.1130/G32733.1
Japan	139	35	<i>Agathoxylon kiiense</i>	Araucariaceae	Barremian-Aptian	4-5	2 Sebayashi Fm., Kwanto, Mountains of central Honshu	https://doi.org/10.1130/G32733.1
Japan	139	35	<i>Agathoxylon pseudohujianimense</i>	Araucariaceae	Barremian-Aptian	4-5	2 Kwanto Mountains of central Honshu	https://doi.org/10.1130/G32733.1
Japan	141	39	<i>Agathoxylon sidugawaense</i>	Araucariaceae	Aptian-Albian	5-6	2 Hiraga, sandstone of the Mkoikorobe, Tanohata-mura, Simo	https://doi.org/10.1130/G32733.1
Japan	141	39	<i>Agathoxylon japonicum</i>	Araucariaceae	Aptian-Albian	5-6	2 Hiraga, sandstone of the Mkoikorobe, Tanohata-mura, Simo	https://doi.org/10.1130/G32733.1
Japan	141	39	<i>Dadoxylon sp. japonicum ?</i>	Araucariaceae	Hauterivian-Barremian	3-4	2 Mossi sandstone of the Mkoikorobe, Tanohata-mura, Simo	https://doi.org/10.1130/G32733.1
Japan	140,8636684	35,7005442	<i>Agathoxylon</i>	Araucariaceae	Barremian-Aptian	4-5	2 Honshu, Chiba Prefecture, Choshi Peninsula, Toriakeura (Outer Zone), Choshi Group	https://doi.org/10.1016/j.iseaes.2010.11.010
Japan	138,8072589	36,0808626	<i>Agathoxylon</i>	Araucariaceae	Barremian-Aptian	4-5	2 Honshu, Gunma Prefecture, Kwanto Mountains (Outer Zone), Sanchu Group, Sebayashi Fm.	https://doi.org/10.1016/j.iseaes.2010.11.010
Japan	136,6773087	36,2147933	<i>Brachoxylon</i>	Araucariaceae	upper Barremian-lower Aptian	4-5	2 Honshu, Ishikawa Prefecture, Do-no-mori (Inner Zone), Upper Totori Group	https://doi.org/10.1016/j.iseaes.2010.11.010
Japan	141	39	<i>Agathoxylon sidugawaense</i>	Araucariaceae	Aptian-Albian	5-6	2 Hiraga, sandstone of the Mkoikorobe, Tanohata-mura, Simo	https://doi.org/10.1130/G32733.1
Japan	141	39	<i>Agathoxylon japonicum</i>	Araucariaceae	Aptian-Albian	5-6	2 Hiraga, sandstone of the Mkoikorobe, Tanohata-mura, Simo	https://doi.org/10.1130/G32733.1
Jordan	37	31	<i>Agathoxylon sp.</i>	Araucariaceae	Aptian-Albian	5-6	2 Zerga River, Inside	https://doi.org/10.1130/G32733.1
Korea	128	36	<i>Agathoxylon byeongpungense</i>	Araucariaceae	Aptian-Albian	5-6	2 Donghwachi Fm., in Andong City, Gyeongsang Basin	https://doi.org/10.1130/G32733.1
Korea	127	35	<i>Agathoxylon togeumense</i>	Araucariaceae	Albian	6	2 Togeum Fm., Togeum, Gurye County, Jeollanam Province	https://doi.org/10.1130/G32733.1
Korea	127	35	<i>Agathoxylon kiiense</i>	Araucariaceae	Albian	6	2 Togeum Fm., Togeum, Gurye County, Jeollanam Province	https://doi.org/10.1130/G32733.1
Korea	128	34	<i>Agathoxylon</i>	Araucariaceae	Albian	6	2 Haman Fm., GungEngland District, Haman County, South Gyeongsang Prov.	https://doi.org/10.1130/G32733.1
Korea	128	36	<i>Brachoxylon sp.</i>	Araucariaceae	Albian	5	2 Dogyedong Fm., Gamcheon, Yeongyang County, Gyeongsang Basin	https://doi.org/10.1130/G32733.1
Korea	128	36	<i>Agathoxylon byeongpungense</i>	Araucariaceae	Aptian-Albian	5-6	2 Donghwachi Fm., in Andong City, Gyeongsang Basin	https://doi.org/10.1130/G32733.1
Korea	126,322879	34,730318	<i>Agathoxylon sp.</i>	Araucariaceae	Albian-Cenomanian	6-7	2 Hwawon Fm. at Hwawon-myeon in Jeollanam-do	https://doi.org/10.1016/j.cretres.2013.02.003
Lebanon	35	33	<i>Agathoxylon sp.</i>	Araucariaceae	Valanginian-Barremian	2-4	2 Besiktas, Barale	https://doi.org/10.1130/G32733.1
Mali	2,71597816	18,6651714	<i>Agathoxylon septatum</i>	Araucariaceae	Berriasian-Albian	1-6	2 Ti-n-Essako, western side of the Adrar des Iforas, Continental Intercalaire rocks	https://doi.org/10.1016/j.iseaes.2012.04.007
Mexico	-100	18	<i>Agathoxylon sp.</i>	Araucariaceae	Albian-Cenomanian	6-7	2 Mal-Paso Fm., Huetamo, Michoacan	https://doi.org/10.1130/G32733.1
Norge	16	78	<i>Araucariopitys</i>	Araucariaceae	Aptian-Albian	5-6	2 Carolinefjellet Fm., Lundstromdalen, N Adventfjorden, Spitsbergen	https://doi.org/10.1130/G32733.1
Norge	16	78	<i>Araucariopitys (Protocedroxylon)</i>	Araucariaceae	Aptian-Albian	5-6	2 Carolinefjellet Fm., Lundstromdalen, N Adventfjorden, Spitsbergen	https://doi.org/10.1130/G32733.1
Norge	17,27603679	78,0222052	<i>Araucariopitys</i>	Araucariaceae	Aptian-Albian	5-6	2 Lundstromdalen, Svalbard, Spitsbergen	https://doi.org/10.1130/G32733.1
Poland	19	51	<i>Agathoxylon</i>	Araucariaceae	Barremian	4	2 Stempiny, literature, Philippe	https://doi.org/10.1130/G32733.1
Portugal	9,22728211	39,0184673	<i>Dadoxylon teixeirae</i>	Araucariaceae	upper Barremian-lower Aptian	4-5	2 Torres Vedras, near Serra do Socorro, Cadriceira	https://doi.org/10.1130/G32733.1
Slovakia	22	48	<i>Agathoxylon</i>	Araucariaceae	Aptian	5	2 Benatina, literature, unpublished	https://doi.org/10.1130/G32733.1
South Africa	25	-33	<i>Agathoxylon sp.</i>	Araucariaceae	Aptian-Albian	5-6	2 Kirkwood Fm., Algoa Basin	https://doi.org/10.1130/G32733.1
South Africa	25	-33	<i>Agathoxylon</i>	Araucariaceae	Aptian-Albian	5-6	2 Kirkwood Fm., Woodbury farm, Amakhala	https://doi.org/10.1130/G32733.1
South Africa	25	-33	<i>Agathoxylon</i>	Araucariaceae	Aptian-Albian	5-6	2 Kirkwood Fm., Kirkwood	https://doi.org/10.1130/G32733.1
Spain	-2,42823205	42,2872133	<i>Agathoxylon riogense</i>	Araucariaceae	Aptian-Albian	5-6	2 Kirkwood Fm., Kirkwood	https://doi.org/10.1130/G32733.1
Spain	-0,39788415	40,7399583	<i>Agathoxylon sp.</i>	Araucariaceae	Berriasian-Barremian	1-4	2 Ladrúñ, Seno and Oliete, Maestrazgo Basin, Teruel	https://doi.org/10.1016/j.geobios.2005.09.003
Spain	-3,25714213	41,9885889	<i>Agathoxylon sp.</i>	Araucariaceae	Barremian-Aptian	4	2 Castrillo de la Reina, Hacinas	https://doi.org/10.1016/j.geobios.2005.09.003
Spain	-2,47517713	42,219343</						

China	129	42	<i>Taxodioxylon</i>	Cupressaceae	Hauterivian–Aptian	3–5	2	Liaoyuan Basin, Jilin	https://doi.org/10.1130/G32733.1
China	131,0991667	45,5352778	<i>Protocupressinoxylon</i>	Cupressaceae	Barremian	4	2	Heilongjiang, Mishan, Chengzhe Fm.	https://doi.org/10.1130/iseaes.2010.11.010
China	121	42	<i>Taxoxylon</i>	Cupressaceae	Aptian–Albian	5–6	2	West Liaoning, NE China	https://doi.org/10.1130/G32733.1
China	130	43	<i>Pseudofrenelopsis dalatzensi</i>	Cupressaceae	Aptian–Albian	5–6	2	Dalai Fm., Zhiqing, Xiang, Yanji county, Jilin	https://doi.org/10.1130/G32733.1
China	132	46	<i>Cupressinoxylon baomiqiaense</i>	Cupressaceae	Barremian–Albian	4–6	2	Yunshan Fm., Baqiao, Heilongjiang	https://doi.org/10.1130/G32733.1
China	121	42	<i>Elatides harrisi</i>	Cupressaceae	Aptian–Albian	5–6	2	Halzhou Fm., Fusin coal mine, Liaoning	https://doi.org/10.1130/G32733.1
England	0	52	<i>Pseudofrenelopsis</i> ?	Cupressaceae	Valangian–Barremian	2–4	2	Wessex Fm., Hanover Point, Sudmoor Point	https://doi.org/10.1130/G32733.1
England	0	51	<i>Cupressinoxylon</i>	Cupressaceae	Aptian	5	2	Lower Greensand, Folkestone Beds near Ightham, Kent	https://doi.org/10.1130/G32733.1
England	-1	50	<i>Sequoia aiguisagrensis</i>	Cupressaceae	Aptian	5	2	Lower Greensand, Luccomb Chine, Isle of Wight	https://doi.org/10.1130/G32733.1
England	0	51	<i>Cupressinoxylon succumbense</i>	Cupressaceae	Aptian	5	2	Lower Greensand, Luccomb Chine, Isle of Wight	https://doi.org/10.1130/G32733.1
England	0	52	<i>Taxoxylon anglicum</i>	Cupressaceae	Aptian	5	2	Lower Greensand, Woburn, Bedfordshire	https://doi.org/10.1130/G32733.1
England	0	52	<i>Cupressinoxylon</i> sp.	Cupressaceae	Aptian	5	2	Lower Greensand, Woburn Sands, Bedfordshire	https://doi.org/10.1130/G32733.1
England	0	52	<i>Taxoxylon anglicum</i>	Cupressaceae	Aptian	5	2	Lower Greensand, Woburn Sands, Bedfordshire	https://doi.org/10.1130/G32733.1
England	0	52	<i>Cupressinoxylon hortii</i>	Cupressaceae	Aptian	5	2	Lower Greensand, Fuller's Earth, Woburn Sands, Bedfordshire	https://doi.org/10.1130/G32733.1
England	-1	50	<i>Cupressinoxylon vectense</i>	Cupressaceae	Aptian	5	2	Lower Greensand, Shanklin, Isle of Wight	https://doi.org/10.1130/G32733.1
England	1	50	<i>Protocupressinoxylon vectense</i>	Cupressaceae	Aptian	5	2	Lower Greensand, Dunrose Point	https://doi.org/10.1130/G32733.1
England	-1	50	<i>Cupressinoxylon</i>	Cupressaceae	Aptian–Albian	5–6	2	Greensand, literature, Stopes	https://doi.org/10.1130/G32733.1
England	-1	50	<i>Cupressinoxylon vectense</i>	Cupressaceae	Aptian	5	2	Lower Crioseras bed, Sandown, Isle of Wight	https://doi.org/10.1130/G32733.1
England	0	52	<i>Pseudofrenelopsis</i>	Cupressaceae	Barremian	4	2	Wealden Group	https://doi.org/10.1130/G32733.1
England	-1	50	<i>Pseudofrenelopsis parceramosa</i>	Cupressaceae	Aptian	5	2	Lower Greensand, Isle of Wight	https://doi.org/10.1130/G32733.1
England	0	52	<i>Pseudofrenelopsis</i>	Cupressaceae	Barremian	4	2	Brook Fm., Shipard's Compton	https://doi.org/10.1130/G32733.1
England	-3	50	<i>Cupressinoxylon</i>	Cupressaceae	Albian	6	2	Upper Greensand, Exeter	https://doi.org/10.1130/G32733.1
England	-3	50	<i>Cupressinoxylon</i>	Cupressaceae	Albian	6	2	Upper Greensand, Semley, Wiltshire	https://doi.org/10.1130/G32733.1
England	0	51	<i>Cupressinoxylon</i>	Cupressaceae	Aptian–Albian	5–6	2	Greensand, literature, Stopes	https://doi.org/10.1130/G32733.1
France	4	50	<i>Cupressinoxylon</i>	Cupressaceae	Hauterivan–Barremian	1–3	2	Feron–Glaeon, literature, Lemoigne	https://doi.org/10.1130/G32733.1
France	0	49	<i>Cupressinoxylon</i>	Cupressaceae	Aptian–Albian	5–6	2	Normandie	https://doi.org/10.1130/G32733.1
France	5	44	<i>Taxodioxylon</i>	Cupressaceae	Aptian	5	2	Col de la Vallouse	https://doi.org/10.1130/G32733.1
France	4	48	<i>Cupressinoxylon</i>	Cupressaceae	Aptian–Albian	5–6	2	Louvemont, literature, Bertrand	https://doi.org/10.1130/G32733.1
France	0	48	Undetermined wood	Cupressaceae	Albian	6	2	Gault, Gault	https://doi.org/10.1130/G32733.1
France	1	50	<i>Cupressinoxylon</i>	Cupressaceae	Albian	6	2	Wissant, Dept. du Pas-de-Calais	https://doi.org/10.1130/G32733.1
France	1	50	<i>Tetradinoxylon amedroi</i>	Cupressaceae	Albian	6	2	Wissant, Dept. du Pas-de-Calais	https://doi.org/10.1130/G32733.1
France	1	50	<i>Widdringtonioxylon borealis</i>	Cupressaceae	Albian	6	2	Wissant, Dept. du Pas-de-Calais	https://doi.org/10.1130/G32733.1
France	4	49	<i>Taxodioxylon</i>	Cupressaceae	Albian	6	2	Ardennes, literature-Na, unpublished	https://doi.org/10.1130/G32733.1
France	4	49	<i>Cupressinoxylon</i>	Cupressaceae	Albian	6	2	Ardennes, literature-Na, unpublished	https://doi.org/10.1130/G32733.1
France	0	49	<i>Cupressinoxylon</i>	Cupressaceae	Aptian–Albian	5–6	2	Normandie	https://doi.org/10.1130/G32733.1
France	4	48	<i>Cupressinoxylon</i>	Cupressaceae	Albian	6	2	Aube, literature, Fliche	https://doi.org/10.1130/G32733.1
France	4	48	<i>Cupressinoxylon</i>	Cupressaceae	Albian	6	2	Aube, literature, Pons	https://doi.org/10.1130/G32733.1
France	6	44	<i>Taxodioxylon</i>	Cupressaceae	Albian	6	2	Chabrieres, literature, Cotillon	https://doi.org/10.1130/G32733.1
France	5	44	<i>Taxodioxylon</i>	Cupressaceae	Albian	6	2	Drome	https://doi.org/10.1130/G32733.1
France	4	44	<i>Taxodioxylon</i>	Cupressaceae	Albian	6	2	Bevons, literature	https://doi.org/10.1130/G32733.1
France	4	48	<i>Cupressinoxylon</i>	Cupressaceae	Aptian–Albian	5–6	2	Louvemont, literature, Bertrand	https://doi.org/10.1130/G32733.1
India	85	23	<i>Taxaceoxylon rajmahalense</i>	Cupressaceae	Aptian	5	2	Rajmahal hills, Jharkhand	https://doi.org/10.1130/G32733.1
India	85	23	<i>Taxaceoxylon indicum</i>	Cupressaceae	Aptian	5	2	Rajmahal hills, Jharkhand, Amarjola	https://doi.org/10.1130/G32733.1
India	85	23	<i>Taxaceoxylon</i>	Cupressaceae	Aptian	5	2	Rajmahal hills, Jharkhand	https://doi.org/10.1130/G32733.1
India	85	23	<i>Taxodioxylon</i> sp.	Cupressaceae	Aptian	5	2	Rajmahal hills, Jharkhand	https://doi.org/10.1130/G32733.1
India	85	23	<i>Cupressinoxylon rajmahalense</i>	Cupressaceae	Aptian	5	2	Rajmahal hills, Jharkhand, Amarjola	https://doi.org/10.1130/G32733.1
Japan	136	36	<i>Taxodioxylon</i>	Cupressaceae	Valangian–Barremian	2–4	2	Akaiwa Subgroup, Honshu, Ishikawa Prefecture, Shiramine Inner	https://doi.org/10.1130/G32733.1
Japan	136	36	<i>Cupressinoxylon</i>	Cupressaceae	Valangian–Barremian	2–4	2	Akaiwa Subgroup, Honshu, Ishikawa Prefecture, Shiramine Inner	https://doi.org/10.1130/G32733.1
Japan	141	39	<i>Paracupressinoxylon</i> sp.	Cupressaceae	Hauterivan–Albian	3–6	2	Mosi sandstone of the MoKokorobe, Tanohata-mura, Simo	https://doi.org/10.1130/G32733.1
Japan	142	44	<i>Cupressinoxylon</i> sp.	Cupressaceae	Hauterivan–Albian	3–6	2	Trigonia sandstone, Hokkaido, Top to eusina, Ponmosiri, Asibetu-mura, Isikari	https://doi.org/10.1130/G32733.1
Japan	140	35	<i>Taxodioxylon</i>	Cupressaceae	Barremian–Aptian	4–5	2	Choshi Group, Honshu, Chiba Prefecture, Choshi	https://doi.org/10.1130/G32733.1
Japan	140	35	<i>Taxaceoxylon japonomesozolicum</i>	Cupressaceae	Barremian–Aptian	4–5	2	Choshi Group, Honshu, Chiba Prefecture, Choshi	https://doi.org/10.1130/G32733.1
Japan	140	35	<i>Mesembryoxylon</i> (Taxodioxylon)	Cupressaceae	Barremian–Aptian	4–5	2	Choshi Group, Honshu, Chiba Prefecture, Choshi	https://doi.org/10.1130/G32733.1
Japan	140	35	<i>Cupressinoxylon</i>	Cupressaceae	Barremian–Aptian	4–5	2	Choshi Group, Honshu, Chiba Prefecture, Choshi	https://doi.org/10.1130/G32733.1
Japan	141	39	<i>Paracupressinoxylon</i> sp.	Cupressaceae	Hauterivan–Albian	3–6	2	Mosi sandstone of the MoKokorobe, Tanohata-mura	

England	0	51	Pityoxylon	Pinaceae	Aptian	5	2	Lower Greensand, Folkestone Beds near Ightham, Kent	https://doi.org/10.1130/G32733.1
England	0	51	Pityoxylon sp.	Pinaceae	Aptian	5	2	Lower Greensand, near Maidstone, Kent	https://doi.org/10.1130/G32733.1
England	0	51	Protocedroxylon maidstoneensis	Pinaceae	Aptian	5	2	Lower Greensand, Kentish Rag, Igauodon Quarry	https://doi.org/10.1130/G32733.1
England	0	51	Pityoxylon bennesti	Pinaceae	Aptian	5	2	Lower Greensand, Kentish Rag, near Maidstone, Kent	https://doi.org/10.1130/G32733.1
England	0	52	Pityoxylon woodwardi	Pinaceae	Aptian	5	2	Lower Greensand, Woburn, Bedfordshire	https://doi.org/10.1130/G32733.1
England	0	52	Protocedroxylon pottoniense	Pinaceae	Aptian	5	2	Lower Greensand, Bedfordshire, Potton	https://doi.org/10.1130/G32733.1
England	0	51	Protopiceoxylon edwardsi	Pinaceae	Aptian	5	2	Lower Greensand, Berwick Green, Sussex	https://doi.org/10.1130/G32733.1
England	0	51	Protopiceoxylon	Pinaceae	Aptian-Albian	5-6	2	Greensand, literature, Stopes	https://doi.org/10.1130/G32733.1
England	0	51	Pityoxylon	Pinaceae	Aptian-Albian	5-6	2	Greensand, literature, Stopes	https://doi.org/10.1130/G32733.1
England	-3	50	Protocedroxylon	Pinaceae	Albian	6	2	Upper Greensand, Exeter	https://doi.org/10.1130/G32733.1
England	0	51	Protopiceoxylon	Pinaceae	Aptian-Albian	5-6	2	Greensand, literature, Stopes	https://doi.org/10.1130/G32733.1
England	0	51	Pityoxylon	Pinaceae	Aptian-Albian	5-6	2	Greensand, literature, Stopes	https://doi.org/10.1130/G32733.1
England	0	51	Protocedroxylon	Pinaceae	Aptian-Albian	5-6	2	Greensand, literature, Stopes	https://doi.org/10.1130/G32733.1
England	0	51	Pityoxylon	Pinaceae	Albian	6	2	Gillingham, Kent	https://doi.org/10.1130/G32733.1
France	0	49	Protocedroxylon	Pinaceae	Aptian-Albian	5-6	2	Normandie	https://doi.org/10.1130/G32733.1
France	1	50	Pityoxylon	Pinaceae	Aptian	5	2	Boulogne, literature, Carpenter	https://doi.org/10.1130/G32733.1
France	0	48	Pityoxylon	Pinaceae	Albian	6	2	Gault, Gault	https://doi.org/10.1130/G32733.1
France	1	50	Piceoxylon boureaui	Pinaceae	Albian	6	2	Wissant, Dept. du Pas-de-Calais	https://doi.org/10.1130/G32733.1
France	0	49	Protocedroxylon	Pinaceae	Aptian-Albian	5-6	2	Normandie	https://doi.org/10.1130/G32733.1
France	0	49	Protocedroxylon	Pinaceae	Albian	6	2	Gault de Bleville, Normandie	https://doi.org/10.1130/G32733.1
France	4	48	Pityoxylon	Pinaceae	Albian	6	2	Aube, literature, Fläche	https://doi.org/10.1130/G32733.1
France	4	48	Pinuxylon	Pinaceae	Albian	6	2	Aube, literature, Pons	https://doi.org/10.1130/G32733.1
France	0	47	Protocedroxylon	Pinaceae	Albian	6	2	Aube, literature, Fläche	https://doi.org/10.1130/G32733.1
France	1	50	Pinuxylon bononiense	Pinaceae	Albian	6	2	literature, Pons	https://doi.org/10.1130/G32733.1
France	2	49	Pityoxylon	Pinaceae	Albian	6	2	Villers-St.-Barthelemy, literature, Koeniguer	https://doi.org/10.1130/G32733.1
Japan	140	35	Protocedroxylon	Pinaceae	Barremian-Aptian	4-5	2	Choshi Group, Honshu, Chiba Prefecture, Choshi	https://doi.org/10.1130/G32733.1
Japan	140	35	Protocedroxylon pseudocaruaroides	Pinaceae	Barremian-Aptian	4-5	2	Choshi Group, Honshu, Chiba Prefecture, Choshi	https://doi.org/10.1130/G32733.1
Japan	140	35	Protocedroxylon vectense	Pinaceae	Barremian-Aptian	4-5	2	Choshi Group, Honshu, Chiba Prefecture, Choshi	https://doi.org/10.1130/G32733.1
Japan	141	39	Protocedroxylon yoshidai	Pinaceae	Aptian	5	2	Miyako Series, Miyako, Iwate Prefecture	https://doi.org/10.1130/G32733.1
Japan	141	43	Pinuxylon dakotense	Pinaceae	Hauterivian-Albian?	3-6	2	Honkeiko Beds, Hokkaido, Pen-hsi-hu, Fengtien Province	https://doi.org/10.1130/G32733.1
Japan	140,8413889	35,7219444	Protocedroxylon	Pinaceae	Barremian-Aptian	4-5	2	Honshu, Chiba Prefecture, Choshi Peninsula (Outer Zone), Choshi Group	https://doi.org/10.1016/iseaes.2010.11.010
Japan	141,8902778	39,5741667	Protocedroxylon	Pinaceae	Aptian?	5	2	Honshu, Iwate Prefecture (Outer Zone), Miyako Series	https://doi.org/10.1016/iseaes.2010.11.010
Kazakhstan	71	43	Piceoxylon	Pinaceae	Albian	6	2	Central Kyzylkum, literature	https://doi.org/10.1130/G32733.1
Libya	13	32	Protocedroxylon paronai	Pinaceae	Albian?	6	2	Tripolitania, Negri	https://doi.org/10.1130/G32733.1
Norge	28	78	Protopiceoxylon extinctum	Pinaceae	Barremian	4	2	Harfagrehaugen, SandstonKing, Charles Land, Svalbard, Spitzbergen	https://doi.org/10.1130/G32733.1
Norge	28	78	Protocedroxylon (Anomaloxylon)	Pinaceae	Barremian	4	2	Harfagrehaugen, SandstonKing, Charles Land, Svalbard, Spitzbergen	https://doi.org/10.1130/G32733.1
Norge	28	78	Piceoxylon extinctum	Pinaceae	Barremian	4	2	Harfagrehaugen, SandstonKing, Charles Land, Svalbard, Spitzbergen	https://doi.org/10.1130/G32733.1
Norge	28	78	Protocedroxylon transiens	Pinaceae	Barremian	4	2	Harfagrehaugen, SandstonKing, Charles Land, Svalbard, Spitzbergen	https://doi.org/10.1130/G32733.1
Norge	28	78	Protocedroxylon cedroides	Pinaceae	Barremian	4	2	Harfagrehaugen, SandstonKing, Charles Land, Svalbard, Spitzbergen	https://doi.org/10.1130/G32733.1
Norge	16	78	Piceoxylon	Pinaceae	Aptian-Albian	5-6	2	Carolinefjellet Fm., Lundstromdalen, N Adventfjorden, Spitsbergen	https://doi.org/10.1130/G32733.1
Norge	16	78	Protopiceoxylon	Pinaceae	Aptian-Albian	5-6	2	Carolinefjellet Fm., Lundstromdalen, N Adventfjorden, Spitsbergen	https://doi.org/10.1130/G32733.1
Norge	16	78	Piceoxylon	Pinaceae	Aptian-Albian	5-6	2	Carolinefjellet Fm., Lundstromdalen, N Adventfjorden, Spitsbergen	https://doi.org/10.1130/G32733.1
Norge	16	78	Protopiceoxylon	Pinaceae	Aptian-Albian	5-6	2	Carolinefjellet Fm., Lundstromdalen, N Adventfjorden, Spitsbergen	https://doi.org/10.1130/G32733.1
Norge	17,27972222	78,0213889	Piceoxylon	Pinaceae	Aptian-Albian	5-6	2	Lundstromdalen, Svalbard, Spitsbergen	https://doi.org/10.1130/G32733.1
Norge	17,27972222	78,0213889	Laricioxylon	Pinaceae	Aptian-Albian	5-6	2	Lundstromdalen, Svalbard, Spitsbergen	https://doi.org/10.1130/G32733.1
Norge	17,27972222	78,0213889	Protopiceoxylon	Pinaceae	Aptian-Albian	5-6	2	Lundstromdalen, Svalbard, Spitsbergen	https://doi.org/10.1130/G32733.1
Norge	17,27972222	78,0213889	Piceoxylon	Pinaceae	Aptian-Albian	5-6	2	Lundstromdalen, Svalbard, Spitsbergen	https://doi.org/10.1130/G32733.1
Russia	135	45	Protocedroxylon primoryense	Pinaceae	Aptian-Albian	5-6	2	Lipovtys Fm., Firssov Cape, Muravyov-Amursky Peninsula, Russia Far East, southern Primorye	https://doi.org/10.1016/cretes.2014.04.002
Russia	165,142068	62,193743	Protocedroxylon gregussii	Pinaceae	Albian	6	2	Kamchatka Peninsula (Russia Far East), Melkaya River, Talovka River Basin, eastern coast of Penzhin	https://doi.org/10.1016/cretes.2014.04.002
Russia	165,142068	62,193743	Cedrus penzinensis	Pinaceae	Albian	6	2	Kamchatka Peninsula (Russia Far East), Melkaya River, Talovka River Basin, eastern coast of Penzhin	https://doi.org/10.1016/cretes.2014.04.002
Russia	158	58	Keteleeriioxylon kamtschatiense	Pinaceae	Albian	6	2	Kedrovka Fm., Penzhin Bay, northwestern Kamchatka Peninsula	https://doi.org/10.1134/S0031030106060104
Russia	135	45	Protocedroxylon primoryense	Pinaceae	Aptian-Albian	5-6	2	Lipovtys Fm., Firssov Cape, Muravyov-Amursky Peninsula, Russia Far East, southern Primorye	https://doi.org/10.1016/cretes.2014.04.002
Russia	166	61	Protocedroxylon	Pinaceae	Albian	6	2	Kamchatka, literature, Blokhina	https://doi.org/10.1130/G32733.1
Spain	-2,426944444	42,2883333	Pinoxylon riogranus	Pinaceae	Aptian	5	2	Soto de Cameros, La Rioja	https://doi.org/10.1130/G32733.1
USA	-122,609074								

India	79,43467758	19,2654655	<i>Podocarpoxylon rajmahalense</i>	Podocarpaceae	Barremian–Aptian	4–5	2	Gangapur Fm., Near village Gangapur, Adilabad, Telangana	https://doi.org/10.1106/j.palwor.2017.12.004
India	77	28	<i>Podocarpoxylon</i> sp.	Podocarpaceae	Early–Middle Albian	6	2	Pariwar Fm., Hapur, 45 km NW of	https://doi.org/10.1106/j.palwor.2017.12.004
Italy	12	43	<i>Metapodocarpoxylon subdiphiticum</i>	Podocarpaceae	Aptian–Albian	5–6	2	«Marne a fucidi» dell'Appennino Umbro-Marchigiano	https://doi.org/10.1106/j.palwor.2017.12.004
Italy	11	46	<i>Protopodocarpoxylon petrotii</i>	Podocarpaceae	Albian	6	2	Vervo, Trento, Alps	https://doi.org/10.1106/j.palwor.2017.12.004
Japan	140	35	<i>Circoporoxylon</i>	Podocarpaceae	Barremian–Aptian	4–5	2	Choshi Group, Honshu, Chiba Prefecture, Choshi	https://doi.org/10.1106/j.palwor.2017.12.004
Japan	140	35	<i>Phylocladoxylon gothani</i>	Podocarpaceae	Barremian–Aptian	4–5	2	Choshi Group, Honshu, Chiba Prefecture, Choshi	https://doi.org/10.1106/j.palwor.2017.12.004
Japan	140	35	<i>Mesembrioxylon nifretakagii</i>	Podocarpaceae	Barremian–Aptian	4–5	2	Choshi Group, Honshu, Chiba Prefecture, Choshi	https://doi.org/10.1106/j.palwor.2017.12.004
Japan	140	35	<i>Mesembrioxylon woburnense</i>	Podocarpaceae	Barremian–Aptian	4–5	2	Choshi Group, Honshu, Chiba Prefecture, Choshi	https://doi.org/10.1106/j.palwor.2017.12.004
Japan	140	35	<i>Mesembrioxylon pseudobedfordense</i>	Podocarpaceae	Barremian–Aptian	4–5	2	Choshi Group, Honshu, Chiba Prefecture, Choshi	https://doi.org/10.1106/j.palwor.2017.12.004
Japan	139	35	<i>Circoporoxylon</i>	Podocarpaceae	Barremian–Aptian	4–5	2	Sebayashi Fm., Kwanto, Mountains of central Honshu	https://doi.org/10.1106/j.palwor.2017.12.004
Japan	135	34	<i>Podocarpoxylon woburnense</i>	Podocarpaceae	Barremian?	4	2	Minaziri Bed? of the Mon Wakayama-Ken, Minaziri, Huzinamimura	https://doi.org/10.1106/j.palwor.2017.12.004
Japan	140,843669	35,719989	<i>Circoporoxylon</i>	Podocarpaceae	Barremian–Aptian	4–5	2	Honshu, Chiba Prefecture, Choshi Peninsula (Outer Zone), Choshi Group	https://doi.org/10.1016/j.iseaes.2010.11.010
Japan	138,8072989	36,0808626	<i>Circoporoxylon</i>	Podocarpaceae	Barremian–Aptian	4–5	2	Honshu, Gunma Prefecture, Kwantu Mountains (Outer Zone), Sanchu Group, Sebayashi Fm.	https://doi.org/10.1016/j.iseaes.2010.11.010
Kazakhstan	71	43	<i>Podocarpoxylon</i>	Podocarpaceae	Albian	6	2	Central Kyzylkum, literature	https://doi.org/10.1106/j.palwor.2017.12.004
Kerguelen Island	69	49	<i>Podocarpoxylon</i> sp.	Podocarpaceae	Albian	6	2	Drilling, Kerguelen Plateau	https://doi.org/10.1106/j.palwor.2017.12.004
Lebanon	35	33	<i>Metapodocarpoxylon libanicum</i>	Podocarpaceae	Valanginian–Barremian	2–4	2	Beskinta, Philippe	https://doi.org/10.1106/j.palwor.2017.12.004
Libya	12	32	<i>Metapodocarpoxylon</i> sp.	Podocarpaceae	Albian	6	2	Tripolitania, near Fessato	https://doi.org/10.1106/j.palwor.2017.12.004
Mali	-2,71597816	18,6651714	<i>Metapodocarpoxylon libanicum</i>	Podocarpaceae	Berrriasian–Albian	1–6	2	Ti-n-Essako, western side of the Adrar des Iforas, Continental Intercalaire rocks	https://doi.org/10.1016/j.iseaes.0031-0182(02)00447-9
Nigeria	6,47108916	16,4351986	<i>Metapodocarpoxylon libanicum</i>	Podocarpaceae	Aptian–Albian	5–6	2	Road Agadez-Tahoua	https://doi.org/10.1106/j.palwor.2017.12.004
Nigeria	8	16	<i>Metapodocarpoxylon</i> sp.	Podocarpaceae	Aptian–Albian	5–6	2	km 167, Agadez-Tahoua	https://doi.org/10.1106/j.palwor.2017.12.004
Nigeria	11	10	<i>Metapodocarpoxylon</i> sp.	Podocarpaceae	Aptian–Albian	5–6	2	Gombe	https://doi.org/10.1106/j.palwor.2017.12.004
Norge	-28	78	<i>Phylocladoxylon</i> sp.	Podocarpaceae	Barremian	4	2	Harfagrehaugen, SandstoneKing, Charles Land, Svalbard, Spitzbergen	https://doi.org/10.1106/j.palwor.2017.12.004
Peru	-80	-5	<i>Metapodocarpoxylon libanicum</i>	Podocarpaceae	Early Albian	6	2	Lancones, 99 km of the border	https://doi.org/10.1106/j.palwor.2017.12.004
Romania	28	44	<i>Protopodocarpoxylon</i>	Podocarpaceae	Aptian	5	2	Medgidia, literature, lamandei	https://doi.org/10.1106/j.palwor.2017.12.004
Romania	26	48	<i>Protopodocarpoxylon</i>	Podocarpaceae	Aptian	5	2	Cuza Voda, literature	https://doi.org/10.1106/j.palwor.2017.12.004
Spain	-3,25714213	41,9885889	<i>Protopodocarpoxylon hacinensis</i>	Podocarpaceae	Barremian–Aptian	4	2	Castillo de la Reina, Hacinas	https://doi.org/10.1016/j.geobios.2005.09.003
Tunisia	10,60096702	33,0657389	<i>Metapodocarpoxylon libanicum</i>	Podocarpaceae	Aptian–Albian	5–6	2	Bir Miteur	https://doi.org/10.1106/j.palwor.2017.12.004
Tunisia	10	32	<i>Protocircoporoxylon</i> sp.	Podocarpaceae	Aptian	5	2	Tataouine area, South Tunisia	https://doi.org/10.1106/j.palwor.2017.12.004
Tunisia	10	32	<i>Metapodocarpoxylon libanicum</i>	Podocarpaceae	Aptian–Albian	5–6	2	Tataouine area, South Tunisia	https://doi.org/10.1106/j.palwor.2017.12.004
Tunisia	9	34	<i>Metapodocarpoxylon</i>	Podocarpaceae	Aptian	5	2	base of secuence, Gued, Zefar	https://doi.org/10.1106/j.palwor.2017.12.004
Tunisia	10	32	<i>Metapodocarpoxylon libanicum</i>	Podocarpaceae	Hauterivian–Barremian	3–4	2	Tataouine area, South Tunisia	https://doi.org/10.1106/j.palwor.2017.12.004
Tunisia	9	37	<i>Metapodocarpoxylon libanicum</i>	Podocarpaceae	Aptian–Albian	5–6	2	Bir, Miteur, literature, Philippe	https://doi.org/10.1106/j.palwor.2017.12.004
Tunisia	10,60096702	33,0657389	<i>Metapodocarpoxylon libanicum</i>	Podocarpaceae	Aptian–Albian	5–6	2	Bir Miteur	https://doi.org/10.1106/j.palwor.2017.12.004
Tunisia	10	32	<i>Protocircoporoxylon</i> sp.	Podocarpaceae	Aptian	5	2	Tataouine area, South Tunisia	https://doi.org/10.1106/j.palwor.2017.12.004
Tunisia	9	34	<i>Metapodocarpoxylon libanicum</i>	Podocarpaceae	Aptian–Albian	5–6	2	Tataouine area, South Tunisia	https://doi.org/10.1106/j.palwor.2017.12.004
Romania	28,283333	44,22	<i>Protopodocarpoxylon dobrogiacus</i>	Podocarpaceae	Aptian	5	2	Ghergina Fm., South Dobroudja, Medgidia	https://doi.org/10.1016/j.iseaes.2006.05.003
Romania	28	44	<i>Protopodocarpoxylon</i> sp.	Podocarpaceae	Aptian	5	2	Ghergina Fm., South Dobroudja, Cernavoda	https://doi.org/10.1016/j.iseaes.2006.05.003
Argentina	-70,78933577	44,8674409	<i>Agathoxylon</i>	Araucariaceae	Valanginian	2	1	Tres Lagunas Fm., southern Fontana Lake, north of Alto Rio Senguer town, Chubut	https://doi.org/10.1016/j.cretres.2019.104322
Chad	23	18	<i>Agathoxylon distichum</i> aff.	Araucariaceae	Berrriasian–Barremian	1–4	1	Continental Intercalaire, Erdi, literature	https://doi.org/10.1106/j.palwor.2017.12.004
Chad	23	18	<i>Agathoxylon distichum</i>	Araucariaceae	Berrriasian–Barremian	1–4	1	Continental Intercalaire, Erdi, literature	https://doi.org/10.1106/j.palwor.2017.12.004
Chad	15	9	<i>Agathoxylon dolonii</i>	Araucariaceae	Berrriasian–Barremian	1–4	1	Literature, Duperon and Laudoueneix	https://doi.org/10.1106/j.palwor.2017.12.004
Chad	23	18	<i>Agathoxylon lugrense</i> aff.	Araucariaceae	Berrriasian–Barremian	1–4	1	Bartoszewski	https://doi.org/10.1106/j.palwor.2017.12.004
Chad	15	9	<i>Agathoxylon brachiphyloides</i>	Araucariaceae	Berrriasian–Barremian	1–4	1	Literature, Laudoueneix	https://doi.org/10.1106/j.palwor.2017.12.004
Chad	15	9	<i>Agathoxylon lagunense</i>	Araucariaceae	Berrriasian–Barremian	1–4	1	Literature, Laudoueneix	https://doi.org/10.1106/j.palwor.2017.12.004
Chile	-71	-46	<i>Agathoxylon</i> sp.	Araucariaceae	Hauterivian–Albian	3–6	1	Apeleg and Katerfeld Fms., Puerto Ibañez	https://doi.org/10.1106/j.palwor.2017.12.004
China	119	45	<i>Araucariopsitys (Protocedroxylon) orien</i>	Arauc					

Australia	146	-38	<i>Podocarpoxylon</i> sp.	Podocarpaceae	Valanginian–Barremian	2–4	1	Rintoul Creek Fm., Gippsland Basin, Rintoul Creek	https://doi.org/10.1130/G32733.1
Australia	113	-24	<i>Circoporoxyton</i> sp.	Podocarpaceae	Hauterivian–Barremian	3–4	1	Cardabia, Perth area	https://doi.org/10.1130/G32733.1
Australia	114	-22	<i>Podocarpoxylon, Phyllocladoxylon?</i>	Podocarpaceae	Valanginian–Aptian	2–5	1	Birdrong Sandstone, Carnarvon Basin	https://doi.org/10.1130/G32733.1
Cambodia	104	11	<i>Protophylocladoxylon xenoxioides</i>	Podocarpaceae	Valanginian	2	1	Phnom, Ker	https://doi.org/10.1130/G32733.1
Chile	-71	-46	<i>Podocarpoxylon</i> sp.	Podocarpaceae	Hauterivian–Albian	3–6	1	Apeleg and Katterfeld Fms., Puerto Ibáñez	https://doi.org/10.1130/G32733.1
China	119	45	<i>Phyllocladoxylon eboraense</i>	Podocarpaceae	Hauterivian	5	1	Huolinhe Fm., Jarud, Inner Mongolia	https://doi.org/10.1130/G32733.1
China	121	44	<i>Podocarpoxylon</i> sp.	Podocarpaceae	Hauterivian	5	1	Huolinhe Fm., Huolinhe, Inner Mongolia	https://doi.org/10.1130/G32733.1
China	121	44	<i>Phyllocladoxylon</i> sp. 2	Podocarpaceae	Hauterivian	5	1	Huolinhe Fm., Huolinhe, Inner Mongolia	https://doi.org/10.1130/G32733.1
China	121	44	<i>Phyllocladoxylon</i> sp. 1	Podocarpaceae	Hauterivian	5	1	Huolinhe Fm., Huolinhe, Inner Mongolia	https://doi.org/10.1130/G32733.1
China	121	44	<i>Podocarpoxylon dacyrioides</i>	Podocarpaceae	Hauterivian	5	1	Huolinhe Fm., Huolinhe, Inner Mongolia	https://doi.org/10.1130/G32733.1
China	128,8972467	42,6738997	<i>Phyllocladoxylon</i>	Podocarpaceae	Hauterivian–Aptian	3–5	1	Helong, Jilin Basin	https://doi.org/10.1130/G32733.1
China	125,346992	43,6751024	<i>Phyllocladoxylon</i>	Podocarpaceae	Hauterivian–Aptian	3–5	1	Changchun, Jilin Basin	https://doi.org/10.1130/G32733.1
Colombia	-73	4	<i>Metapodocarpoxylon rosablancense</i>	Podocarpaceae	Hauterivian	3	1	Ubalá	https://doi.org/10.1130/G32733.1
Egypt	26	22	<i>Metapodocarpoxylon saadawi</i>	Podocarpaceae	Berriasian–Hauterivian	1–3	1	Gebel Kâmil	https://doi.org/10.1130/G32733.1
England	-2	50	<i>Circoporoxyton</i>	Podocarpaceae	Late Jurassic–Berriasian	1	1	Purbeck Fm., Dorset, Purbeck	https://doi.org/10.1130/G32733.1
France	0	43	<i>Podocarpoxylon</i>	Podocarpaceae	Hauterivian	3	1	Oyonnax, Martignat, literature, unpublished	https://doi.org/10.1130/G32733.1
France	5	46	<i>Podocarpoxylon</i>	Podocarpaceae	Hauterivian	3	1	Martignat, literature, unpublished	https://doi.org/10.1130/G32733.1
Germany	11	52	<i>Protocircoporoxyton</i>	Podocarpaceae	Hauterivian	3	1	Harzvorland, literature, Vogellehner	https://doi.org/10.1130/G32733.1
India	150,9801133	12,9643511	<i>Podocarpoxylon parthasarathyi</i>	Podocarpaceae	Berriasian–Valanginian	1–2	1	Sriperumbudur Fm., near Sriperumbudur, Tamil Nadu	https://doi.org/10.1016/j.palwor.2017.12.004
India	150,9801133	12,9643511	<i>Podocarpoxylon tirumangalense</i>	Podocarpaceae	Berriasian–Valanginian	1–2	1	Sriperumbudur Fm., near Sriperumbudur, Tamil Nadu	https://doi.org/10.1016/j.palwor.2017.12.004
India	78	11	<i>Podocarpoxylon tricholiopinense</i>	Podocarpaceae	Berriasian–Valanginian	1–2	1	Uttatur, Tamil Nadu	https://doi.org/10.1130/G32733.1
India	78	11	<i>Podocarpoxylon sarmai</i>	Podocarpaceae	Berriasian–Valanginian	1–2	1	Uttatur, Tamil Nadu	https://doi.org/10.1130/G32733.1
India	78	11	<i>Podocarpoxylon</i> sp.	Podocarpaceae	Berriasian–Valanginian	1–2	1	East Coast, Tamil Nadu	https://doi.org/10.1130/G32733.1
India	78	11	<i>Podocarpoxylon parthasarathyi</i>	Podocarpaceae	Berriasian–Valanginian	1–2	1	East Coast, Tamil Nadu	https://doi.org/10.1130/G32733.1
India	78	11	<i>Podocarpoxylon tirumangalense</i>	Podocarpaceae	Berriasian–Valanginian	1–2	1	East Coast, Tamil Nadu	https://doi.org/10.1130/G32733.1
India	78	11	<i>Podocarpoxylon trichinopoliense</i>	Podocarpaceae	Berriasian–Valanginian	1–2	1	Garudamagalam, East Coast,	https://doi.org/10.1130/G32733.1
India	80,79584527	23,5063177	<i>Podocarpoxylon bansaeense</i>	Podocarpaceae	Berriasian–Hauterivian	1–3	1	Jabalpur Fm., Marwar Ghat, Umaria, Madhya Pradesh	https://doi.org/10.1016/j.palwor.2017.12.004
Japan	133,6419672	33,8070676	<i>Podocarpoxylon</i>	Podocarpaceae	Hauterivian	3	1	Honshu, Kochi Prefecture (Outer Zone), Shikoku, Monobegawa Series	https://doi.org/10.1016/j.iseaes.2010.11.010
Lebanon	35	33	<i>Metapodocarpoxylon libanoticum</i>	Podocarpaceae	Valanginian–Barremian	2–4	1	Beskinta, Philippe	https://doi.org/10.1130/G32733.1
Mali	-2,71597816	18,6651714	<i>Metapodocarpoxylon libanoticum</i>	Podocarpaceae	Berriasian–Albian	1–6	1	Ti-n-Essako, western side of the Adrar des Iforas, Continental Intercalaire rocks	https://doi.org/10.1016/S0031-0182(02)00447-9
Portugal	-9	39	<i>Protopodocarpoxylon</i> ? <i>teixeirae</i>	Podocarpaceae	Berriasian–Hauterivian	1–3	1	Cadriceira, South of Torres Vedras	https://doi.org/10.1130/G32733.1
Russia	49	58	<i>Phyllocladoxylon</i>	Podocarpaceae	Valanginian	2	1	Kirov Region, literature, Shil'kina	https://doi.org/10.1130/G32733.1
Russia	49,37664484	59,0108516	<i>Phyllocladoxylon dorofeevii</i>	Podocarpaceae	Valanginian	2	1	Kirov, Russia	https://doi.org/10.1016/j.revpalbo.2006.05.003
South Africa	25	-33	<i>Protocircopoxyton capense</i>	Podocarpaceae	Valanginian–Hauterivian	2–3	1	Sundays River Fm., Algoa Basin, Eastern Cape	https://doi.org/10.1130/G32733.1
Tunisia	10	32	<i>Metapodocarpoxylon libanoticum</i>	Podocarpaceae	Hauterivian–Barremian	3–4	1	Tataouine area, South Tunisia	https://doi.org/10.1130/G32733.1

We include references that do not have DOI and are not in open access in Internet.

Supplementary A references

- Borkent, A., 1997. Upper and Lower Cretaceous Biting Midges (Ceratopogonidae: Diptera) from Hungarian and Austrian Amber and the Koonwarra Fossil Bed of Australia. *Stuttgarter Beiträge zur Naturkunde*, Ser. B, 249, 10 pp.
- Gomez, B., Roghi, G., Giusberti, L., Ragazzi, E., Fornaciari, E., Daviero-Gomez, V., Angelini, I., 2018. Plant assemblage and amber from the Coniacian–Santonian of Vernasso, Friuli-Venezia Giulia, Northeastern Italy. *10th European Palaeobotany & Palynology Conference*, p. 158, Dublin, Ireland.
- Khanchuk, I.A., Ratkin, V.V., Ryazantseva, M.D., Golozubov, V.V., Gonokhova, N.G., 1996. *Geology and Mineral Deposits of Primorsky Krai (Territory)*. Vladivostok “ Dalnauka”, 61 pp.
- McKellar, R.C., Wolfe, A.P., 2010. Canadian amber. In: Penney D. (Ed.). *Biodiversity of Fossils in Amber from the Major World Deposits*. Siri Scientific Press, 149–166, Manchester.
- Peñalver, E., Delclòs, X., 2010. Spanish amber. In: Penney D. (Ed.). *Biodiversity of Fossils in Amber from the Major World Deposits*. Siri Scientific Press, 236–270, Manchester.
- Poinar Jr., G.O., 1992. *Life in amber*. Stanford University Press, 350 pp., Stanford.
- Rice, P.C., 2006. *Amber: Golden Gem of the Ages*. AuthorHouse, 4th edition, 456 pp.
- Savkevich, S.S., Skalski, A.W., Veggiani, A. 1990. Fossil resin in deep deposits of the Persian Gulf. *Prace Muzeum Ziemi* 41, 51–52.
- Zherikhin, V.V., Escov, K.Y., 1999. Mesozoic and Lower Tertiary resins in the former USSR. *Estudios del Museo de Ciencias Naturales de Álava* 14 (nº especial 2), 119–132.

Supplementary B references

- Collinson, M.E., Featherstone, C., Cripps, J.A., Nichols, G.J., Scott, A.C., 2000. Charcoal-rich plant debris accumulations in the Lower Cretaceous of the Isle of Wight, England. *Acta Palaeobotanica*, Supl 2 for 1999, 93–105. [Free Access in RG](#).
- De Oliveira, E.P., 1936. Madeiras petrificadas do planalto dos Parecis. *Notas Preliminares e Estudos do Serviço Geológico e Mineralógico* 3, 2–14.

Supplementary data C. Database of the charcoal/fusain record in Cretaceous rocks worldwide

NORTH HEMISPHERE												
Country	Location	Longitude	Latitude	Stage/s	Maps	Charcoal - Plants	Comments in the paper	References	Other references			
Alaska (USA)	Cantwell Fm., Colville River, Wrangell-St. Elias National Park & Preserve	-141.4323056	61.17875742	Campanian-Maastrichtian	4	charcoal-horsetails, ferns and gymnosperm wood	related to volcanism	https://doi.org/10.1016/j.cretres.2012.04.013				
Austria	Gosau Fm.	13,53267464	47,56704293	Campanian	4	inertinite - charcoal		https://doi.org/10.1038/geo923				
Austria	Sievering Fm., Vienna Flish	16,30136841	48,26293926	Campanian-Maastrichtian	4	charcoal		Knobloch and Mai (1991)				
Canada	Comox Fm., Vancouver Island	-125.0323566	49,69382378	Turonian-Santonian	4	charcoal-inertinite		https://doi.org/10.1038/geo923				
Canada	Oldman Fm., Dinosaur Provincial Park, Alberta	-111.5723924	50,73112712	Campanian	4	charcoalfied gymnosperms		https://doi.org/10.1016/j.cretres.2012.02.008	https://doi.org/10.1007/s12549-013-0123-y			
Canada	Dinosaur Park Fm., Dinosaur Provincial Park, Alberta	-111,5023958	50,79835023	Campanian	4	charcoalfied gymnosperms		https://doi.org/10.1016/j.cretres.2012.02.008				
Canada	Hasen Point Volcanic Unit, unnamed peninsular between Emma Fiord & Audhild Bay, NW Ellesmere Isla	-89,19143286	79,88630353	Campanian-Maastrichtian	4	charcoal-taxodiaceae dominated	related to volcanism	https://doi.org/10.1016/j.palaeo.2004.05.016				
Canada	Kanguk Fm., Sverdrup Basin	-91,7074909	79,27122202	latest Cenomanian-Campanian	4	charcoal-inertinite	HALIP related volcanism	https://doi.org/10.1016/j.glopacha.2021.103515				
Canada	Frenchman Fm., Saskatchewan	-109,2897744	53,44479665	late Maastrichtian	4	charcoal		https://doi.org/10.1016/j.palaeo.2014.02.020				
Canada	Rock Creek East, Saskatchewan	-106,8859000	50,03360055	Maastrichtian-Danian boundary	4	charcoal	K-Pg impact	https://doi.org/10.1144/0016-764904-104				
Canada	Wood Mountain Creek, Saskatchewan	-106,3467431	49,51282664	Maastrichtian-Danian boundary	4	charcoal	K-Pg impact	https://doi.org/10.1144/0016-764904-104				
Canada	Eden Main, Vancouver Island, British Columbia	-123,1263253	49,2521587	Coniacian	4	charcoal-Bennettitales		https://doi.org/10.1086/655963				
China	Qingshankou Fm., Changling Sag, southern Songliao Basin	123,311467	44,7518322	early Cenomanian-early Coniacian	4	charcoal		https://doi.org/10.1016/S1876-3804(21)60049-6				
Croatia	Islands of Hvar and Šćedro	16,68679045	43,13303726	Senonian	4	charcoal		https://doi.org/10.1016/j.cretres.2017.02.003				
Cuba	Monos Fm., south of the Presa Damuji's spillway, Rodas, Cienfuegos Province	-80,54889487	22,27828129	upper Campanian-lower Maastrichtian	4	charcoalfied Cupressaceae		https://doi.org/10.1016/j.cretres.2021.105067				
Czech Republic	Slezské Pavlovce borehole, Silesia	17,7119187	50,30581565	Upper Turonian-Lower Coniacian	4	charcoal		Knobloch and Mai (1991)				
Czech Republic	Klikov Fm., South Bohemia	14,9329645	48,89211245	Turonian-Santonian	4	charcoalfied angiosperms		https://doi.org/10.3140/bull.geosci.1100				
Czech Republic	Flyš, Moravian-Silesian Bezkyd Mts.	18,56002952	49,58274139	Campanian-Maastrichtian	4	charcoal		Knobloch and Mai (1991)				
Egypt	Quseir Fm., Baris Oasis, south Western Desert	30,5941538	24,6560454	Campanian	4	charcoalfied gymnosperms	evidences that wildfire are still scarce in Gondwana	https://doi.org/10.1016/j.cretres.2015.09.012				
Egypt	Quseir/Qusier Fm., Dakhla oasis	28,95770952	25,49910327	lower-middle Campanian	4	charcoal		https://doi.org/10.1016/j.cretres.2021.104783				
Egypt	Quseir/Qusier Fm., Kharga oasis	30,59553655	25,43716894	lower-middle Campanian	4	charcoal		https://doi.org/10.1016/j.cretres.2021.104783				
France	NW Bagnoles-sur-Cèze, Département Gard, Vocontian Basin	4,62720176	44,14762452	Late Turonian-Coniacian	4	charcoal		https://doi.org/10.1016/j.cretres.2008.05.029				
France	Tercis les Bains	-1,11598625	43,6783741	Campanian-Maastrichtian	4	fusain		https://doi.org/10.1016/S0920-5446(01)80018-2				
Germany	Aachen Fm., Aachen	6,35702173	50,87122974	late Santonian-early Campanian	4	charcoalfied diverse angiosperms		Knobloch and Mai (1991)				
Germany	Walbeck	11,49468195	51,66411969	Maastrichtian	4	charcoalfied diverse angiosperms		Knobloch and Mai (1991)				
Germany	Eisleben	11,51774363	51,52689216	Maastrichtian	4	charcoalfied diverse angiosperms		Knobloch and Mai (1991)				
Germany	Gosau Fm., Kossen Niederdorf, Hartmannsdorf	12,71198261	50,87938394	Maastrichtian	4	charcoalfied Magnoliophyta, Theraceae, Cyrtaceae		Knobloch and Mai (1991)				
Greenland	Nanok-1 borehole, Østersletten Fm., Hold with Hope, NE Greenland	-19,74574156	74,44094441	middle Coniacian-lower Campanian	4	charcoal/fusain		https://doi.org/10.1016/j.marpetgeo.2020.104414				
Holland	Aachen Fm., South Limburg	-5,84198454	50,85573038	late Santonian-early Campanian	4	charcoalfied diverse angiosperms		Knobloch and Mai (1991)				
Hungary	Ajka Fm., Bakony Mtns	17,81173102	47,25291961	late Santonian-early Campanian	4	charcoalfied Magnoliophyta		Knobloch and Mai (1991)				
Hungary	Csehbányá Fm., Németbánya and Bakonyjákó, Iharkút, Bakony Mts	17,652555894	47,23069462	Santonian	4	charcoal		https://doi.org/10.1016/j.cretres.2013.08.001				
India	Mandleshwar Fm., Malwa Group of the Deccan trap, Bagh valley of Madhya Pradesh, Karam river east c	75,52071334	22,41994772	early Maastrichtian	4	charcoal	associated to volcanism	https://doi.org/10.18520/cs/v11a/07/1540-1544				
Japan	Ashizawa Fm., Asamigawa Mbr, Kamikita, Fukushima Pref., NE Honshu	140,963436	37,22693444	early Santonian	4	charcoalfied Taxodiaceae and diverse angiosperms		https://doi.org/10.1007/pl00013872				
Mexico	Olmos Fm., Fuentes - Rio Escondido cal basin boreholes (ED-131, VF-12, GN-7), Coahuila region	-100,5357751	28,62186546	Maastrichtian	4	fusain		https://doi.org/10.1038/geo923				
Mexico	Arroyo el Mirbal, San Miguel de Ubaldo, Tamaulipas	-99,72491885	23,32282778	Maastrichtian-Danian boundary	4	charcoal/fusain	related with Chicxulub crater in Yucatán	https://doi.org/10.1016/0016-7037(94)90394-8				
Mexico	Chicxulub crater, Borehole site M0077	-89,9176151	21,74737993	Maastrichtian-Danian boundary	4	charcoal		https://doi.org/10.1073/pnas.2004596117	https://doi.org/10.1038/s41598-022-15566-z			
Nigeria	Agwu Fm., Middle Benue Trough	7,45675922	6,08242285	Coniacian	4	inertinite		https://doi.org/10.1038/geo923				
Nigeria	Manu Fm., Benue Trough Basin	3,93806206	7,12294842	Maastrichtian	4	inertinite		https://doi.org/10.1038/geo923				
Nigeria	Awgu Fm., Benue Trough Basin	7,45675922	6,08242285	Turonian-Santonian	4	fusain		https://doi.org/10.1038/geo923				
Nigeria	Lamja Sandstone Fm., Upper Benue Trough Basin	12,21212302	9,30023228	Santonian	4	fusain		https://doi.org/10.1038/geo923				
Pacific Ocean	Shatsky Rise, Pacific Ocean	160,0151206	35,0082387	Maastrichtian-Danian boundary	4	charcoal		https://doi.org/10.1016/j.epsl.2020.116476				
Portugal	"Arenitos e argillas de Aveiro", Esgueira, north-east Aveiro	8,61950823	40,6610118	Coniacian-Maastrichtian	4	charcoalfied gymnosperms and angiosperms		https://doi.org/10.1016/0034-6667(91)90004-M				
Portugal	"Agilas de Vagos" and "Conglomerado de Mira", Mira, south of Aveiro	-8,74700644	40,42628289	Campanian-Maastrichtian	4	charcoalfied flowers of Fagales		https://doi.org/10.1007/s00600-017-00766				
Romania	Bozeş Fm., Petreşti-Ariňi near Sebes, Hateg Island, Transylvanian Basin	23,62448333	45,93599045	Campanian	4	charcoal		https://doi.org/10.1016/j.cretres.2014.02.002				
Turkmenistan	Niy Klov, Sumbar river	56,2402169	38,47114928	Maastrichtian-Danian boundary	4	charcoal-fusain		https://doi.org/10.1016/0016-7037(90)90444-P	http://meetingorganizer.copernicus.org/EGU2012/			

USA	Raritan Fm., Staten Island, Charleston (Kreischerville), New York	-74,23601189	40,533348837	Turonian	3	charcoaled conifers	Hollick and Jeffrey (1909)		
USA	Baritan Fm., Cape Sable, Magoth River, Ann-Arundel County, Maryland	-76,49037411	39,04177817	Turonian	3	charcoal	Troost (1821)		
USA	Raritan Fm., Fire Clay Mbr., South Amboy, Crossman, New Jersey	-74,27765786	40,46682064	middle-late Turonian	3	charcoaled angiosperms	https://doi.org/10.1016/0034-6667(95)00090-9		
USA	Mancos Shale, Ferron Sandstone Mbr., Emery Coalfield, Utah	-111,2505666	38,87693181	Turonian-Coniacian	3	inertinite	https://doi.org/10.1038/geo923		
USA	Crevasse Canyon Fm., New San Juan River Coalfield, southern San Juan Basin	-108,3217372	35,57559153	Turonian-Santonian	3	inertinite	https://doi.org/10.1038/geo923		
USA	Woodbine Fm., Arlington Archosaur Site, N Texas	-97,081	32,811	Cenomanian	3	charcoal	https://doi.org/10.1016/j.palaeo.2019.109491		
USA	Naturita Fm., Cottonwood Canyon, Utah	-111,8927528	37,28277423	latest Cenomanian	3	charcoal	https://doi.org/10.1130/B35097_1		
USA	Naturita Fm., Wahweap Wash, Arizona	-111,5238723	36,89416898	latest Cenomanian	3	charcoal	https://doi.org/10.1130/B35097_1		
USA	Naturita Fm., Big Hill and Kanarra Mountains localities, western Markagunt Plateau, Utah	-113,1541029	37,51970953	Cenomanian	3	charcoal	https://doi.org/10.1130/B35097_1		
USA	Moreno Hill Fm. (low. mem.), southern Zuni Basin, Balloon Hoodoo, west-central New Mexico	-108,7058821	34,48949127	Turonian	3	charcoal	https://doi.org/10.1016/0034-6667(09)00401		
USA	Dakota Fm., Rose Creek Pit, south of Fairbury on Highway 15, Nebraska	-97,17601867	40,05538158	Albian-Conomanian boundary	3	charcoal	https://doi.org/10.1130/G21998_1		
Alaska (USA)	Corwin Fm., Kukpukruk River, Howard Syncline	-162,5615467	69,32531896	Albian-earliest Cenomanian	2	charcoal-Podozamites	https://doi.org/10.1006/cres.2000.0238		
Bahamas	Site 534, Deep Sea Drilling Project, Blake-Bahama Basin, western North Atlantic	-75,38433297	28,34684716	Aptian-Albian	2	charcoal	https://doi.org/10.2973/dsdp.proc.76.116.1983		
Belgium	Hautrage Fm., Mons Basin, Danube-Bouchon Quarry	3,77441003	50,48706553	early Barremian-early late Barremian	2	fusain-Weichselia	Gomez et al. (2018)	https://doi.org/10.1016/j.palaeo.2015.11.026	
Belgium	Clay pit of Danube-Bouchon's, Hautrage quarry, Mons Basin	3,7741696	50,48762112	Barremian-Aptian	2	fusain-Frenelopsis and Taxodiaceae cf. <i>Sphenolepis</i>	Gomez et al. (2008)		
Belgium	Bernissart, Mons Basin,	3,68222262	50,47311375	middle Barremian-earliest Aptian	2	charcoal-Matoniaceae and Dicksoniaceae	https://doi.org/10.1016/j.cretres.2021.104814		
Brazil	Serra do Tucano Fm., Morro da Sereia, Takutu Basin, Roraima	-60,18227432	3,27589301	Aptian-Albian	2	charcoal-Weichselia	https://doi.org/10.1111/pala.12627		
Canada	Gething Fm., Alberta and British Columbia	-120,0212709	56,13559984	Aptian	2	charcoal-inertinite	https://doi.org/10.1038/geo923		
Canada	Boulder Creek Fm., Peace River, British Columbia	-133,3847406	59,6531444	Albian	2	charcoal-inertinite	https://doi.org/10.1038/geo923		
Canada	Maniville Gp.	-111,2869089	53,4639458	Albian	2	charcoal-inertinite	https://doi.org/10.1038/geo923		
Canada	Suncor Millennium Mine, Clearwater Fm., northern Alberta	-111,4331256	57,57541283	early Albian	2	charcoal-Polyplodiiidae ferns, cycad-cycadophyte, and trace conifer foliage	https://doi.org/10.1098/rsos.200305		
Canada	Drillholes, southeast Moose River Basin, James Bay Lowlands, Cochrane District, northern Ontario	-82,51151318	51,50152852	middle-Albian	2	fusain	https://doi.org/10.1139/e87-100		
Canada	Gates Fm., Honeymoon pit, Monkman, south of the Peace River, North East Coal Block, British Columbia	-121,5531191	54,76945664	early Albian	2	fusain	https://doi.org/10.1139/e87-100		
Canada	Gates Fm., Rocky Mountain Footills, northeastern British Columbia	-123,0583422	56,35931343	early-middle Albian	2	inertinite	https://doi.org/10.1016/0031-0182(95)00043-7	https://doi.org/10.1038/geo923	
China	Yimin Fm., Jiuqiao Sag, Hailar Basin	119,2618542	48,00671381	Albian	2	fusain/inertinite	https://doi.org/10.1016/j.cretres.2021.104815		
China	Yimin Fm., Hailar Basin, Yimin coal mine, Inner Mongolia	119,1871497	48,38478042	Albian	2	fusain/inertinite	https://doi.org/10.1016/j.cretres.2020.104674		
China	Chujinbao Fm., Juixi Basin, Huxia Section, Gansu Province	97,2618131	39,89171505	Barremian	2	charcoal	https://doi.org/10.1016/j.palaeo.2021.109968		
China	Xiagou Fm., Yujingzi Basin, Gansu Prov., northwest China	98,5008	39,9289	Aptian	2	charcoal	https://doi.org/10.1080/00724634.2018.1510412		
China	Hulinhe Fm., Hulinhe coal-mining area, eastern Inner Mongolia	119,5845205	45,49026002	late Barremian-earliest Aptian	2	fusain	associated to volcanism	Susannah et al. (2003)	
China	Zhongou Fm., Yujingzi Basin, Gansu Prov., northwest China	98,5008	39,9289	Albian	2	charcoal	https://doi.org/10.1080/00724634.2018.1510412		
China	Xinchang Petrified Wood National Geopark, Guantou Fm., Zhejiang province	120,7882116	29,30534015	Aptian	2	charcoaled Araucarioxylon	associated to volcanism	https://doi.org/10.2110/palo.2013.130	
China	Shahezi shale, Changling Fault Depression, Songliao Basin	124,1774219	40,50674466	middle Aptian-early Albian	2	fusain	https://doi.org/10.1177/1045987211044831		
China	Seam #16, Yimin Fm., Hailar Basin, Inner Mongolia	119,2393753	48,44172315	Albian	2	charcoal	https://doi.org/10.1016/j.palaeo.2022.111050		
China	Saihantala Fm., Jiergalangtu Sag, Erlan Basin, NE China	116,2608143	44,08474384	Albian	2	fusain-inertinite	https://doi.org/10.1186/s42501-019-0035-5		
China	Yimin Fm., Yimin sag, Hailar Basin, NE China	118,7746998	49,46315078	Albian	2	fusain-inertinite	https://doi.org/10.1186/s42501-019-0035-5		
China	Chengzhi Fm., lixi mine, Sanjiang Basin, NE China	130,9370898	45,41445529	Barremian	2	fusain-inertinite	https://doi.org/10.1186/s42501-019-0035-5		
England	Wessex Fm., Hanover Point Assemblage, Isle of Wight	-1,46795406	50,65358432	Hauterivian-Barremian	2	charcoaled Araucariaceae and Podocarpaceae	Collinson et al. (2000)		
England	Vectis Fm., Sheperds Chine Mbr., Sheperds Chine Assemblage, Isle of Wight	-1,37239379	50,61636245	Hauterivian-Barremian	2	fusainized Weichselia	Alvin (1974)		
England	Upper Weald Clay Fm., Smokejacks clay pit, Ockley, Surrey	-0,41683124	51,12501084	Barremian	2	charcoaled Weichselia	https://doi.org/10.1006/cres.1998.0116		
England	Wessex Fm., Wealden Marl, Chilton Chine, Isle of Wight	-1,42461858	50,63664003	Barremian	2	charcoaled ferns	amber globules, possibly Taxodiaceous	https://doi.org/10.1017/S0016756800023207	
England	3m below the Gault Fm., Mundays Hill Quarry near Leighton Buzzard, Bedfordshire	-0,641044	51,94142767	early Albian	2	charcoaled gymnosperms	https://doi.org/10.1086/297609		
England	Upper Soft Cockle beds, Lulworth Fm., Durlston Bay, Swanage, Dorset	-1,95324462	50,60218442	lower Berriasian	2	charcoal	https://doi.org/10.1016/j.cretres.2011.10.001		
England	Purbeck Limestone Group, Durlston Bay, Dorset	-1,93657782	50,61051838	middle Berriasian	2	charcoal	https://doi.org/10.1016/j.ipgeola.2021.03.001		
England	"Silty Beds" of Bedfordshire, Mundays Hill Quarry near Leighton Buzzard	-0,65160039	51,95142788	early Albian	2	fusain Weichselia and Gleichenites	https://doi.org/10.1086/297609		
England	Wessex Fm., Sheperd's Chine, Isle of Wight	-1,36739348	50,61302908	Barremian	2	fusain	not related to volcanism	https://doi.org/10.1006/cres.1996.0002	
England	"Pseudofrenelopis bed" in the Isle of Wight, Wessex Fm., Hanover Point, Wessex Sub-Basin	-1,46906538	50,65747334	Barremian	2	charcoal	not related to volcanism	https://doi.org/10.1006/cres.1996.0002	
England	"Weichselia bed", Vectis Fm., Hanover Point, Isle of Wight	-1,46906538	50,65747334	lowermost Albian	2	charcoal	not related to volcanism	https://doi.org/10.1006/cres.1996.0002	
England	"Pine Raft" bed, in the Isle of Wight, Hanover Point	-1,46906538	50,65747334	Barremian	2	charcoal	not related to volcanism	https://doi.org/10.1006/cres.1996.0002	
France	Beauvais	2,1277099	49,39610123	Barremian	2	charcoal	https://doi.org/10.1111/pala.12627		
Germany	Balve, fissure fillings, Sauerland	8,01178468	51,3479422	late Barremian-Aptian	2	charcoal	https://doi.org/10.1016/j.cretres.2020.104606		
Germany	Prangenhaus								

Ukraine	Crimean Peninsula, southern slope of Belya Mt., northwestern Verkhorichchia	33,96935221	44,70186231	Hauterivian	1	charcoal		https://doi.org/10.1016/j.egsl.2005.09.001	
SOUTH HEMISPHERE									
Country	Location	Longitude	Latitude	Stage/s	Maps	charcoal - Plants	Comments	Reference	Other references
Antarctica	Table Nunatak Fm., Kenyon Peninsula, Eastern side of Antarctic Peninsular	-62,72825759	-68,45837467	late Santonian	4	charcoalfied Siparunaceae, Winteraceae and Myrtaceae		https://doi.org/10.1016/S0034-6667(03)00120-9	
Antarctica	Rip Point, Nelson Island, South Shetland Islands	-59,00723133	-62,2465536	Campanian	4	charcoal	related to volcanism	https://doi.org/10.1016/j.cretres.2022.105185	
Antarctica	Santa Marta Fm., James Ross Island	-57,93155388	-63,90405371	Campanian	4	charcoal		https://doi.org/10.33265/polar.v40.5487	
Antarctica	Rip Point outcrop, Nelson Island, South Shetland Islands	-59,00112037	-62,24459991	Campanian	4	charcoal	related to volcanism	https://doi.org/10.1016/j.palaeo.2014.11.012	
Antarctica	Table Nunatak Fm., Kenyon Peninsula	-62,72825759	-68,45837467	late Santonian	4	charcoal		https://doi.org/10.1016/j.cretres.2003.11.004	
Argentina	Lago Cahué Huapi Fm., Golfo San Jorge Basin,	-68,52353605	-45,57718174	Campanian-Maastrichtian	4	charcoal		https://doi.org/10.1016/j.cretres.2022.105229	
Atlantic Ocean	Walvis Ridge, South Atlantic Ocean	3,04427529	-27,99534835	Maastrichtian-Danian boundary	4	charcoal		https://doi.org/10.1016/j.egsl.2020.116476	
Australia	Bundey Basin, which hosts the corehole HUC11 sediments, 140 km northeast of Alice Springs	135,2529188	-22,65739273	late Campanian-Maastrichtian	4	charcoalfied Proteaceae	not related to volcanism	https://doi.org/10.3732/ajb.1500343	
Brazil	São Carlos Fm., Ibaté Bed, Bauru Group, Paraná Basin	-47,98812806	-21,99526784	Upper Santonian	4	charcoalfied Olacaceae		https://doi.org/10.1016/j.egsl.2017.11.014	
Brazil	Sea boreholes in Santos Basin (Rio de Janeiro)	-43,08422067	-23,07637728	Santonian	4	fusain	related to volcanism	Arai et al. (2005-6)	
Brazil	Sea boreholes in Campos Basin (Sao Paulo) -	-41,68643192	-22,83139144	Santonian	4	fusain	related to volcanism	Arai et al. (2005-6)	
France	Kerguelen Plateau	69,43778182	-49,45049769	Maastrichtian-Danian boundary	4	charcoal		https://doi.org/10.1016/j.egsl.2020.116476	
New Zealand	Members 3 & 4, Pike River Coalfield, Paparoa Range	171,483946	-42,20535205	Campanian-Maastrichtian	4	charcoal		https://doi.org/10.1038/geo923	
New Zealand	Rewanui Coal Measures, Pike River Coalfield	171,4792239	-42,20729647	Campanian Maastrichtian	4	charcoal		https://doi.org/10.1038/geo923	
New Zealand	Taratu Fm., Kaitangata Coalfield, Kai Point Mine, South of Dunedin	169,8798777	-46,2710694	latest Maastrichtian	4	charcoalfied Podocarpaceae and Lauraceae		https://doi.org/10.1016/j.cretres.2010.11.006	
New Zealand	Maungataniwha Sandstone Mb., Tahora Fm., Urewera Ranges, Mangahouanga Stream, northern Hawke	176,7996132	-38,93766059	late Campanian-early Maastrichtian	4	charcoal		https://doi.org/10.1080/03115518.2010.486642	
Argentina	Kachaike Fm., Austral Basin, Santa Cruz Prov., Bajo Comisión, north of San Martín Lake, Patagonia	-72,98723583	-48,85398127	Albian-Cenomanian	3	charcoal		https://doi.org/10.1016/j.cretres.2006.12.006	
Australia	Winton Fm., Eromanga-1 bore hole, Eromanga Basin, Queensland	143,2656642	-26,64942888	late Albian-Cenomanian	3	charcoal		https://doi.org/10.1006/cres.1999.0164	
Australia	Mackunda Fm., Blackall-1 bore hole, Eromanga Basin, Queensland	145,4514595	-24,37949808	late Albian-Cenomanian	3	charcoal		https://doi.org/10.1006/cres.1999.0164	
Australia	Allaru Fm., Tickalara-1 bore hole, Eromanga Basin, Queensland	142,2151361	-28,64214514	late Albian-Cenomanian	3	charcoal		https://doi.org/10.1006/cres.1999.0164	
New Zealand	Tupuangi Fm., Pitt Island, Waihere Bay, Chatham Islands	176,2394002	-44,26414328	Cenomanian	3	charcoalfied Cupressaceae	in resin-rich beds	https://doi.org/10.1080/03115518.2017.1417478	https://doi.org/10.1016/j.revpalbo.2018.08.004
Antarctica	Alexander Island	-70,25874054	-71,27514752	latest Aptian-uppermost Albian	2	charcoal		https://doi.org/10.1144/igs.158.4.709	https://doi.org/10.1111/1365-2486.2005.001068.x
Antarctica	President Beaches Fm., Byers Peninsula, Livingston Island, South Shetland Islands	-69,83196745	-62,5129935	Berriasian	2	charcoalfied Podocarpaceae and Araucariaceae	volcanic arc volcanism	https://doi.org/10.1016/j.egsl.2022.103940	
Antarctica	Cerro Negro Fm., Byers Peninsula, Livingston Island, South Shetland Islands	-69,83196745	-62,5129935	early Aptian	2	charcoal		https://doi.org/10.1016/j.egsl.2022.103940	
Antarctica	Lith. Unit IV, Site 750, Raggatt Basin, Kerguelen Plateau	-81,2606532	-57,6089367	early Albian	2	charcoalfied Podocarpaceae	related to volcanism	https://doi.org/10.2973/odp.proc.sr.120.195.1992	
Antarctica	Triton Point Fm., Alexander Island	-68,22550864	-71,69185617	late Albian	2	charcoalfied Podocarpaceae	related to volcanism	https://doi.org/10.1144/igs.158.4.709	
Argentina	Kachaike Fm., Austral Basin, Santa Cruz Prov., Bajo Comisión, north of San Martín Lake, Patagonia	-72,98723583	-48,85398127	Albian-Cenomanian	2	charcoal		https://doi.org/10.1016/j.cretres.2006.12.006	
Australia	Burgowan Coal, Queensland	152,6322127	-25,3322035	Albian	2	inertinite		https://doi.org/10.1038/geo923	
Australia	Winton Fm., Eromanga-1 bore hole, Eromanga Basin, Queensland	143,2656642	-26,64942888	late Albian-Cenomanian	2	charcoal		https://doi.org/10.1006/cres.1999.0164	
Australia	Mackunda Fm., Blackall-1 bore hole, Eromanga Basin, Queensland	145,4514595	-24,37949808	late Albian-Cenomanian	2	charcoal		https://doi.org/10.1006/cres.1999.0164	
Australia	Allaru Fm., Tickalara-1 bore hole, Eromanga Basin, Queensland	142,2151361	-28,64214514	late Albian-Cenomanian	2	charcoal		https://doi.org/10.1006/cres.1999.0164	
Australia	Eumeralla Fm., Otway Basin	142,1808186	-38,28629117	middle-late Albian	2	charcoalfied Araucariaceae		https://doi.org/10.1016/j.palaeo.2018.01.017	
Brazil	Romualdo Mb., Santana Fm., Porteiras, Chapada do Araripe	-39,13499035	-7,50624186	Aptian-Albian	2	charcoal		https://doi.org/10.1007/s12549-018-0359-7	
Brazil	Ipubi Fm., Upubí, Chapada do Araripe	-40,15694115	-7,61818475	Aptian	2	charcoal		https://doi.org/10.1007/s12549-018-0359-7	
Brazil	Crato Fm., Nova Olinda, Chapada do Araripe	-39,6977723	-7,11541922	Aptian	2	charcoal, fusain		https://doi.org/10.1007/s12549-018-0359-7	
Brazil	Romualdo Mb., Santana Fm., Araripe Basin	-39,15554599	-7,54540756	late Aptian-uppermost Albian	2	charcoal		http://dx.doi.org/10.1016/j.cretres.2011.10.011	
Antarctica	Chester Cone Fm., Byers Peninsula, Livingston Island, South Shetland Islands	-69,83196745	-62,5129935	latest Berriasian-mid Valanginian	1	charcoal		https://doi.org/10.1016/j.egsl.2022.103940	
Argentina	Springhill Fm., Tierra de Fuego, Santa Cruz Province, Patagonia	-68,07498874	-53,92286001	Berriasian-Valanginian	1	fusain - Bennetitales	related to volcanism	https://doi.org/10.1006/cres.2001.0266	
Australia	Orallo Fm., Surat Basin	148,5894947	-26,59689842	Valanginian	1	inertinite	related to volcanism	https://doi.org/10.1080/08120099.2020.1781690	
Madagascar	Manja, Menabe district	44,31588439	-21,43194728	Hauterivian	1	charcoalfied ferns, fusain		Appert (2010)	
South Africa	Kirkwood Fm., Algoa Basin, Sundays River, Mfuleni farm	25,36626428	-33,35057371	middle-upper Valanginian	1	fusain	in association with amber	https://doi.org/10.1111/j.1502-3931.2002.tb00090.x	
South Africa	Kirkwood Fm., Algoa Basin, Bezuidenhouts River locality	25,50460203	-33,47696167	Valanginian	1	fusain	in association with amber	http://dx.doi.org/10.1016/j.cretres.2015.04.005	